UAlg
UNIVERSIDADE DO ALGARVE

Faculdade de Ciências e Tecnologia
Departamento de Ciências Biomédicas e Medicina

Nano and microparticles as carriers for alveolar macrophage targeting in pulmonary tuberculosis therapy

Ludmylla Costa Cunha

2018

UAlg
UNIVERSIDADE DO ALGARVE

Faculdade de Ciências e Tecnologia
Departamento de Ciências Biomédicas e Medicina

Nano and microparticles as carriers for alveolar macrophage targeting in pulmonary tuberculosis therapy

Ludmylla Costa Cunha

PhD in Biomedical Sciences

Thesis supervised by Prof. Ana Grenha, PhD.

2018

Nano and microparticles as carriers for alveolar macrophage targeting in pulmonary tuberculosis therapy

Declaração de autoria de trabalho

Declaro ser a autora deste trabalho, que é original e inédito. Autores e trabalhos consultados estão devidamente citados no texto e constam na listagem de referências incluída.

_____

Acknowledgements

Agradeço à professora Ana Grenha por me acolher em seu grupo de investigação e pela orientação no desenvolvimento deste trabalho.
Agradeço aos professores que colaboraram diretamente com a realização desta pesquisa, nomeadamente prof. Ana Costa (UAlg), prof. Deborah Power (UAlg), prof. João Lourenço (UAlg), prof. Leonor Faleiro (UAlg), prof. Manuela Gaspar (iMed UL) e prof. Francesca Buttini (Universidade de Parma).
Igualmente, agradeço aos colaboradores dos serviços técnico e administrativo, que com competência e prestimosidade, contribuíram direta ou indiretamente para a realização deste trabalho. Em especial, destaco a colaboração do Sr. Mário Freitas (UAlg) e Sra. Judith Anakayana (Universidade de Parma).
Agradeço o apoio dos meus colegas de laboratório Filipa, Jorge, Susana, e João.
E, finalmente, meu eterno agradecimento a meus pais, irmão, Vincent e amigos pelo carinho, incentivo e suporte emocional ao longo dessa jornada.
Muito obrigada!

Esta pesquisa foi financiada pela Fundação para a Ciência e Tecnologia, de Portugal (PTDC/DTP-FTO/0094/2012 and UID/BIM/04773/2013). A bolsa de doutoramento foi financiada pela agência brasileira de fomento à pesquisa CAPES – Coordenação de Aperfeiçoamento de Pessoal de Nível Superior – por meio do programa Ciências sem Fronteiras (BEX 1168-13/4).

This page was intentionally left in blank

Contents

This page was intentionally left in blank

Resumo

A tuberculose (TB) é uma das principais causas de morte por infeção no mundo, apesar de uma vacina e vários antibióticos eficazes estarem disponíveis para a prevenção e tratamento da patologia. O controlo global da TB está dificultado por vários fatores, incluindo o diagnóstico tardio e a não adesão do paciente a tratamentos de longo prazo, o que leva a uma alta incidência de resistência aos fármacos tuberculostáticos. Em geral, existem grandes desafios associados à terapêutica convencional, incluindo (i) resistência aos fármacos e toxicidade; (ii) interrupção do tramento pelo paciente, devido à terapêutica prolongada e efeitos secundários graves; (iii) interações medicamentosas, particularmente com antirretrovirais em pacientes co-infectados com TB e HIV. Assim, a gravidade da situação chegou a um ponto em que o desenvolvimento de novas estratégias de intervenção é urgentemente necessário.

Nesse contexto, a administração pulmonar de fármacos tuberculostáticos é uma abordagem promissora no tratamento da TB pulmonar. A doença representa aproximadamente 80% do total de casos e, portanto, o pulmão tem sido explorado como uma via efetiva para a administração de fármacos. Essa estratégia não só permite direcionar instantaneamente os fármacos para o órgão afetado, como também pode reduzir os efeitos adversos sistémicos dos antibióticos, que são as principais razões para a interrupção do tratamento por parte do paciente. No entanto, a administração pulmonar de fármacos enfrenta algumas limitações, como a complexa estrutura das vias aéreas, a degradação local de fármacos e a eliminação mucociliar. A fim de ultrapassar algumas dessas limitações, a microencapsulação de fármacos aparece como uma abordagem com potencial. Nesse sentido, este trabalho teve como objetivo produzir micropartículas inaláveis que associassem eficientemente dois fármacos tuberculostáticos de primeira linha, isoniazida (INH) e/ou rifabutina (RFB), visando uma aplicação na terapia da TB pulmonar. Fucoidan (FUC) e quitosano (CS) foram os biomateriais selecionados para compor a matriz dos transportadores. FUC é um polissacárido composto por unidades de fucose, que foram relatadas como sendo especificamente reconhecidas por recetores de membrana de macrófagos alveolares (a célula hospedeira do agente patogénico da tuberculose - *Mycobacterium tuberculosis*). Da mesma forma, o CS é também um polissacárido composto por resíduos de *N*-

acetilglucosamina e D-glucosamina, sendo os primeiros igualmente reconhecido por macrófagos de acordo com descrições da literatura. Este reconhecimento pelos macrófagos acredita-se que potenciará a fagocitose.

Numa primeira abordagem foram produzidas nanopartículas, tendo-se considerado que o desenvolvimento de uma formulação inalável à base de nanopartículas implicaria uma etapa posterior de microencapsulação para contornar as limitações relacionadas com as propriedades aerodinâmicas dos sistemas nanométricos e as suas dificuldades para alcançar a região alveolar. As nanopartículas foram obtidas por complexação de FUC com CS, tendo-se desenvolvido várias formulações (rácios de massa FUC/CS de 4:1 a 1:4). Os sistemas sem fármaco apresentaram tamanho médio de 159 – 266 nm, PdI entre 0,21 e 0,36 e potencial zeta entre -39 mV e +12 mV, seguindo sensivelmente a alteração das razões de massa. A capacidade das nanopartículas de FUC/CS para associar fármacos tuberculostáticos foi avaliada, tendo-se iniciado estes testes pela incorporação de RFB, associada à razão final polímero/fármaco de 10/1 (m/m). Várias tentativas foram executadas sem sucesso, pelo que o trabalho prosseguiu com uma segunda abordagem metodológica para produção das nanopartículas. Aplicou-se o método de nanoprecipitação, que levou à produção de nanopartículas de FUC e nanopartículas de CS com tamanho médio de 500 nm e 700 nm, respetivamente. No entanto, as nanopartículas obtidas apresentaram uma ampla distribuição de tamanhos, indicada pelos valores de PdI, que variaram entre 0,55 e 0,83. Além disso, um protocolo de nanoprecipitação ideal para obter nanopartículas à base de FUC ou CS que associassem de forma efetiva INH e/ou RFB não foi estabelecido. Tendo em conta a ausência de sucesso da produção de sistemas nanométricos, e considerando as restrições temporais impostas aos trabalhos de doutoramento, foi decidido focar o trabalho no desenvolvimento de micropartículas poliméricas à base de FUC ou CS.

As micropartículas foram produzidas por um processo de atomização, contendo os fármacos modelo (INH e RFB) isoladamente ou de forma combinada. As micropartículas de FUC associaram efetivamente a INH (95%) e a RFB (81%) por separado. Foram igualmente produzidas com sucesso micropartículas de FUC carregadas com os dois fármacos tuberculostáticos simultaneamente, as quais registaram elevada eficácia de associação dos fármacos (97% para INH e 95% para

RFB). Todas as formulações de micropartículas de FUC demonstraram ter propriedades aerodinâmicas favoráveis para a distribuição e penetração pulmonar após inalação. Para as micropartículas que associaram os fármacos isoladamente, obteve-se um diâmetro aerodinâmico no intervalo 2,0-3,8 µm. Da mesma forma, a formulação que associa os dois antibióticos apresentou um diâmetro aerodinâmico de 3,6 – 3,9 µm. Em geral, as formulações não evidenciaram efeitos citotóxicos nas células do epitélio alveolar humano (A549), embora tenha sido observada uma ligeira toxicidade nas células THP-1 diferenciadas em macrófagos, na concentração mais elevada que foi testada (1 mg/mL). Contudo, considera-se que esta concentração seja muito mais elevada em relação àquela que seria efetivamente administrada *in vivo*. As micropartículas de FUC desenvolvidas neste estudo também exibiram propensão para serem capturadas por macrófagos ou células diferenciadas em macrófagos (células-alvo) de forma dose-dependente. Particularmente, as micropartículas que associam os dois fármacos conjuntamente exibiram uma capacidade para ativar as células-alvo e, ainda, inibiram de maneira eficaz o crescimento de micobactéria *in vitro*, sem alterarem a atividade bactericida dos fármacos. A administração pulmonar *in vivo* (ratinhos BALB/c) das micropartículas de FUC (sem fármacos) indicou, num ensaio preliminar, que as mesmas não induziram respostas alérgicas.

As micropartículas de CS também associaram eficientemente INH (90%) e RFB (97%) por separado, tendo a formulação com fármacos combinados resultado em 93% de eficácia de associação para INH e 99% para RFB. Todas as formulações apresentaram propriedades adequadas para administração pulmonar, com diâmetro aerodinâmico entre 2,5 e 4 µm. A ausência de toxicidade foi observada no epitélio alveolar humano (células A549), mas, tal como observado para as micropartículas de FUC, a maior concentração de micropartículas testada (1 mg/mL) diminuiu a viabilidade de células THP-1 diferenciadas em macrófagos, após 24 h de exposição, uma dose considerada sobrestimada, como mencionado anteriormente. As micropartículas de CS evidenciaram ainda uma grande capacidade de internalização por macrófagos (percentagem de fagocitose até 99,9%), de forma independente da dose, e as micropartículas contendo ambos os fármacos numa única formulação, induziram a ativação de macrófagos e inibiram eficazmente o crescimento de micobactérias *in vitro*. Além disso, o biomaterial (CS)

foi, aparentemente, bem tolerado por ratinhos BALB/c, após administração pulmonar das micropartículas de CS sem fármaco. No geral, os dados obtidos fornecem indicações positivas sobre o potencial dos sistemas propostos para uma aplicação na terapia inalável da tuberculose pulmonar.

Keywords: atomização, fucoidan, isoniazida, macrófagos alveolares, micropartículas inaláveis, quitosano, rifabutina, terapia pulmonar, tuberculose.

Abstract

Tuberculosis (TB) is a leading infectious cause of death worldwide, even though a vaccine and several effective antibiotics are available for its prevention and treatment. Global TB control is very difficult due to various factors, including late diagnosis and patient non-compliance to long-term treatments, which leads to a high incidence of extensive resistance to effective anti-TB drugs. Overall, there are significant challenges associated with conventional TB therapy, including (i) drug resistance and toxicity; (ii) patient non-compliance, given the long-term therapy and severe side effects; (iii) and drug-drug interactions, particularly with antiretroviral drugs in patients co-infected with TB and HIV. Thus, the situation has come to a point where the development of novel intervention strategies is urgently needed.

In this context, the pulmonary delivery of anti-TB drugs is a promising approach to treat lung TB. The disease represents approximately 80% of total cases, and thus the lung has been explored as an effective route for the delivery of drugs. This strategy not only allows targeting the infected organ instantly, but it can also reduce the systemic adverse effects of the antibiotics, which are main reasons for patient non-compliance. However, pulmonary drug delivery faces some limitations related with the proper airway structure, local degradation of drugs, and mucociliary clearance. In order to overcome some of these limitations of lung delivery, drug microencapsulation appears as a potential approach. In this sense, this work aimed at producing inhalable microparticles that efficiently associate two anti-TB drugs, isoniazid (INH) and/or rifabutin (RFB), for an application in pulmonary TB therapy. Fucoidan (FUC) and chitosan (CS) were the biomaterials selected to compose the matrix of the carriers. FUC is a polysaccharide composed of fucose units that has been reported to be specifically recognised by surface receptors of alveolar macrophages (the host cells of *Mycobacterium tuberculosis*). Likewise, CS is a polysaccharide composed of *N*-acetylglucosamine and D-glucosamine residues, the former being also specifically recognised by macrophages, according to the literature. This recognition by macrophages is believed to potentiate phagocytosis.

The first approach involved the production of nanoparticles and it was considered that subsequent microencapsulation of the nanocarriers would be necessary to overcome aerodynamic limitations of nanosized carriers and their

ability to reach the alveolar zone. Nanoparticles were spontaneously obtained by complexing FUC with CS, resulting from several formulations (polymeric mass ratio varying from 4:1 to 1:4). The produced unloaded FUC/CS nanoparticles presented average size range of 159 – 266 nm, PdI ranging between 0.21 and 0.36, and zeta potential varying from -39 mV to +12 mV, following the alteration of the mass ratios. The ability of FUC/CS nanoparticles to associate anti-TB drugs was assessed, and tests initiated with the incorporation of RFB, which was associated to obtain final polymer/drug mass ratio of 10/1 (w/w). Several attempts were made unsuccessfully, and therefore the work continued using another production method. Nanoprecipitation technique was then used, resulting in FUC nanoparticles and CS nanoparticles with mean size of 500 nm and 700 nm, respectively. However, the obtained nanoparticles showed little uniformity in size, indicated by PdI values, varying between 0.55 and 0.83. Moreover, an optimal protocol to obtain FUC- and CS-based nanoparticles that efficiently encapsulate INH and RFB could not be established. Taking into consideration the unsuccessful nanoparticle production and time restraints to accomplish the aims of the PhD plan, it was decided to focus the study on the development of polymeric microparticles.

Microparticles were produced by spray-drying, associating the model drugs (INH and RFB), either separately or in combination. FUC microparticles effectively associated INH (95%) and RFB (81%), separately. Likewise, FUC microparticles loaded with the two anti-TB drugs simultaneously were also successfully produced, demonstrating high drug association efficiency (97% for INH and 95% for RFB). All FUC-based microparticles evidenced favourable aerodynamic properties for deep lung delivery upon inhalation. Single drug-loaded FUC microparticles showed aerodynamic diameter (MMAD) in the range of 2.0–3.8 µm. Likewise, the dual drug-loaded dry powder presented aerodynamic diameter of 3.6–3.9 µm. Overall, the formulations evidenced no cytotoxic effects on human alveolar epithelium cells (A549), although mild toxicity was observed on macrophage-differentiated THP-1 cells at the highest tested concentration (1 mg/mL). Nonetheless, this dose is considered overestimated compared to that effectively observed *in vivo*. The produced FUC microparticles also exhibited a propensity to be captured by macrophages or macrophage-like cells (target cells) in a dose-dependent manner. Particularly, dual drug-loaded microparticles displayed ability to activate the target

cells and, moreover, effectively inhibited mycobacterial growth *in vitro*, preserving the bactericidal activity of the drugs. *In vivo* lung administration (BALB/c mice) of unloaded FUC microparticles indicated, in a preliminary assay, that the carriers induced no allergic responses.

CS microparticles also associated INH (90%) and RFB (97%) efficiently, in separate formulations, whereas dual drug-loaded formulation resulted in 93% association efficiency for INH and 99% for RFB. All formulations presented adequate properties for deep lung delivery, with aerodynamic diameters ranging between 2.5 and 4 µm. Absence of toxicity was observed in human alveolar epithelium (A549 cells) but, as observed for FUC carriers, the highest tested concentration of microparticles (1 mg/mL) decreased the viability of macrophage-differentiated THP-1 cells upon 24 h exposure. This dose is however believed to be overestimated, as aforementioned. CS microparticles further evidenced strong ability to be internalised by macrophage-like cells (percentage of phagocytosis up to 99.9%), regardless of the dose. Yet, dual drug-loaded carriers induced macrophage activation and effectively inhibited the growth of mycobacteria *in vitro.* Moreover, the biomaterial (CS) was well tolerated by BALB/c mice upon pulmonary administration of unloadead CS microparticles. Overall, the obtained data gave positive indications on the potential of the proposed systems for an application as inhalable tuberculosis therapy.

Keywords: alveolar macrophage, chitosan, fucoidan, inhalable microparticles, isoniazid, lung therapy, rifabutin, spray-drying, tuberculosis.

List of tables

List of figures

List of abbreviations, acronyms, and symbols

AE – Association efficiency
ACI – Andersen cascade impactor
CCM – Cell culture medium
CD4 – CD4 positive T cells
CD8 – CD8 positive T cells
CS – Chitosan
D_{aer} – Aerodynamic diameter
ED – Emitted dose
EDAC – *N*-(3-dimethylaminopropyl)-*N*′-ethylcarbodiimide hydrochloride
ELISA – Enzyme-linked immunosorbent assay
FBS – Fetal bovine serum
FUC – Fucoidan
FPD – Fine particle dose
FPF – Fine particle fraction
HIV – Human immunodeficiency virus
HPLC – High performance liquid chromatography
Ig – Immunoglobulin
IL – Interleukin
INH – Isoniazid
ISO – International Organization for Standardization
LC – Loading capacity
LDH – Lactate dehydrogenase
LPS – Lipopolysaccharide
Man – Mannitol
MD – Metered dose
MIC – Minimum inhibitory concentration
MMAD – Mass median aerodynamic diameter
MP – Microparticles
MTT – 3-(4,5-dimethylthiazol-2-yl)-2,5-diphenyltetrazolium bromide
NP – Nanoparticles
OADC – Oleic acid, albumin, dextrose and catalase
OVA – Ovalbumin
PBS – Phosphate-buffered saline
PdI – Polydispersity index
PGA – Poly(glycolic acid)
PLA – Poly(lactic acid)
PLGA – Poly(lactic acid-co-glycolic acid) copolymer
PMA – Phorbol 12-myristate 13-acetate
RFB – Rifabutin
SDS – Sodium dodecyl sulphate
SEM – Scanning electron microphotograph
TB – Tuberculosis
TNF – Tumor necrosis factor
WHO – World Health Organization

This page was intentionally left in blank

Chapter One

General Introduction

The information presented in this chapter was partially published in the following publication:

Ludmylla Cunha and Ana Grenha. Sulfated seaweed polysaccharides as multifunctional materials in drug delivery applications. *Marine Drugs* ***2016***, 14, 42; doi: 10.3390/md1403004

This page was intentionally left in blank

1. General Introduction

1.1 Tuberculosis

Since ancient times, tuberculosis (TB) or illnesses resembling TB have been described in several parts of the world from many civilisations. Although it was probably described for the first time in Indian scriptures, pulmonary TB is known since the time of Hippocrates as *phthisis*, which is derived from the Greek for "wasting away". TB-like diseases have also been documented in ancient Chinese and Arabic literature and have been described under many peculiar names during history, such as *consumption* (derived from the Latin *consumer*) and *scrofula*, a rare manifestation form of TB that affects the lymph nodes, especially of the neck (1,2). The meaning of old names has undergone great alterations with time, mainly due to discoveries about the nature of the disease and its effects on people. The disease was given the name of *tuberculosis* in 1839 by J.L. Schonlein, derived from the Latin *tuberculum* ("a small lump"), and came into general use in the last years of the 19th century (3,4).

The information concerning the actual prevalence and mortality of TB over the centuries is uncertain. It is difficult to obtain accurate data from written documents because the diagnosis was then based exclusively on signs and symptoms. Moreover, the expressions *pulmonary consumption* and *phthisis* were often used to designate a variety of unrelated diseases. Therefore, until late in the 19th century, many lung diseases were confused with TB and it was only during modern times that certain types of non-pulmonary infections have been recognised as being caused by tubercle bacilli, and thus belonging to the class of TB (3). Despite all the uncertainties, TB was the greatest single cause of disease and death by the end of the 19th and beginning of the 20th century in Europe. The lack of knowledge on TB diagnosis, its nature and treatment certainly contributed to that fact (2,3).

Over the last century, there has been unquestioned scientific and clinical progress on this matter. The understanding of basic concepts related to the pathogenesis, the isolation and cultivation of the aetiological agent of TB by Robert Koch in 1882, have all led to the development of diagnostic techniques, vaccine and effective chemotherapy. Today, the disease can be cured in more than 95% of

cases, when the correct combination of drugs is used (2,5). However, despite the great advances, TB remains depressingly successful as a global epidemic until nowadays.

In 2017, it was estimated that 10 million people (range 9.0–11.1 million) developed TB worldwide, of which 5.8 million were among men, 3.2 million among women and 1 million among children (aged < 15 years old). People living with human immunodeficiency virus (HIV) accounted for 9% of all TB cases. The estimate is that there were 1.3 million TB deaths (range 1.2–1.4 million) in 2017, and an additional 0.3 million deaths resulting from TB diseases among HIV-positive people cases (6).

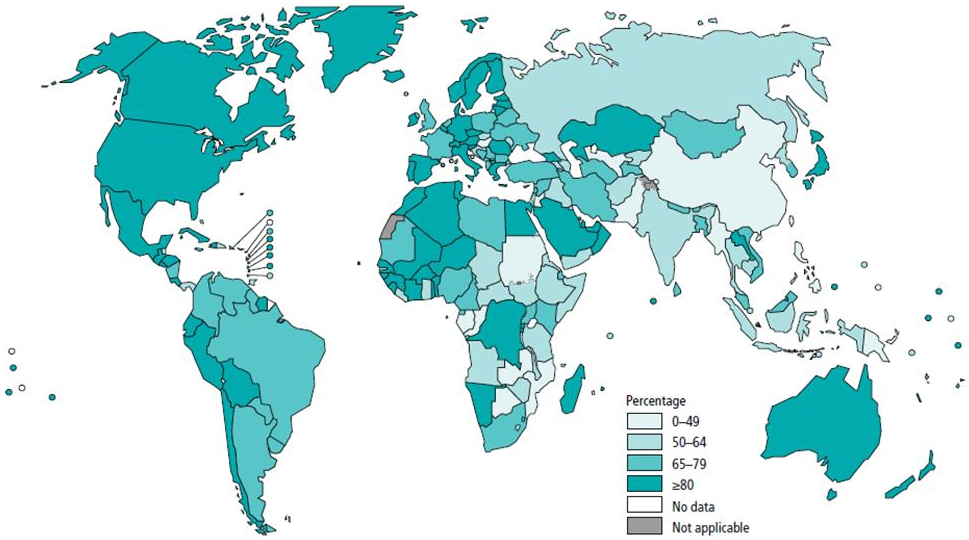

Figure 1.1. Percentage of new and relapse pulmonary TB cases with bacteriological confirmation, 2016 (6)**.**

It has been 25 years since the World Health Organization (WHO) declared TB a public health emergency, and this rallying call has led to significant investment in research over the last two decades (7). Over the time, great advances have been made: TB mortality has fallen 47% since 1990, with nearly all the improvement taking place since 2000 when the Millennium Development Goals were set (8). Despite the remarkable achievements and efforts, and even though nearly all cases can be cured, TB remains one of the world's biggest threats, ranking alongside HIV a leading cause of death from an infectious disease (9).

Global TB control is very challenging, essentially due to the emergence of multidrug-resistant TB and extensively drug-resistant TB, which require longer, more aggressive and expensive treatments. In other words, TB cases are becoming increasingly complex and expensive to treat and, to worsen the situation, the spectre of totally drug-resistant TB is now a reality (10).

The severity of the situation requires careful consideration and efforts to control the disease. In this sense, perhaps one effective way to stop the disease spreading and progression would be to directly interrupt the infectious cycle of TB where it starts, exactly in the lungs.

1.1.1 Pathogenesis of tuberculosis

TB is a contagious infectious disease, predominantly affecting the lungs. The commonest causative agent of TB is *Mycobacterium tuberculosis*, although the disease can be caused by various strains of mycobacteria (4). It is a microscopic, rod-shaped bacterium (0.2-0.6 mm wide and 1-10 mm long), aerobic and non-motile bacillus with a waxy coat that enables retention of the red dye upon treatment with an acidic solution in acid-fast stains (4,11).

There are nearly 60 commonly recognised species of *Mycobacterium*, but most are saprophytic inhabitants of soil (12). Apart from *M. tuberculosis*, other mycobacteria are human pathogens such as *M. africanum* (13), *M. marinum* (14), *M. kansasii* (15), *M. microti* (16), *M. leprae* (17), *M. fortuitum* (18), *M. bovis* (19), *M. scrofulaceum* (20) and members of the *M. avium* complex (21).

The clinical interest in mycobacteria started with Robert Koch (1882), who identified, isolated and cultivated the bacilli *M. tuberculosis* for the first time (2). For clinical purposes, pathogenic mycobacteria are assigned to three main classes: i) *Mycobacterium leprae,* which causes leprosy; ii) *Mycobacterium tuberculosis* complex, which can cause TB and include *M. tuberculosis*, *M. bovis*, *M. africanum,* and *M. microti*; iii) Non-tuberculous mycobacteria or environmental mycobacteria, which are all other strains able to cause lymphadenitis, skin disease or pulmonary diseases resembling TB. These include *M. avium* complex, *M. fortuitum* and *M. kansasii*. The latter can cause both leprosy and TB (4).

As referred before, TB primarily affects the lungs, establishing a condition known as pulmonary TB. However, it can affect any part of the human body (2), in

that case being called extra-pulmonary TB. Nevertheless, only patients with pulmonary TB transmit the infection to new hosts (7). Therefore, transmission of infection within and between species occurs mainly by inhalation. Although *M. tuberculosis* is the most frequent cause of human TB, *M. bovis*, the agent responsible for bovine TB, is also known to infect humans by ingestion of infected milk or meat products, and very rarely by inhalation of animal aerosol micro-droplets when humans have contact with infected animals (22).

The infection with *M. tuberculosis* follows a relatively well-defined sequence of events. Patients with pulmonary TB have tubercle bacilli in their sputum, in a bacterial load that can reach 10 million bacilli/mL (4). When the individual coughs, sneezes or speaks, droplets of saliva containing the pathogen are emitted into the air (12). These droplets can be inhaled by other individuals and the infectious dose is estimated at a single bacterium (23). A cough can generate around 3000 of these droplets, as can talking for 5 minutes, and a single sneeze can produce up to 40000 droplets (24).

In general, the particulate in bioaerosol ranges 0.3 – 100 μm in diameter. However, the infectious aerosols of primary concern are those that are generated as droplets of respirable size (1–10 μm) and have the capability of remaining viable for extended periods in the indoor environment (25,26). The size distribution of infectious aerosols is crucial in the pathogenesis of pulmonary TB. Aerosol particles with an aerodynamic diameter (D_{aer}) over 10 μm will probably be deposited on the upper airways and cleared away by mucociliary action, whereas those in the range of 1–5 μm will most likely penetrate into lower airways (27). The infection is established when aerosol droplets containing few or even single infectious units bypass the bronchial mucociliary structure to reach the alveolar region of the lungs, where bacilli replicate (24).

Once in the alveoli, alveolar macrophages play an important role in the pathogenesis of TB. These cells are involved in phagocytosis and killing of mycobacteria, as well as in the initiation of adaptive T-cell immunity (28). The defence mechanisms of macrophages include the fusion of the phagosomes containing *M. tuberculosis* with lysosomes, originating the so-called phagolysosome, which has the bactericidal capacity (29). Other mycobactericidal mechanisms of macrophages include the lysosomal killing of *M. tuberculosis* mediated by ubiquitin-derived peptides (30) and by the generation of nitric oxide and

other reactive nitrogen intermediates, which have a toxic effect on the bacilli (31). The ubiquitination destroys tubercle bacilli by autophagy as a ubiquitin-derived peptide impairs the integrity of mycobacterial membrane, allowing nitric oxide to act more efficiently (32).

Few microorganisms can survive inside macrophages, due to the abundance of acidic phagocytic vacuoles and hydrolytic enzymes. Despite that, *M. tuberculosis* has evolved mechanisms that potentiate survival and replication inside the host (33). Viable and virulent *M. tuberculosis* displays the capacity of blocking the fusion of phagosomes containing mycobacteria with lysosomes. Furthermore, the mycobacteria appear to have the ability to disrupt the normal functioning of phagosomes, preventing them from developing into acidic hydrolase-rich compartments (34,35). Therefore, antimicrobial activity may require a more aggressive response from the phagocyte, and thus macrophages are equipped with a full range of Toll-like receptors and other pattern-recognition receptors capable of recognising and inducing a preliminary, inflammatory response against a microbial presence (29). Among these pattern-recognition receptors are the complement receptor (the mannose receptor) and scavenger receptors, differing in the pathogen recognition motif. For instance, C-type lectin receptors recognise conserved carbohydrate structures, including mannose and galactose, found on the surface of many respiratory pathogens, as *M. tuberculosis* (36). Additionally, the mannose receptor, like other C-type lectin receptors, is important in the phagocytic and pinocytic uptake of sugar-containing molecules (37). In fact, the mannose receptor is reported as capable of recognising mannose, fucose, *N*-acetylglucosamine units and sulphated sugars (36). Likewise, macrophage scavenger receptors can bind to a wide range of negatively charged macromolecules, including carbohydrates (e.g. fucoidan) (38,39).

All these receptors induce rearrangements in the actin cytoskeleton that lead to the internalisation of the pathogen. Phagocytosis of pathogens by macrophages initiates the innate immune response (40) while inducing the activation of macrophages (32). Activated phagocytes, then, release cytokines that limit the growth of ingested organisms, and recruit additional leukocytes from the peripheral circulation (41).

It should be stressed that the infection with *M. tuberculosis* does not necessarily lead to active disease. In most cases, the individual is asymptomatic

and non-infectious owing to a successful immune response that restrains the pathogen, although not eliminating it (42). In these cases, a condition known as latent TB infection is established (43), which often extends for the lifetime of the individual. In this state, the host does not transmit the infection to others, but reactivation of the latent infection can occur in response to perturbations of the immune response, leading to active TB (23,42).

Briefly, alveolar macrophages trigger an inflammatory response immediately after taking up *M. tuberculosis*. The bacilli that manage to escape the initial intracellular destruction can multiply and cause the apoptosis of macrophage cells (28). The apoptotic cells participate in host defence by inducing the activation of CD4 and CD8 T-cells, which migrate to the site of inflammation, i.e. the lung (32,44). The presence of activated T cells at the infection site attracts other cells of the immune system that are organised in a highly specific way to form the so-called granuloma or tubercle (32,45). The granuloma basically consists of a cluster of infected macrophages surrounded by foamy macrophages, and other defence cells, covered by lymphocytes in association with a fibrous cuff of collagen and extracellular matrix components (23). A schematic representation of the granuloma structure is depicted in Figure 1.2.

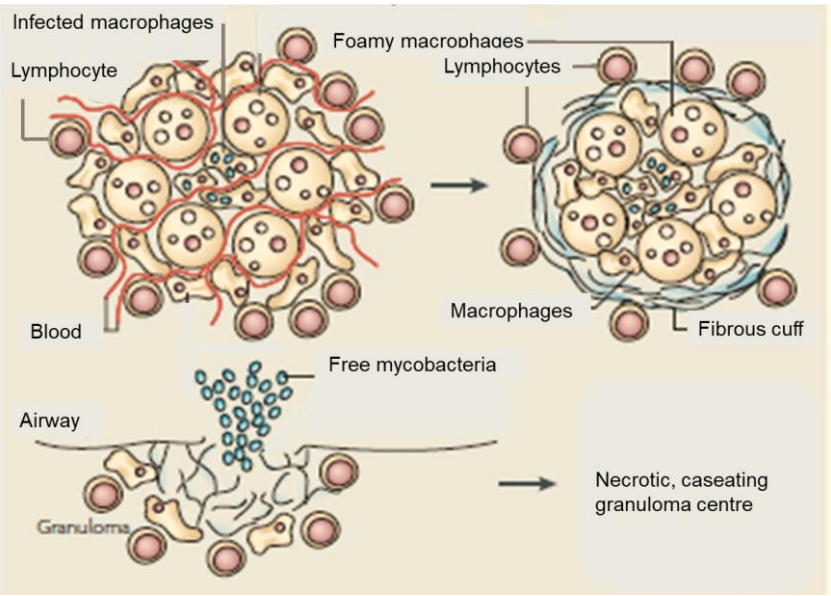

Figure 1.2. Schematic representation of the granuloma structure. Adapted from (23).

In some cases, with granuloma formation, most tubercle bacilli are killed and disease progression is halted (32). In others, the bacilli resist the hostile

environment of the granuloma (e.g. hypoxia, nutrient deficiency, acidic pH) and induce a state of bacteriostasis, allowing them to survive during extended periods of latency (46). In patients with latent TB, reactivation occurs when the granuloma wall shatters and releases thousands of viable/infectious mycobacteria into the host airways, a process known as caseation (23).

The probability of developing active clinical TB (or primary infection) after being infected with *M. tuberculosis* is small. Less than 10% of infected individuals develop symptoms and signs of active disease over a lifetime. However, containment usually fails when the person is immunocompromised (primary TB cases) or when the immune status of the host changes (reactivation of latent TB), which is usually a consequence of ageing, malnutrition, treatment with corticosteroids, alcohol or drug abuse, co-infection with HIV or basically any condition that reduces the number or impairs the function of CD4 T cells, mainly (23,42). Not surprisingly, infection with HIV is the most potent of these risk factors, with the risk of people infected with HIV developing TB being more than 20-times greater than that of people not infected with HIV (47).

1.1.2 Diagnosis and treatment of tuberculosis

The definitive test for TB disease is the detection of *M. tuberculosis* bacilli in clinical specimens from symptomatic patients. Therefore, sputum microscopy and culture, with subsequent drug-susceptibility testing are currently recommended as standard methods to diagnose pulmonary TB (48).

Although much work has been done to develop modern diagnostic tools (e.g. nucleic acid amplification tests), direct sputum smear microscopy remains necessary and it is recommended to evaluate the response of the disease to treatment (49). Overall, detection of TB relies heavily on direct smear microscopy, solid culture and chest radiography, tools that often perform poorly, and require infrastructure frequently unavailable in the periphery of the health system where patients first seek care (50). Moreover, multiple investigations may be necessary over a period of weeks or months before a diagnosis is made. Delay in diagnosis is crucial to both disease prognosis at the individual level and transmission within the community. Most transmissions occur between the onset of a cough and initiation

of treatment. Therefore, early diagnosis and immediate initiation of treatment are essential for an effective TB control program (51,52).

Currently, the recommended treatment for new cases of drug-susceptible TB is a 6-month regimen of four first-line drugs: isoniazid (INH), rifampicin, pyrazinamide, and ethambutol. It involves an initial phase of a four-drug regimen for the first 2 months followed by a continuation phase of two drugs: INH and rifampicin for the next 4 months. Up to 95% of people with drug-susceptible TB reach the cure with this four-drug regimen (53). In cases in which rifampicin resistance is suspected, other rifamycin derivatives, such as rifapentine and rifabutin (RFB) may be used (54). Moreover, RFB is the first-line anti-TB drug recommended for patients who are taking medications incompatible with rifampicin, such as antiretroviral drugs (55).

In summary, TB is a curable disease as long as a rapid diagnosis is performed, and a proper antibiotic therapy is established and followed. Although advances have been made in TB therapy, standard TB regimens are limited and cause severe side effects that include ototoxicity, hepatotoxicity and nephrotoxicity and hyperuricemia, especially in the treatment of drug-resistant TB (56,57). For this reason, new TB drugs have started to emerge from the pipeline, and combination regimens that include new compounds are being tested in clinical trials. However, the evolution of resistance will inevitably follow the introduction of new drugs, making it unlikely that existing agents are removed from clinical use.

The situation has, thus, come to a point where the development of novel therapeutic strategies is urgently needed. In this regard, the advent of drug delivery systems may hold the key to the prevention and treatment of TB disease. The delivery of anti-TB drugs directly to the site of infection would potentially enable the reduction of dosing frequency, possibly shortening treatment duration, thereby avoiding or reducing systemic side effects and improving patient compliance (12).

1.2 Pulmonary drug delivery

Site-specific delivery of drugs permits delivering drugs to a patient in a very specific manner that allows concentrating the drugs in the site of interest while reducing their concentration in the remaining tissues (58). This not only improves the inherent efficacy of drugs, but also potentially reduces side effects. The selective

delivery of drugs is, therefore, very attractive and a real need, as it provides one of the most potent ways to improve the therapeutic effect of drugs.

Since it is very difficult for drug molecules to reach with high efficiency the intended destination in the complex cellular network of an organism, the assistance of a drug carrier may strongly benefit the process. Drug delivery systems offer an intelligent approach for carrying and protecting drugs, while in many cases providing simultaneous modulation of their release and absorption. However, their success is frequently limited by short residence times at the site of absorption or action. For this reason, it is deemed advantageous to potentiate the intimate contact of drug delivery systems with the referred sites.

In light of this, particulate carriers are one of the most used classes of drug delivery systems. They offer many advantages that include the possibility of tailoring particle sizes and surface characteristics, improvement of drug pharmacokinetics and pharmacodynamics, and the possibility for delivery through various routes of administration, including the respiratory route (59,60). As it is well demonstrated in Figure 1.3, the pulmonary delivery of drugs has been increasingly studied over the last two decades, given the advantages over traditional routes.

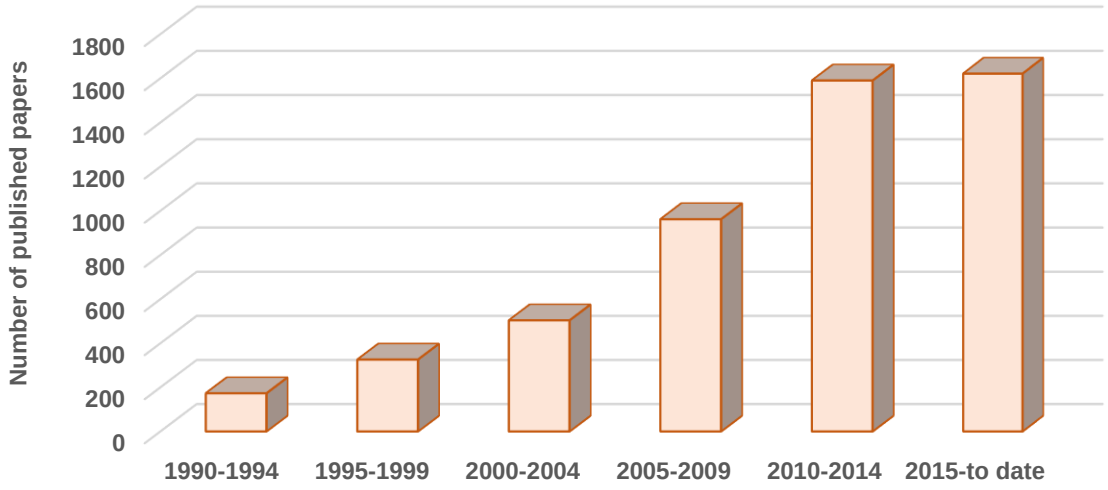

Figure 1.3. Number of scientific papers published on the topic "pulmonary drug delivery" on ISI Web of Science (October/2018), as a function of publication years.

In general, the main reasons why the lung is an attractive route for drug delivery are non-invasiveness, the possibility of direct delivery to the site of action when treating pulmonary diseases, avoidance of the first-pass metabolism, and the

availability of a large surface area for systemic delivery of drugs, along with highly vascularised epithelium (61). Besides, drug efflux transporters and metabolising enzymes are present in the lung at much lower levels comparing with the gastrointestinal tract, which is the most common route of delivery (62). Table 1.1 summarises the most relevant advantages and limitations of drug delivery by inhalation.

Table 1.1. The most relevant advantages and limitations of pulmonary drug delivery.

Advantages	Limitations
Non-invasive route	Respiratory tract is structurally complex
Avoidance of the first-pass metabolism and limitation of side effects	Lung defence mechanisms
Extensive vascularisation	Specific aerodynamic requirements needed to reach each zone of respiratory tree
Possibility of administering lower drug doses	Inhalation devices and special dosage form are required for drug delivery

Despite marked advantages of pulmonary administration, delivery of free drugs is not easy and their efficiency has been potentiated by means of the use of drug carriers, which need to be specifically designed to meet aerodynamic requirements (63). Nevertheless, lung drug delivery is not only affected by characteristics of the inhalable formulation, further having great contribution from biophysical and physiological factors, e.g. aerosol particle size and breathing manoeuvre (inspired volume, inspiratory flow, and end-inspiratory breath holding time). Importantly, the physical and biochemical stability of pharmaceutical formulations designed for aerosolisation (dry powder, suspensions or solutions) are preconditions for the administration of adequate and reproducible drug doses via the pulmonary route (64). In parallel, inhalation devices are required to be designed to overcome all the obstacles and potentiate the performance of formulations.

1.2.1 Challenges for pulmonary delivery

The lung presents several defence mechanisms that comprise relevant limitations to drug delivery, including cough, mucociliary apparatus and airway anatomic barriers. Understanding the complex architecture of the respiratory tract is important because it is a biophysical factor affecting the deposition of particulate drug delivery systems in the airways (64). As depicted in Figure 1.4, there are several mechanisms involved in aerosol transport and deposition in the human lung, including inertial impaction, gravitational sedimentation and Brownian diffusion, which are the most prevalent (65). Inertial impaction refers to the inability of particles (larger than 5 µm) to adjust its course according to the sudden change in air flow direction at airway bifurcations (65,66). Gravitational sedimentation is the settling of particles under the action of gravity and occurs mainly in small airways and alveolar region. Deposition by Brownian diffusion results from the random motion of particles of size lower than 0.5 µm, as a consequence of their collisions with gas molecules. It increases with decreasing particle size and is the dominant mechanism of deposition for particles in this size range (65,67).

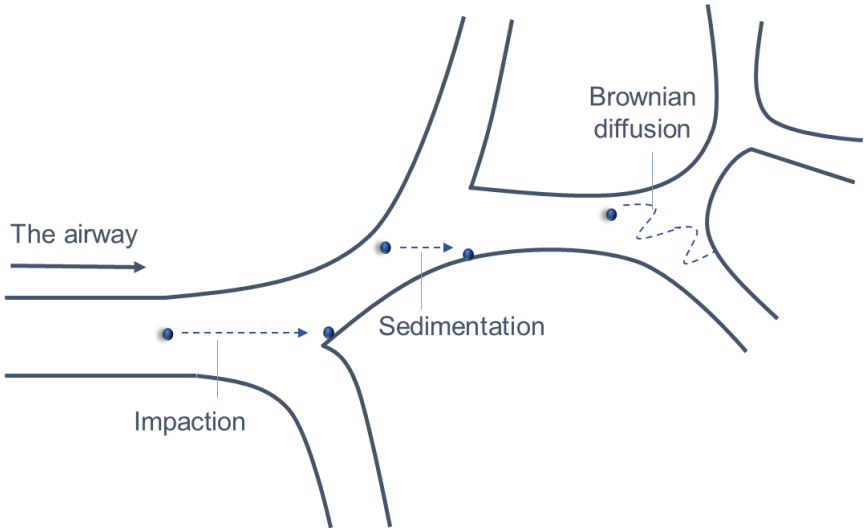

Figure 1.4. Scheme describing the main mechanisms affecting aerosol transport and deposition in the human lung. Adapted from (68).

As a consequence of the physical forces acting on aerosol particles, their deposition in the lungs is highly dependent on diameter (66). The size of particles aimed at inhalation is conventionally defined as the Daer, which is the diameter of

a spherical particle with unit density that has the same settling velocity as the particle in consideration (69). Some equations have been proposed to be used in the theoretical calculation of Daer of aerosol particles. One of the most used is displayed below (70,71):

$$D_{aer} = d\left(\frac{\rho}{\lambda\,\rho_0}\right)^{1/2}$$

where **d** is the particle geometric diameter, **ρ** is the particle density, ρ_0 = 1 g/cm^3 and **λ** is the dynamic shape factor of the particle, which is 1 in the case of spherical particles (72). Nevertheless, accurate determination of Daer is only possible experimentally, which is routinely performed using techniques based on inertial impaction (e.g. cascade impactors, twin-stage impinger, etc.) as indicated in the European Pharmacopeia (73). Although several terminologies are used to characterise this parameter, the mass median aerodynamic diameter (MMAD) is that commonly used after characterisation by cascade impaction. MMAD represents the median of the distribution of airborne particle mass with respect to the aerodynamic diameter. This is usually accompanied by the geometric standard deviation, which characterises the variability of the particle size distribution, referring to mono- or polydisperse aerosols (66,74). Additionally, the fine particle fraction (FPF) is defined as the percentage relative to the total quantity of drug collected in the impactor that has the size equal or lower than 5 µm (75).

In other words, aerosols with larger MMADs will deposit higher in the respiratory tract and a polydisperse aerosol is also more likely to show greater deposition in the tracheobronchial region than a monodisperse aerosol of the same MMAD (66). The MMAD of aerosols is, therefore, critical factors in determining the deposition patterns within the lung, although other conditions will also affect this behaviour, as detailed above. Figure 1.5 represents the relationship between Daer and deposition of aerosol particles in the human respiratory tract.

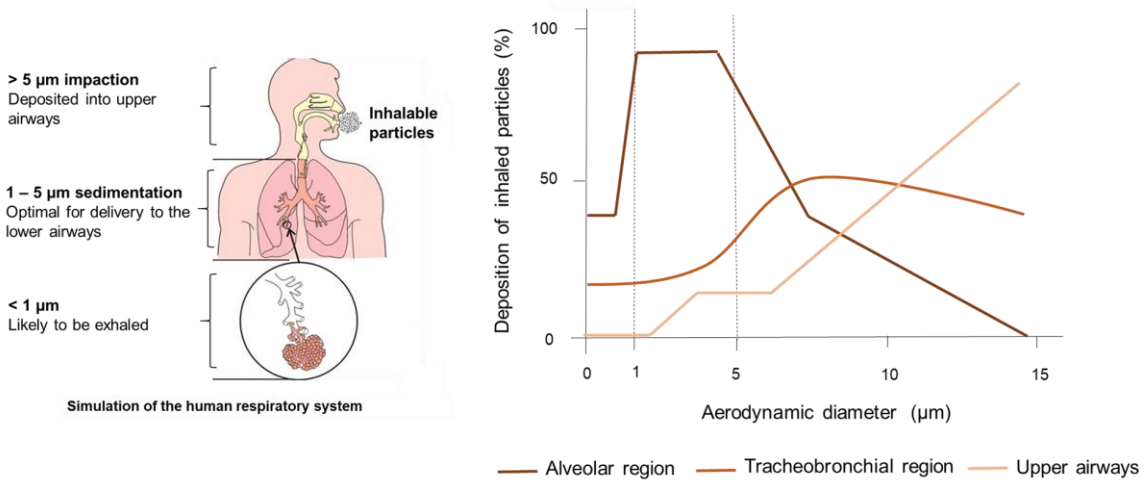

Figure 1.5. Relationship between aerodynamic diameter and deposition of aerosol particles in the human respiratory tract. Adapted from (27,76).

In brief, particles greater than 5 µm in diameter will mostly impact in the upper airways and are rapidly removed by coughing and mucociliary processes. In turn, smaller particles in the size range of 1–5 µm may escape impaction in the upper airways and will deposit in the lower tracheobronchial and alveolar regions. On the other hand, particles <1 µm may not be deposited at all, since many will be removed from the lung on the exhaled air stream before sedimentation can occur (66,77). Therefore, to reach the lower respiratory tract, particularly the alveoli, and optimise pulmonary drug deposition, aerosols should have aerodynamic diameters <5 µm. (65,78).

1.3 Nano and microparticles as drug delivery systems for inhalation purposes

Nanoparticles (NP) and microparticles (MP) are the most cited of the particulate carriers, in most cases presenting a matrix composed of polymeric materials. The International Organization for Standardization (ISO) defines nanoparticles as particles having at least one dimension below 100 nm (79). The definition is, however, not consensual in the area of drug delivery and the term is frequently used for spherical particles with submicron size (<1000 nm) (80,81). Microparticles present diameters in the micrometre range (from 1 µm to 1000 µm). Structurally, these systems are typically divided into two categories, according to a classification that is now widely accepted: nanocapsules/microcapsules, when the

drug is mainly confined to a cavity surrounded by a polymer membrane (shell); and nanospheres/microspheres when the drug is dispersed within the polymeric matrix (82). The drug release mechanism from carriers primarily involves drug diffusion through the carrier material. Additional mechanisms depend on the considered drug carrier. For instance, the drug may be released through pores present in the carrier or by water penetration into the systems or by hydrolysis/erosion of polymeric matrix (83).

In general, carrier systems aim to minimise drug degradation and loss, enhance the solubility of poorly soluble drugs, prevent adverse effects (targeted therapy) and increase the availability of the drug at the target site. To reach these goals, carriers can be designed to slowly degrade, react to stimuli or to be site-specific. Targeted therapy generally requires lower total doses to achieve clinically effective results, comparing with conventional approaches (62). In this context, the use of polymeric systems offers potential advantages over free drug formulations or even other carriers (such as liposomes), considering their higher stability and the possibility to modulate the systems for targeted delivery (84). For instance, inhalable PLGA particles containing rapamycin were more effective in clearing intracellular mycobacteria and presented lower cytotoxicity compared to the free drug (85). Nonetheless, the development of polymeric drug carriers presents some limitations, including lower reproducibility compared to conventional formulations, higher cost of materials and processing, and even the environmental impact of degradation products (86).

There are many methods available to prepare nano and microparticles and it is not uncommon that the same method can be used to prepare both types of particles. Obtaining one system or the other naturally depends on specific conditions of the process, such as the used concentrations, intensity of stirring, etc. (87). Methods such as polyelectrolyte complexation, ionic gelation, solvent evaporation, coacervation, supercritical fluids technology and spray-drying, have been frequently reported (88,89). Polyelectrolyte complexation is a widely used technique to obtain polymeric carrier systems, because it generally offers simple and mild preparation processes that do not involve harsh conditions. The absence of additives results in low toxicity and low cost. This technique is based on electrostatic interactions between oppositely charged polymers, which allow spontaneous formation of complexes (90,91). Another method commonly used is coacervation, that also

occurs spontaneously upon desolvation of a homogeneous polymeric solution. The method is based on liquid-liquid phase separation which is promoted by the addition of a non-solvent (e.g. ethanol) or a salt into the polymeric solution. The non-solvent/salt reduces the solvation of the polymer, leading to the formation of coacervates which can be nano- or micron sized particles (92,93). Concerning the production of microparticles, spray-drying is one of the most reported techniques, as it provides several advantages over other methods. First, it offers great control over critical parameters of resulting microparticles, including their size, shape and density. It also allows the incorporation of different excipients into the formulation to be spray-dried, including dispersibility enhancers to improve the aerosolisation characteristics of the resultant powder (94). Furthermore, it is a unique single step method for microencapsulation of drugs in polymeric carriers (95). Briefly, the polymer is first dissolved in a suitable solvent and the drug is then dispersed/solubilised in the polymer solution under homogenisation. This dispersion is then atomised in a stream of hot air, leading to the formation of small droplets. This happens in a drying chamber where temperature is set to enable instantaneous solvent evaporation, leading to the formation of microparticles. In the end, these are separated from the hot air by means of a cyclone separator (86). This method is highly reproducible, relatively easy to scale up, and offers a narrow particle size distribution (95). Conventional spray-dryers permit producing microparticles in a size ranging from 1 to several μm, but more recent equipments are also reported to produce particles at the nanoscale (96).

Particle size distribution is an important feature to be considered in drug delivery, because it may determine the *in vivo* distribution of nano and microparticles (97). In general, microparticles are unlikely to cross most biological barriers, so they are often delivered directly to the site of interest. On the contrary, nanoparticles of adequate size may cross such barriers. In this regard, the smaller the particle size, the better is the absorption through epithelia (98). Nevertheless, the effectiveness of drug delivery systems, in some cases, depends on the internalisation of the systems. Generally, particles enter cells by a process termed endocytosis, which comprises phagocytosis and pinocytosis. Phagocytosis is a means of taking up material up to 10 μm in diameter and this process is limited to a certain type of cells, such as macrophages, neutrophils and dendritic cells. Differently, pinocytosis is a process characteristic of all cell types in which liquid and small non-specific particles

are ingested, including nanosized materials in solution (99). Taking into account the above considerations, both nano and microparticles have potential to be internalised by living cells with variable efficiency depending on their size. Some researchers have taken advantage of this difference, for instance, to provide targeting to phagocytes, such as macrophages (100,101). Additionally, other characteristics like surface charge, lipophilicity, etc. are also described to affect internalisation of particulates by cells, namely macrophages (102,103).

As stated, phagocytosis is a process highly dependent on particle size, as reported in several studies addressing the subject. These have revealed that particles possessing diameters between 1–6 μm were the most susceptible to phagocytosis (37,104). In this context, pulmonary drug delivery systems have been designed to target alveolar macrophages, the predominant phagocytic cells involved in lung defence (105). Targeting alveolar macrophages has the distinct advantage of delivering high concentrations of drugs to a cell that plays a central role in immune responses and progression of certain diseases, as is the case of TB (62). As a matter of fact, the literature describes several works devoted to the delivery of anti-TB drugs, upon inhalation, mediated by nano (106–108) and microparticles (109–111). The advantage of using nanoparticles for pulmonary delivery resides on the fact that they are sufficiently small to avoid inertial deposition in the upper airways, penetrating into the lung. However, in the ambit of macrophage-targeted therapy, nanoparticles may find difficulties in cell internalisation, given the apparent preference of macrophages for microparticles. For instance, the uptake of titanium dioxide nanoparticles (20 nm) by rat alveolar macrophages upon aerosol inhalation was described as unspecific and inefficient. Within 24 h after particle deposition, there was only about 0.1% of the deposited nanoparticles taken up by macrophages (112). This is coincident with reports of avoidance of macrophage clearance by nanoparticles of sizes < 100 nm (37,113). Once deposited, nanosized particles smaller than 100 nm can readily translocate across epithelia of respiratory tract (113). Yet, the deposition of nanoparticles in the deep lung can be also a limitation, as these are reported to be exhaled due to their small size and mass (114). To overcome this limitation, many works have been proposing the microencapsulation of drug-loaded nanoparticles (115–117). The approach endows nanoparticles with the adequate aerodynamic properties to reach the respiratory region. This has been typically provided by spray-drying of nanoparticles, although other methods may

also apply (118). Moreover, the microencapsulation of nanoparticles can improve the internalisation of the nanosized systems by alveolar macrophages (116), considering that nanoparticles of small size can evade phagocytosis by virtue of their small size (119,120). Additionally, this approach can improve nanoparticles aerosolisation from inhaler devices, given that they often aggregate under shear forces (62).

In summary, the design of inhalable nano and microparticles is a major contribution to enhancing drug availability and therapeutic effectiveness in the respiratory zone (114). Particularly, this approach appears to be a feasible strategy for the treatment of TB, as inhalable systems could overcome some of the problems that were mentioned for conventional TB therapy and enhance the therapeutic efficacy of anti-TB drugs. Yet, carrier systems targeted to alveolar macrophages can also improve bactericidal activity on intracellular pathogens, which is especially valuable to fight multi-drug resistant strains (121). Therefore, inhalable drug carriers are considered a promising approach in the treatment of respiratory infections, such as pulmonary TB.

1.4 Biopolymers for designing drug delivery systems

Drug delivery systems can be manufactured from a large variety of raw materials, either natural or synthetic, and by many different preparation techniques, as already referred. Both the raw materials and the producing techniques allow the preparation of an enormous variety of carriers, regarding composition, morphology, surface chemistry, and size distribution (122). From the wide diversity of materials that are available, polymers have been extensively investigated to compose the matrix of drug delivery systems (123).

Polymers remain the most versatile class of materials because they can be synthesised (or modified) to have appropriate chemical, physical, interfacial and biomimetic characteristics, which permit various specific applications. Compared with other types of materials, such as metals and ceramics, polymers offer the advantage of enabling different compositions with a wide variety of structures and physicochemical properties (124). In general, polymers used as matrix of drug delivery systems can be naturally occurring, synthetic or a combination of both (125). For instance, polyester alone or in combination with other polymers has been

widely investigated for designing drug carriers (126). Poly(lactic acid) (PLA), poly(glycolic acid) (PGA) and the copolymer poly(lactic-co-glycolic acid) (PLGA) are among the most well-known choices for drug delivery applications, including in TB therapy (127–130). Although PLGA represents the 'gold standard' of synthetic biodegradable polymers (exemplified by more than 500 patents), increased local acidity due to degradation can lead to irritation at the application site (131). Indeed, the primary difficulty of most synthetic materials is the general lack of biocompatibility.

In this regard, polysaccharides present favourable characteristics in comparison with synthetic polymers used in drug delivery. These include the higher propensity for biocompatibility and biodegradability, and abundant renewable sources (132). On the other hand, natural polymers often render extraction and purification difficulties due to their structural complexity. Additionally, significant batch-to-batch variations may occur because of their 'biopreparation' in living organisms, e.g. plants, crustaceans (124).

Anyway, polysaccharides and their derivatives are commonly used for the preparation of both nano and microparticles (133–136). Polysaccharides are long carbohydrate polymers composed of repeated monosaccharide units joined together by glycosidic bonds. These molecules are usually considered biocompatible and biodegradable in a general manner, but these characteristics must be contextualized with the used carrier, the dosage and the route of administration (137). Because of the presence of various functional groups on their molecular chains, polysaccharides can be chemically modified for specific purposes, such as tissue and cell targeting (138). Yet, most polysaccharides have hydrophilic groups, including hydroxyl, carboxyl and amino groups, which may affect the polymer charges and also interact with functional molecules, as well as with cell receptors (132).

Taking into account the promising applications of polysaccharides in drug delivery, research in the field of polysaccharides of marine origin has considerably increased in the last decades (139). As well, the discovery of metabolites from marine resources showing biological activity has increased significantly. Among marine resources, seaweeds and crustaceans are valuable sources of structurally diverse bioactive compounds. These include sulphated polysaccharides, such as fucoidan (FUC), abundantly found in the cell wall of algae; and chitosan (CS), a

polysaccharide derived from the exoskeleton of marine crustaceans (140). It should be stressed that FUC and CS are the selected biomaterials for composing the matrix of the delivery systems developed in the present work. The literature reports numerous studies on the development of nanosized drug delivery carriers based on FUC (80,141–147) and also works that use the polysaccharide in the composition of micron sized carriers (148–150). Likewise, CS has been widely proposed as biomaterial to compose nano (151–156) and microcarriers (157–160).

The following sections detail the most relevant characteristics of each of the polymers.

1.4.1 Fucoidan

FUC is the major sulphated polysaccharide found in marine brown algae. In this regard, the candidate has authored a review addressing the use of sulphated seaweed polysaccharides as multifunctional materials in drug delivery applications (161). FUC designates a family of sulphated polysaccharides extracted from brown seaweeds (Phaeophycophyta) and some echinoderms (sea urchin and sea cucumber). The term fucoidan is commonly applied to complex sulphated polysaccharides, often isolated from marine algae, mainly containing fucose residues, but also many other monosaccharides. In turn, the term sulphated fucan is reserved for polysaccharides with a regular structure, mostly containing sulphated fucose, which is often extracted from marine invertebrates such as sea cucumber and sea urchin. However, not all authors consider these denominations and, therefore, the polymer is usually indistinctly termed fucoidan or fucan, while other terms like fucosan may also be referred (162,163).

Origin and chemical structure

Brown algae (Phaeophyta), the second most abundant group of algae, produce a range of active components. The structure of their cell walls consists of an amorphous matrix of acid polysaccharides, linked to each other by proteins. These acid polysaccharides are mainly composed of FUC and alginic acid, which confer structural toughness and flexibility to seaweed (164). In recent years, these fucose-containing polysaccharides have been isolated from different sources,

including the main genera *Fucus* (165), *Laminaria* (166), *Sargassum* (167), *Ascophyllum* (168), and *Undaria* (169). Before choosing the source, it is important to consider that FUC can differ in structure among algal species and may even vary within the same species (170). It is also known that the use of different extraction methods may affect the bioactivity and physicochemical properties of the biopolymer (171).

Although FUC has been known for over a century, its chemical structure is still incompletely determined, owing to its heterogeneity and irregularity. This is due to the fact that marine brown algae synthesise highly branched polysaccharides, which structures and proportion vary in dependence of the specific taxonomic position. For instance, it has been shown that FUC obtained from representatives of Chordariales and Laminariales may display different backbone structure compared with that isolated from algae belonging to the order Fucales (163,172,173). The main sugar backbone of the polysaccharide is fucose, consisting essentially of α-L-fucose units. These units are sulphated in some positions, having species-related sulphation pattern (174,175). Apart from fucose and sulphate, FUC may also contain additional sugar constituents, including mannose, galactose, glucose, xylose, uronic acids and yet acetyl groups (167,176–178). Although it is not a pattern, a certain similarity in the backbone structure of different FUC molecules has been observed, regarding the positions of inter-glycosidic linkages. In this context, many studies show that several representatives of the orders Chordariales and Laminariales contain FUC with a linear backbone composed of (1→3)-linked α-L-fucose residues. However, the polysaccharide isolated from algae belonging to the order Fucales mostly displays a backbone composed of alternating (1→3)- and (1→4)-linked α-L-fucose residues (175,178–180). Representative backbone structures of fucoidan molecules are depicted in Figure 1.6.

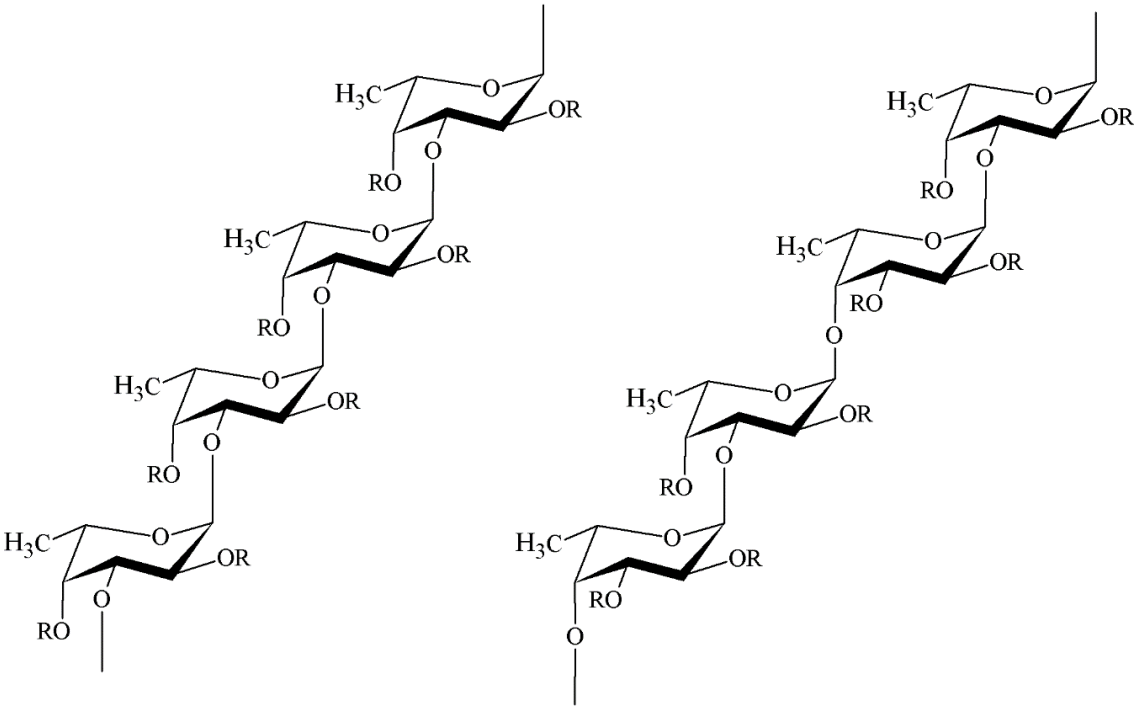

Figure 1.6. Scheme of α-L-fucose chains observed in fucoidans isolated from several algae belonging to the taxonomic orders Chordariales and Laminariales (a) and Fucales (b); (a) The chain is only composed of repeating (1→3)-linked α-L-fucose residues; (b) The chain consists of alternating (1→3)- and (1→4)-linked α-L-fucose residues. R represents the positions of potential attachment of carbohydrate.

In general, FUC polysaccharides may be branched, presenting a variety of substituting groups and side chain compositions, as aforementioned. The reported structural data for FUC isolated from different brown seaweed species clearly indicates that there is no consistent basic structure of this polymer. The investment observed in recent years in research dedicated to obtaining highly purified fractions of the polysaccharide is expected to permit a better understanding of FUC structures (166,181,182).

Physicochemical properties and biological activity

The physicochemical and biological properties of algal polysaccharides, including FUC, are strongly correlated to their chemical composition (183). In seaweeds, this is the result of many factors such as harvesting region, season and the specific algal species (184). For instance, the natural sulphation grade of FUC

may range between 4% and 8%, depending on the site and season of collection of the algae (185).

In general, FUC molecular weight may vary from 10 (186) to approximately 2000 kDa (187). It is very soluble in water, producing non-viscous solutions, and its solubility is related to the level of branching, depending on the content of sulphate groups (188). Moreover, there is little evidence about gelling and film-forming properties of FUC (189). In fact, gelation of FUC was not observed up to 25% concentration (190).

The functional properties of FUC have rendered the polymer potential applications in pharmaceutical and biomedical-related fields (164,191). The biopolymer and its oligosaccharides have been extensively studied regarding the evidence of diverse biological activities. These include antitumor effect (192), anti-inflammatory (193) and antiviral activities. For instance, it has been shown that FUC has an antiviral effect against herpes simplex virus type 1, and human cytomegalovirus (194). As well, the anti-metastasis and immunomodulatory effect of the polymer have been demonstrated (195,196). From all the reported biological activities, the potent anticoagulant property of FUC is by far the most widely investigated (197–199). Based on the reports, the referred physicochemical and biological properties are related to molecular size, type of sugar content, sulphation degree and molecular structure of the biopolymer.

Lung biodegradability

The pharmacokinetics of FUC is an important consideration to be taken for the purpose of the present work, particularly within the context of pulmonary administration.

Although FUC has been indicated in the literature as a biomaterial for biomedical applications, studies regarding the *in vivo* distribution, degradation and elimination of the polymer are scarce (187). Importantly, to date, there are no reports regarding the metabolisation of FUC in the lung environment. It is well known that FUC can be enzymatically degraded (200,201). In this context, lung tissue is recognised as a source of endogenous β-galactosidase, an enzyme able to degrade FUC in marine invertebrates (200). In humans, the activity of β-galactosidase has been demonstrated in airway epithelial cells and in alveolar macrophages (202).

Nevertheless, to the best of our knowledge, there is no data about FUC degradation by the referred enzyme, except in marine microorganisms and invertebrates (200). In addition, fucose-containing macromolecules can be degraded by α-L-fucosidase, a lysosomal enzyme widely present in human cells, blood and body fluid (203). Notwithstanding this fact, no data has been reported yet on the enzymatic activity of human α-L-fucosidase regarding FUC degradation. In summary, the metabolism of the polysaccharide has been poorly studied in mammals, especially in humans (204), but there are indications that lung biodegradation may be possible.

1.4.2 Chitosan

CS is a polysaccharide derived from the deacetylation of the naturally occurring polymer chitin. Chitin, in turn, is a biopolymer synthesised by an enormous number of living organisms. It occurs in nature as ordered crystalline microfibrils comprising the principal structural component in the exoskeleton of arthropods (e.g. crustaceans) or in the cell walls of fungi and yeast (e.g. *Aspergillus* and *Mucor*). It is the second most abundant polysaccharide after cellulose (205,206).

Origin and chemical structure

CS is synthesised by (partial) deacetylation of chitin. Despite the widespread occurrence of chitin, up to now the main commercial sources of chitin have been crab and shrimp shells (206). The resulting chitin needs to be graded in terms of purity since residual substances can cause problems for further utilisation (206). In this respect, the complete removal of protein is especially important for biomedical applications, as a percentage of the human population is allergic to shellfish, the primary culprit being the protein component (207).

Chitin can be converted to CS by enzymatic means (208,209) or chemical processes, the latter using either acids or alkalis. Because glycosidic bonds are very susceptible to acid, alkaline deacetylation is used more frequently (210). Usually, deacetylation of chitin is achieved by treatment with concentrated sodium hydroxide solution (40-50%) at 100°C or higher temperature (211). Although many experimental conditions can be found in the literature for chitin isolation and

subsequent CS production, effects on molecular weight and acetylation degree cannot be avoided (207).

Structurally, CS is a copolymer composed of glucosamine and *N*-acetylglucosamine. Its chemical structure thus consists of repeating alternated units of *N*-acetylglucosamine and D-glucosamine, linked by β-(1→4) glycosidic bonds, as depicted in Figure 1.7. The polysaccharide is available in a variety of forms that mainly differ in the molecular weight and degree of deacetylation (212).

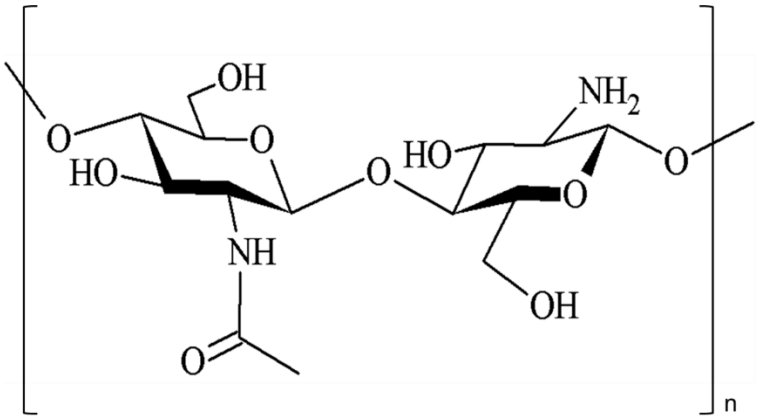

Figure 1.7. Structure of chitosan showing alternated units of *N*-acetylglucosamine and D-glucosamine, linked by β-(1→4) glycosidic bonds.

Commercially, the biopolymer is available as chitosan base (low and high molecular weight) and as chitosan salts (213,214), which provides versatility for different applications of CS and its derivatives (215).

Physicochemical properties and biological activity

The physicochemical properties of CS are generally determined by its chemical structure, mainly molecular weight and deacetylation degree. The biopolymer has functional hydroxyl and amino groups which may vary in sequence and quantity (216).

In general, the biopolymer is insoluble in water, but it is readily soluble in dilute acidic solutions below pH 6, as it possesses primary amino groups with p*K*a of 6.5. The protonation of the amino groups along the polymeric chain allows CS to dissolve in aqueous acidic solutions (212,217). Yet, solubility properties seem to depend on the distribution of acetyl groups (218). In the same way, the viscosity is

influenced by CS deacetylation degree pattern as well as pH and strength of the solvent. Additionally, other parameters affect the intrinsic viscosity, including temperature, shear rate, concentration and molecular weight of the polymer (219,220). The latter varies from approximately 10000 to 1 million Dalton and it also presents variable degrees of deacetylation, depending on the method of preparation (207,221,222). In addition to CS preparation, its origin (i.e. crustacean species) may also result in different distribution of functional groups, thus influencing other physicochemical properties, such as solubility and viscosity (207,223).

Physicochemical properties of CS are of utmost importance in developing drug formulations (205). For instance, the degree of deacetylation and the degree of polymerisation, which in turn decide the molecular weight of the biopolymer, are two major characteristics dictating the use of CS for various applications (222). The interest in using CS, particularly in pharmaceutical and biotechnological fields, is also related with the flexibility of its molecular structure that allows chemical modifications. Chemical modification can improve original physicochemical properties (e.g solubility) and provide desired and distinctive biological functions, as receptor-mediated gene delivery (224), cell penetration enhancement (225) or site-specific delivery (226), to cite a few examples.

Moreover, CS has been shown to possess mucoadhesive properties, a feature that has been widely exploited in drug delivery, as mucoadhesion can prolong retention in the site of action or increase absorption (227). Yet, different bioactivities have been attributed to CS, such as antitumor (228,229), antimicrobial (229), anti-inflammatory (228), antioxidant (229), and hypocholesterolemic effect (230,231). The cationic character of CS, by virtue of the primary amino groups, seem to be pivotal to determine its biological activities and to confer many of its applications in several fields (232,233).

Lung biodegradability

The biodegradability of CS is far more explored than that of FUC. CS can be degraded *in vivo* by several proteases, mainly by lysozyme, in a process that depends on the deacetylation degree, the distribution of acetyl groups, and the molecular weight of the polymer (234,235). Still, very few studies on *in vivo* degradation of CS have been reported thus far (236,237), especially addressing

pulmonary administration. It is well known that lysozyme is highly expressed in submucosal glands of the human airway. Yet, surface airway epithelial cells appear to also express lysozyme at lower levels (238). Therefore, it can be reasonably assumed that CS could be enzymatically degraded in the lungs. However, further studies are required to confirm this assumption.

Chapter Two

Motivation and Objectives

This page was intentionally left in blank

2. Motivation and objectives

TB is a major cause of mortality worldwide, even though a vaccine and several effective antibiotics are available for its prevention and treatment. Particularly, pulmonary TB represents approximately 80% of total cases and therefore the lung has been explored as an effective route for the delivery of drugs in the ambit of TB therapy (239). Pulmonary delivery of anti-TB drugs is considered a promising approach because it allows targeting the infected organ instantly, thus possibly decreasing severe systemic side effects, such as hepatotoxicity and nephrotoxicity, which are main reasons for patient non-compliance. However, several limitations of pulmonary delivery must be considered as well, mainly related with airway structure and specific defense mechanisms, such as the mucociliary clearance (240). Overcoming these limitations demands the design of aerodynamically suitable carriers that can potentially reach the alveoli, where infected alveolar macrophages reside (host cells of *Mycobacterium*). Additionally, drug delivery systems may target and stimulate cells by surface ligands, an effect that can be mediated by the composition of the carriers, favouring recognition and phagocytosis by alveolar macrophage, for instance.

For an active targeting approach, carriers must either have a matrix composed of materials that act as targeting moieties themselves or incorporate surface ligands with selective affinity for specific receptors. For instance, polysaccharides of marine origin, such as FUC and CS, have been shown to intensify macrophage activation, mediated by membrane receptors (241). In fact, the use of both FUC (242,243) and CS (107,244) has been proposed for targeted therapy, particularly toward macrophage cells. Apparently, the two polysaccharides are endowed with specific features that enable macrophage targeting. As previously mentioned, these phagocytic cells express a variety of surface receptors capable of recognising, mannose, fucose, *N*-acetylglucosamine units and sulphated sugars (40,245), moieties that compose the chemical structure of the referred polymers. Considering all the above, FUC and CS may be of potential use in facilitating the internalisation of anti-TB delivery systems and possibly stimulating macrophage activation.

Due to its chemical structure, FUC has been finding some applications in the design of polymeric nano and microparticles, which are of the most used of drug

carriers. In the ambit of drug delivery, the almost totality of FUC-based carriers relies on the so-called fucospheres, which are microparticles obtained by polyelectrolyte complexation with CS (148,150). Fucoidan has also been used in the development of nanoparticles. Again, polyelectrolyte complexation was the predominant technique and CS was used in most cases as counterion (80,120,141,147,246).

Comparatively, CS has been the focus of research as a pharmaceutical excipient due to several favourable chemical and biologically features. Apart from applications such as wound dressing and tissue engineering, CS showed promising features as a supporting agent in drug delivery (247). For instance, it was found that CS interacts with cells, which is related to changes in the characteristics of the cell membrane or uptake by phagocytic cells (248), an interesting feature for targeted cell therapies. Over the last decades, a considerable amount of work has been published on CS and its potential use in the design of drug delivery carriers (155–160), as referred in the previous chapter.

In this sense, patients with pulmonary TB could benefit from targeted therapy, since most anti-TB drugs currently in use, cannot suitably reach the lung and alveolar macrophages via oral administration, allowing for prolonged survival of mycobacteria in the host (110,249). Yet, the pulmonary delivery of antibiotics would maximise drug delivery to the site of infection, since alveolar macrophages are fundamentally involved in mediating the removal of inhaled particles. This approach could reduce drug doses and delivery frequency, improve patient compliance and decrease antibiotic resistance. Furthermore, inhaled antibiotic therapy targeted to alveolar macrophages should increase the therapeutic effect of drugs, while limiting the potential for systemic side effects. Yet, this strategy would represent a major advance in the treatment of pulmonary TB.

Considering the motivations mentioned above, the aim of the present work was to explore the potential of FUC and CS as matrix of polymeric nano and microparticles for the pulmonary administration of anti-TB drugs. To demonstrate the feasibility of the approach, INH and RFB, two first-line anti-TB drugs, were used as models. The working mechanism herein proposed for inhalable carriers is illustrated in Figure 2.1.

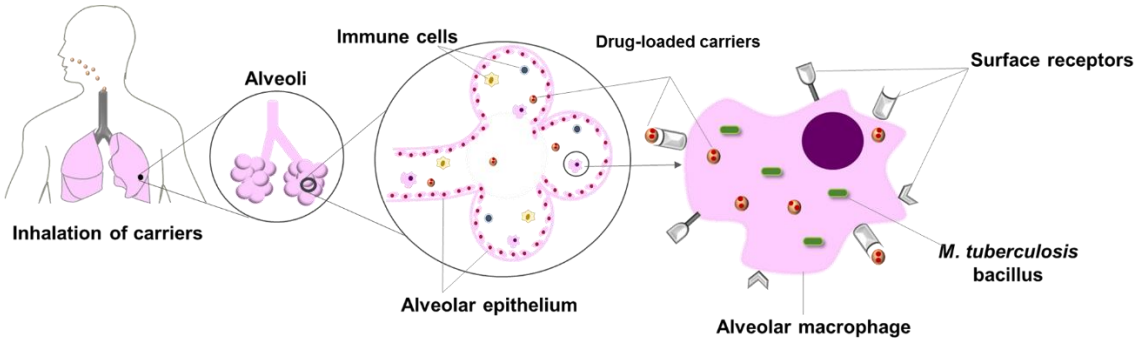

Figure 2.1. Illustration of carrier uptake by alveolar macrophages, assuming targeted drug delivery mediated by the polysaccharides (fucoidan or chitosan). Drug-loaded carriers reach the alveoli upon dry powder aerosolisation. Next, alveolar macrophages, infected with *M. tuberculosis*, engulf the particles. The polymer is expected to facilitate phagocytosis, because it possesses chemical moieties that are recognisable by the macrophage surface receptors.

In order to achieve the referred general objectives, several partial goals were established, which are displayed below:

i. To develop nano and microparticles based on FUC and CS;
ii. To microencapsulate the produced nanoparticles to provide them with adequate morphological and aerodynamic properties for deep lung deposition;
iii. To evaluate the ability of carriers to associate anti-TB drugs, individually and in combination, and to characterise aerodynamic properties of the systems;
iv. To determine the drug release profiles in media relevant for pulmonary delivery applications;
v. To evaluate the cytotoxicity of the systems in human pulmonary epithelial (A549) and macrophage-like cells (differentiated THP-1 cells);
vi. To assess the capacity of polymeric carriers to activate alveolar macrophages;
vii. To certify the ability of alveolar macrophages to uptake the proposed systems;
viii. To determine the potential antibacterial activity of the produced formulations against a strain of mycobacteria.
ix. To perform preliminary *in vivo* study to verify signs of inflammatory and allergic responses, possibly induced by the carriers after inhalation.

As a result, it is expected to develop natural polymeric carriers which efficiently associate antibiotics, present adequate aerodynamic properties for pulmonary administration and display the ability to target alveolar macrophages.

Chapter Three

Nanoparticles

This page was intentionally left in blank

3. Nanoparticles

3.1 Materials and methods

3.1.1 Preparation and characterisation of nanoparticles by polyelectrolyte complexation

Nanoparticles based on FUC (*Laminaria japonica*, M_w 598.4 g/mol, Chemos GmbH, Germany) and CS (Protasan UP CL 113, FMC Biopolymers, Novamatrix, Norway) were prepared by polyelectrolyte complexation (FUC/CS nanoparticles; Figure 3.1). Firstly, stock solutions of the polymers were prepared at concentrations of 0.1% (w/v) by dissolving the polymers in water. Given that low molecular weight CS is highly insoluble in water (250), water-soluble ultrapure CS (Protasan^{TM}) was used in the process. Then, stock solutions were diluted and mixed respecting the required concentration of each polymer. It is worth mentioning that the initial pH of FUC (unadjusted pH 6.2 – 6.8) and CS solutions (unadjusted pH 3.8 – 4.1) slightly varied according to the polymer concentration (0.25; 0.334; 0.5; 1 mg/mL).

Polymeric nanoparticles were spontaneously obtained by mixing the negatively-charged FUC and positively-charged CS under gentle magnetic stirring at room temperature. FUC solution (2 mL) was added dropwise to the CS solution (2 mL) to achieve FUC/CS mass ratios varying from 4:1 to 1:4. The concentration of CS was maintained at 1 mg/mL, while that of FUC solutions varied to reach the desired ratio. After 15 min of stirring, nanoparticles were concentrated on a 10 µL-glycerol layer by centrifugation at 16000 *xg*, at 15 ºC for 30 min (Centrifuge 5804R, Eppendorf, Germany). The supernatants were discarded, and nanoparticles resuspended in 200 µL purified water. The size, polydispersity index (PdI) and zeta potential of the prepared nanoparticles were evaluated using a Zetasizer Nano ZS (Malvern Instruments, Malvern, UK).

The loading of anti-TB drugs in the formulations was performed by following a protocol similar to that described above. Drug-loaded nanoparticle formulations were prepared with FUC/CS mass ratios between 4:1 and 1:1. The amount of associated drug was calculated to represent a theoretical content of 10% (w/w) of the amount of polymers. Considering only RFB (M_w 847.00 g/mol), the drug was

previously dissolved (HCl 0.01M) and then dropped into the CS solution under mild magnetic stirring, prior to the addition of FUC solution. After preparing the nanoparticles, the supernatant obtained upon centrifugation was analysed by spectrophotometry at 500 nm to indirectly determine the RFB content of nanoparticles. In other words, the drug association efficiency was calculated by the difference between the total amount of drug added to the nanoparticles and the amount of non-entrapped drug, which remained in the aqueous supernatant.

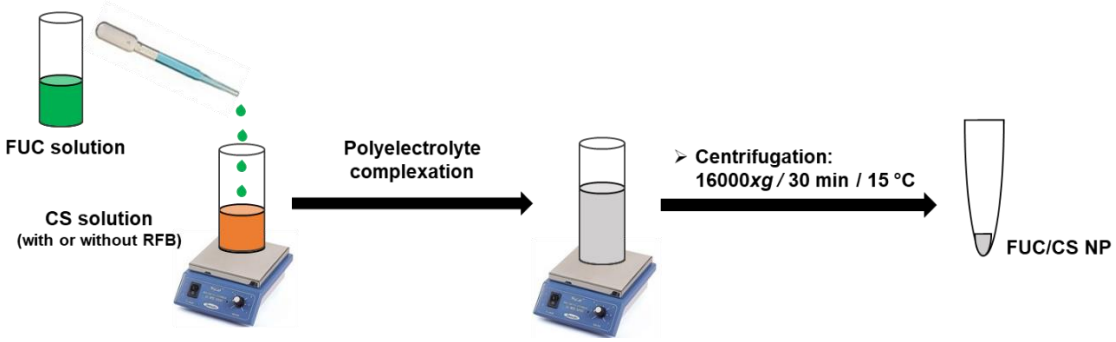

Figure 3.1. Illustration of fucoidan/chitosan nanoparticle (FUC/CS NP) preparation by polyelectrolyte complexation.

It is important to highlight that attempts to produce FUC/CS nanoparticles loaded with INH (M_w 137.14 g/mol) were made, however it was soon discovered that drug content could not be quantified by UV-Vis spectrophotometry. A screening of the matrix materials (both FUC and CS), and of the drugs revealed that FUC interferes with the spectrophotometric analysis of INH content at the selected wavelengths (268.5 nm). Taking that into consideration, it was decided to quantify INH content by HPLC, but until a HPLC protocol was optimised, experiments continued using only RFB.

3.1.2 Preparation and characterisation of nanoparticles by nanoprecipitation

Unloaded FUC NP and CS NP were prepared by nanoprecipitation method, introducing some modifications in a previously reported methodology (251). FUC was dissolved in ultrapure water (0.2%, w/v), while CS low molecular weight (75-85% deacetylation degree, 116 kDa, Sigma-Aldrich, Germany), was prepared by solubilisation in 1% (v/v) acetic acid, to obtain concentrations of 0.2% and 0.5%

(w/v). Absolute ethanol was used as the non-solvent. In the case of CS nanoparticles, the ethanol (10 mL) was added dropwise to the polymeric solution (5 mL), at a volume ratio of solvent/non-solvent of 1:2, under mild magnetic stirring (10 and 30 min, 1, 3 and 6 h) (Figure 3.2a). In the case of FUC nanoparticles, the mixing of solvent/non-solvent was performed in the other way around, that is, the polymeric solution was dropped into absolute ethanol (Figure 3.2b). Two solvent/non-solvent volume ratios were tested for this polymer (polymeric solution/ethanol of 1:2 and 1:5). The nanoprecipitation occurred under mild magnetic stirring (10 and 30 min) and the concentration of FUC solution (0.2%, w/v) was kept constant in all trials. In order to optimise the protocol to produce both FUC and CS-based formulations of nanoparticles, several approaches were tested using surfactants (Tween® 20 and Tween® 80), sonication (ultrasonic bath; VWR, USA), and high-speed homogenisation (IKA® Ultra-Turrax® T25 Digital Homogeniser, Germany).

For both polymers, nanoparticles were concentrated on a 10 µL-glycerol layer by centrifugation at 16000 *xg*, at 15 ºC for 30 min. The supernatants were discarded, and nanoparticles resuspended in 1 mL of milliQ water. The particle size and PdI were evaluated using a Zetasizer Nano ZS (Malvern Instruments, Malvern, UK).

Both INH and RFB were associated, separately, to CS nanoparticles (10%, w/w relative to the amount of polymer). The association was performed in two different ways (Figure 3.2): i) the drug was dissolved in the non-solvent (absolute ethanol), or ii) the drug was dissolved in the polymeric solution. In the latter approach, RFB was first solubilised in HCl 0.01M, and then added to the polymeric solution, a procedure unnecessary for INH, which is hydrophilic. The association of RFB to FUC nanoparticles was also conducted following the same protocol illustrated in Figure 3.2b. In turn, INH was not associated to FUC nanoparticles, at this stage, due to the analytical limitation that was previously explained.

For the two polymers, nanoparticles were recovered by centrifugation as described above and the supernatants were used to indirectly determine the drug association efficiency by spectrophotometry at 268.5 nm for INH and 500 nm for RFB. Nanoparticles were characterised in terms of size and PdI using a Zetasizer Nano ZS (Malvern Instruments, Malvern, UK). Calibration curves were performed using, as medium of dissolution, the supernatant resulting from the production of unloaded nanoparticles using the same solvent/non-solvent volume ratios used in the experiments.

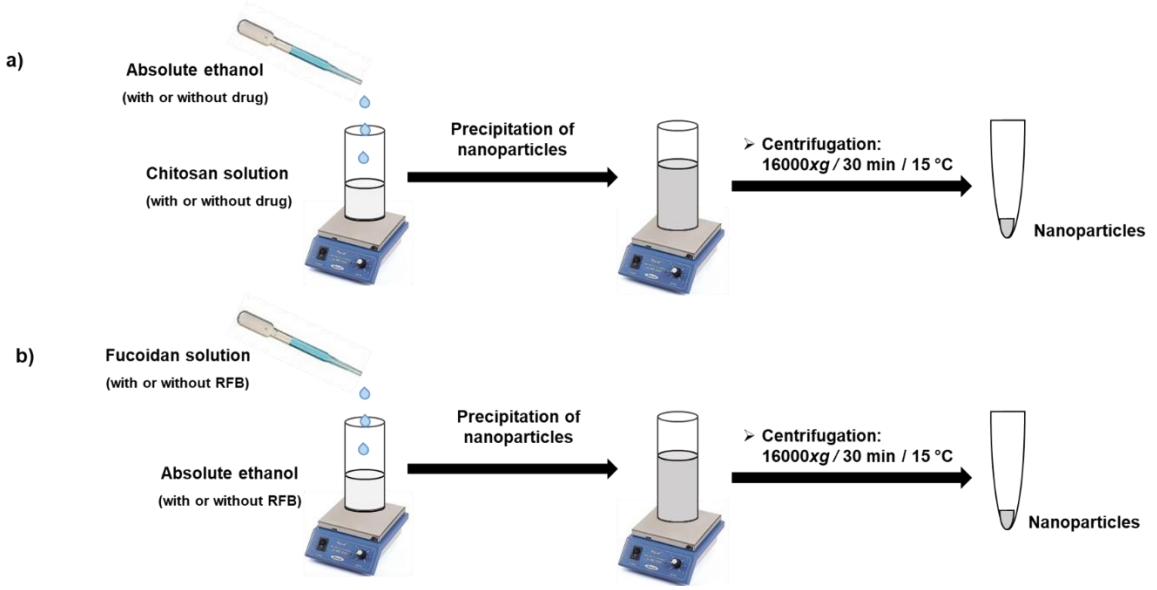

Figure 3.2. Illustration of the method to produce (a) chitosan and (b) fucoidan nanoparticles by nanoprecipitation. Drug was solubilised either in the non-solvent (absolute ethanol) or in the polymeric solution. In the latter approach, RFB required solubilisation in HCl 0.01M prior to the addition to the polymeric solution, to address its hydrophobicity.

3.2 Results and discussion

Polysaccharides have long been showing potential in drug delivery applications and CS is one major material with broad application in this field (250), as aforementioned. Many reported NP-based formulations have, thus, relied on CS. The exploration of FUC abilities in this regard is much more recent but numerous works report its use in nanoparticle production by polyelectrolyte complexation, as previously referred. The ionic nature of FUC enables the formation of complexes with oppositely charged polyelectrolytes and CS appears, in this case prominently, as the most used counterion, as referred in the previous chapter (80,120,141,147,246). However, the production of FUC-based nanoparticles produced by other methods, with no use of counterions has also been reported (145,146,252).

Polyelectrolyte complexation has been very useful in the design of drug carriers, permitting drug entrapment during complex formation. Afterwards, the drug is released from the complex either by ion exchange mechanism or by charge interaction, as well as by polymer breakdown and dissolution of the complex (91). Although the literature reports FUC/CS nanoparticles obtained by polyelectrolyte complexation, to date, there are no reports describing the encapsulation of either INH or RFB in such systems. Nevertheless, the entrapment of anti-TB drugs, including INH, in nanocomplexes of other composition has been reported (253,254).

3.2.1 Production of FUC/CS nanoparticles by polyelectrolyte complexation

Nanoparticles were spontaneously obtained by complexing FUC with CS, a process that occurred in a hydrophilic environment with mild preparation conditions, that is in the absence of organic solvents and high shear forces that could interfere with the stability of encapsulated drugs (133). By mixing FUC and CS solutions, an electrostatic interaction was established between the negatively charged sulphate groups of FUC and the positively charged amino groups of CS, leading to nanoparticles formation.

Several formulations of unloaded FUC/CS nanoparticles were produced with polymeric mass ratio varying from 4:1 to 1:4. Considering that the mixing order of

polymeric solutions influences nanoparticle stability (255), all formulations were prepared by adding FUC solution into CS solution. The opposite approach resulted in macroscopic precipitation for certain polymeric mass ratios, certainly as a consequence of reduction or elimination of electrostatic repulsion (133). In fact, when dropping CS into FUC solution, that has initial pH around 6, the relative charge density of the protonated amino group of CS, at pH 6, is lower than or equal to the relative charge density of sulphated ions of anionic FUC, as previously demonstrated (256). Therefore, visible aggregates were formed as the system approached an isoelectric condition.

The developed FUC/CS nanoparticles (unloaded) were characterised in terms of size, PdI, and zeta potential. The detailed results are displayed in Table 3.1.

Table 3.1. Characterisation of unloaded FUC/CS nanoparticles in terms of size, polydispersity index (PdI) and zeta potential (mean ± SD, *n* = 3). Different letters represent significant differences in each parameter (p<0.05).

FUC/CS (w/w)	Size (nm)	PdI	Zeta potential (mV)
4:1	[a] 246 ± 10	0.36 ± 0.04	- 39 ± 2 [a]
3:1	[a] 243 ± 21	0.26 ± 0.03	- 39 ± 3 [a]
2:1	[b] 159 ± 5	0.21 ± 0.03	- 30 ± 4 [a]
1:1	[a] 234 ± 4	0.31 ± 0.04	+18 ± 3 [b]
1:2	[a] 226 ± 20	0.30 ± 0.05	+13 ± 1 [b]
1:3	[a] 266 ± 5	0.35 ± 0.05	+13 ± 2 [b]
1:4	[b] 171 ± 16	0.26 ± 0.03	+12 ± 2 [b]

As can be observed, the tested formulations resulted in nanoparticles with average size range of 159 – 266 nm, PdI ranging between 0.21 and 0.36, and zeta potential varying from -39 mV to +12 mV, following the alteration of the mass ratios. The surface charge of nanoparticles resulted from the excess of one of the polysaccharides. Therefore, it was observed that the values of zeta potential varied, increasing the positive charge density as the amount of CS was raised in the formulation, as expected. The current results agree with previous studies that showed similar zeta potential variation in terms of absolute value and charge, also demonstrating that the excessive amount of either FUC or CS confers the final zeta potential (143,257). This is a relevant parameter, as the distribution of the surface charge on a delivery system defines its stability, considering that high surface

potential reduces particle agglomeration, making the carriers stable for a longer period (258).

Alterations in polymer ratios not only modify the amount of charges available, but also may result in nanoparticles with different mean sizes. Overall, the produced nanoparticles evidenced average diameters around 200 nm, which is coincident with other studies that tested similar FUC/CS mass ratios (147,259). However, it should be mentioned that FUC/CS nanoparticles with larger sizes, varying from 365 to 900 nm, have been reported (246), corroborating other studies on the production of FUC/CS nanoparticles that have demonstrated an effect of polymeric mass ratios as well as pH on the average size of FUC/CS nanocarriers (80,120,143). Polymer molecular weight may also have an impact on the particle size (260).

In the present study, differences in the size mean of unloaded FUC/CS nanoparticles were observed, however, it was not significant among all tested mass ratios, except for formulations at ratios 2:1 and 1:4. These formulations resulted in nanoparticles with the lowest average sizes (159 and 171 nm, respectively). Thus, these nanoparticles were significantly smaller ($p < 0.05$) than those obtained from formulations 4:1 (246 nm), 3:1 (243 nm), and 1:3 (266 nm), the latter being the one that produced nanoparticles with the highest average size.

Considering that this work aimed at producing drug delivery nanocarriers for TB therapy via inhalation, the ability of FUC/CS nanoparticles to associate anti-TB drugs was evaluated. For this phase of the work, nanoparticle formulations were prepared with equal or higher amount of FUC respect to CS, as we intended to take benefit from the theoretical ability of FUC to target macrophages, the host cells of tuberculosis pathogenic bacteria. In this sense, drug-loaded nanoparticles with FUC/CS mass ratios between 4:1 and 1:1 were prepared. Initially, it was intended to incorporate the model drugs separately in order to assess the effect of each drug on the developed systems. However, our final interest was to develop a system able to carry the two drugs simultaneously, thus complying with the combined therapeutic regimen of TB that is recommended by WHO (261). To the best of our knowledge, to date, very few studies have reported the co-encapsulation of drugs in polysaccharide-based nanoparticles, prepared by polyelectrolyte complexation (262).

Firstly, the ability of FUC/CS nanoparticles to associate RFB was assessed by adding the drug to obtain final polymer/drug mass ratio of 10/1 (w/w). As indicated

in the methodology, the amount of drug associated to nanoparticles was quantified indirectly by analysing the supernatants resulting from nanoparticle isolation by centrifugation. The analysis showed that RFB was not associated with any of the tested formulations. The literature displays already several works on FUC/CS nanoparticles prepared by the same technique described herein, which report the successful association of different drugs (120,255,263,264). In most cases, these are charged molecules, which certainly facilitates the interaction with the polymers and entrapment within the matrix. Nevertheless, the encapsulation of neutral materials has also been reported in nanoparticles with different composition but prepared by polyelectrolyte complexation (90).

It is well known that the formation and stability of polyelectrolyte complexes depends on many factors, including the concentration of the polymers, their mixing order, the polymeric mass ratios, solution pH, etc. (255,265). Accordingly, drug entrapment is also affected by polymeric ratios or by whether the resulting complex is loosely or tightly assembled, a condition mostly determined by the charge density of the constituent materials (90). As charge density is directly affected by solution pH (256), this parameter was then addressed as a variable condition to promote drug entrapment. Initially, FUC solutions had pH 6 while the pH of CS solution was around 4, approximately. After mixing FUC and CS solution, the final pH was registered as 6.2 for the formulation FUC/CS 4:1 (w/w). In other words, as the mass ratio of FUC increases, the pH of the nanoparticle production medium comes close to the initial pH of FUC solution.

At pH 6, FUC is likely to be fully charged given that it is a strong polyelectrolyte with p*K*a between 1 and 2.5 (266). On the other hand, at this pH, few CS amino groups remain protonated, owing to a p*K*a of 6.5 (144). With this in mind, nanoparticles were prepared in acidic medium, knowing that it would lead to the protonation of CS (267). As mentioned in the methodology section, RFB was solubilized with HCl 0.01M, given its hydrophobic nature, allowing RFB to be protonated in the acidic dissolution medium (268). Nevertheless, both ultrapure CS and FUC were dissolved in miliQ water. Thus, for further tests, CS solution was prepared using HCl 0.01M to ensure that most amino groups of CS were protonated. In the same way, FUC solution had the pH adjusted from 6 to 4, in order to maintain the nanoparticle production medium at low pH. The pH of FUC solution could not be lower than that, because at pH 2, the anionic sulphate groups of FUC are partially

uncharged, meaning that electrostatic interactions between FUC and CS are weaker (141). With this approach, we expected to promote drug association.

Surprisingly, varying the pH of polymeric solutions and polysaccharide mass ratios did not promote drug association at all. A possible explanation may lie in the nature of the drugs or even in the polysaccharide couple. In this respect, a study with dextran sulphate/CS complexes has shown an average efficiency of insulin loading varying from 48.6 to 96.4%. However, the complexes barely incorporated hydrophilic low molecular weight drugs, since they easily escape from the matrices (269). Actually, drug entrapment has been reported not only to depend on the nature of drugs, but also on the concentration of polymeric solutions, drug/polymer ratios and ionic strength, among other factors (262,269). Nanocomplexes of alginate/CS and PGA/CS, for instance, encapsulated 5-fluorouracil and temozolomide with variable efficiencies (16–82%), depending on: i) CS concentration, ii) the polysaccharide pair, iii) polymer ratios, and iv) whether the systems contained one or two drugs encapsulated simultaneously (262).

Unfortunately, the several attempts to associate RFB to FUC/CS nanoparticles produced by polyelectrolyte complexation did not succeed. Therefore, it was decided to continue the work by using another methodology to produce the nanoparticles.

3.2.2 Production of FUC and CS nanoparticles by nanoprecipitation

As the complexation of FUC and CS was not successful in producing nanoparticles with ability to effectively associate the selected anti-TB drugs, an attempt was made to produce nanoparticles by nanoprecipitation. The technique is defined as a process that generates dispersible colloidal systems of polymeric compounds in the form of nanoparticles. It is a simple method conducted in one step and usually does not require the more aggressive conditions involving high temperatures, shear forces and sonication, or even the application of surfactants (270). The literature reports the preparation of polymeric nanoparticles using this technique, which is also known as solvent displacement method (271,272). Nanoprecipitation was originally designed for the encapsulation of hydrophobic molecules, but it has also been investigated for the entrapment of hydrophilic drugs into the nanoparticles (270,273). Basically, the approach requires two miscible

phases (organic and aqueous), and the polymer is soluble in one phase (solvent), but not in the other (non-solvent). Ultimately, nanoparticle formation results from the instability created at the interface by the interfacial tension between solvent and non-solvent. In this way, the polymer immediately precipitates, entrapping the drug present in the medium (273).

Chitosan

The initial application of this method employed hydrophobic polymers as matrix materials, which were dissolved in organic solvents. Consequently, water was usually the aqueous phase (non-solvent) used in the process (274). In the present study, CS was dissolved in aqueous solution of 1% (v/v) acetic acid, and absolute ethanol was employed as the non-solvent. Firstly, unloaded CS nanoparticles were produced, in order to optimise the conditions. For that reason, several formulations were prepared by varying polymer concentration (0.2% and 0.5%, w/v), stirring time (10 and 30 min, 1, 3 and 6 h), and using a constant volume ratio of solvent/non-solvent (1:2). Ethanol was used as non-solvent. Comparing with other alcohols which application has been reported for the same end (e.g. propanol and methanol), ethanol has been shown to have milder effect on particle size (270). Yet, it is a chemical reagent of easy access and manipulation in the laboratory.

It has been reported that polymer concentration and stirring time are determinant parameters for obtaining nanosized particles by this technique. In this work, it was found that the use of CS solution at 0.5% (w/v) and magnetic stirring time of 30 min rendered nanoparticles with an average size around 700 nm. Under all the other tested conditions, the mean size of the precipitated particles was in the micron size range.

The present work intended to produce nanoparticles for pulmonary drug delivery. Although it has been reported that submicron particles can potentially deposit in the deep lung (275,276), some researchers claim that nanosized systems are mostly exhaled due to their small size and mass (114). Because of that, the microencapsulation of nanoparticles is a strategy that could overcome this limitation, as previously mentioned in the introduction (Section 1.3). Anyway, obtaining particles with larger diameters (between 500 – 700 nm) was preferable in the present work.

The produced unloaded CS nanoparticles displayed high PdI values (0.83 ± 0.10), indicating diversity in particle size that can occur due to aggregation (271). In general, nanoparticle formation by nanoprecipitation is believed to arise from the nucleation of small aggregates of macromolecules with subsequent aggregation of these nuclei. The aggregation process occurs until the colloidal stability is reached (274). Usually, particle agglomeration can be prevented by using different approaches. For instance, stabilising agents (e.g surfactants), high-speed homogenisation and sonication may be applied in the process to produce smaller particles with narrower unimodal distribution (97,277).

In this sense, several tools were attempted to prevent particle aggregation, allowing the production of CS nanoparticles with narrower size distribution. Firstly, 4% (v/v) Tween® 20 or Tween® 80 were added into CS solution and used as stabilisers in the production process. The presence of surfactants during the precipitation process prevents nanoparticle coalescence and subsequently formation of aggregates (277). Therefore, it was expected that the use of surfactants would avoid particle aggregation, subsequently narrowing particle size distribution. Surprisingly, the addition of Tween® 20 resulted in micron-sized CS particles with PdI values around 1.0. The increase in size in the presence of surfactant has been previously reported and this effect can raise with higher concentrations of stabiliser (272). Contrarily, the inclusion of Tween® 80 significantly reduced the mean size of CS nanoparticles (50 – 100 nm) but did not narrow the particle size distribution as much as expected, with PdI values remaining between 0.8 – 1.0.

In this manner, experiments proceeded applying sonication along with the use of Tween® 20. Sonication was applied for 5 min, right after the mixing of non-solvent and CS solution, containing the surfactant. Longer periods were also tested (15, 30, 60 min), but the evaporation of ethanol (non-solvent) was perceived during the process, since the volume content in the beaker was visually reduced. The strategy resulted in micron-sized particles with high PdI values (0.9 –1.0).

In the same way, high speed homogenisation (Ultra-Turrax®) was applied instead of sonication, combined with Tween® 20, also resulting in the production of particles over 1000 nm in size. Next, the described approaches were also performed using Tween® 80, combined with either sonication or high-speed homogenisation. In general, the strategies decreased the size range of CS nanoparticles under 100 nm, a result not desirable for the intended application of the carriers. It is known that

nanosized particles smaller than 100 nm can readily translocate across the epithelia of respiratory tract (113). It should be mentioned that when only sonication was applied (with no surfactant), it resulted in the production of micron-sized particles with wide size distribution (PdI around 1.0). As well, the application of high-speed homogenisation in the absence of surfactants originated particles with mean diameter over 1000 nm.

Although particle size distribution had not been properly controlled, attempts to encapsulate the model drugs were made. For this phase of the present study, surfactants, sonication, and high-speed homogenisation were not used at all. As illustrated in Figure 3.2a, each drug (INH or RFB) was dissolved either in the solvent (CS solution at 0.5%, w/v) or in ethanol (non-solvent), and nanoparticles were produced at solvent/non-solvent volume ratio of 1:2. The mixing of polymeric solution/ethanol was conducted under mild magnetic stirring (30 min). The approaches illustrated in Figure 3.2a were tested and neither of them succeeded in encapsulating the antibiotics.

Despite the numerous attempts to produce CS nanoparticles by nanoprecipitation, the obtained results were not in line with the desirable nanoparticle characteristics. PdI values clearly evidenced wide size distribution of particles, suggesting particle agglomeration. In spite of the use of several approaches, the formation of aggregates was not sufficiently minimised. In most cases, the distribution curves indicated the presence of two different particle size populations. The bimodal curves mostly consisted of a fraction of submicron particles and a second population over 1000 nm. Nanoprecipitation often enables the production of small nanoparticles (100 – 300 nm) with narrow unimodal distribution (270), which contrasts with the results obtained herein. However, particles with larger diameters (400 – 800 nm) have also been reported using this technique (278,279). In fact, some of the tested approaches generated CS particles in that size range (around 700 nm), which was acceptable for the purpose of this work. Nevertheless, we realised that this was difficult to replicate. More importantly, the technique did not result in the encapsulation of the model drugs, a crucial element for the development of this research work.

Fucoidan

As described for CS, several experimental approaches were performed to identify the most appropriate conditions to control the size and polydispersity of FUC nanoparticles prepared by nanoprecipitation. The production of these resulted from the dropwise addition of the polymeric solution into ethanol, since the opposite approach did not enable nanoparticle formation. Similarly to CS, FUC nanocarriers were initially produced without drugs.

As described in the methodology, the concentration of FUC solution (0.2%, w/v) was kept constant in all trials, since the first attempts to produce unloaded FUC nanoparticles resulted well, at this concentration. In addition, two solvent/non-solvent volume ratios (1:2 and 1:5) were used and revealed that this variation had little influence on particle size, which varied between 535 – 564 nm (1:3, v/v) and 507 – 551 nm (1:5, v/v). This observation is coincident with that of a recent study on starch nanoparticles, which evaluated the effect of solvent/non-solvent volume ratio on the particle size (271). However, the literature displays various studies of this effect with variable results, reporting that the decrease in the solvent/non-solvent ratio can lead to a rise or a reduction in the particle size (280,281). This suggests strong influence of the proper polymers on this parameter.

As described before, the nanoprecipitation procedure was conducted under mild magnetic stirring, which was kept for 10 min or 30 min. In this case, applying magnetic stirring for longer was not considered, given that it could generate micron sized particles, as observed for CS. In terms of average size, similar values were obtained after stirring FUC solution and ethanol (ratio 1:2) for 10 min (535 ± 78 nm) and 30 min (564 ± 123 nm). Regarding the solvent/non-solvent volume ratio of 1:5, the corresponding mean diameters were 507 ± 43 nm (magnetic stirring for 10 min) and 551 ± 101, after 30 min of stirring. Hence, the approaches resulted in unloaded FUC particles in the nanosized range (around 500 nm), regardless of the operated variations in both magnetic stirring time and solvent/non-solvent volume ratio.

Nevertheless, the obtained unloaded FUC nanoparticles displayed little uniformity in size, indicated by PdI values, varying within 0.55 and 0.67. Thus, as described for CS, several approaches regarding the process were used to address this issue and obtain FUC nanoparticles with narrower size distribution. It was expected that the use of Tween®, sonication and/or high-speed homogenisation

would inhibit the aggregation of the particulate carriers. Nonetheless, the used tools did not improve the characteristics of the produced FUC nanoparticles, under the tested conditions, with PdI values remaining high in order of 0.8 – 1.0. In light of this, the experiments continued, using no surfactants, sonication, or ultra-turrax®, and the encapsulation of drug was attempted. As previously explained, the tests initiated with RFB, rather than INH, because the latter imposed an analytical limitation that hindered the determination of drug content in INH-loaded FUC nanoparticles by spectrophotometry. In this case, drug content would be determined by HPLC, but a protocol had not been optimised by then. Thus, drug encapsulation experiments started with RFB.

RFB (10% w/w in relation to the polymer) was dissolved in ethanol, followed by the dropwise addition of 0.2% (w/v) FUC solution, resulting in none or very low drug entrapment (5.4 – 7%). For this reason, the experiments persisted, but the dissolution of RFB started to be performed in HCl 0.01M instead. In this medium RFB becomes protonated, which could affect positively the encapsulation. After the dissolution step, the drug was mixed with the polymeric solution following the same approach. The strategy rendered submicron FUC particles showing variable entrapment efficiency of RFB, ranging from zero to 46%, which indicated difficulties in the replicability.

Although it has been observed in the initial assays that the volume of the non-solvent (ethanol) did not influence particle size, different solvent/non-solvent ratios were tested because these could interfere with drug association efficiency (282). The 1:2 volume ratio resulted in drug-loaded FUC nanoparticles with mean size of 517 ± 57 nm and PdI around 0.46. The average RFB content of these carriers was 15 ± 20%, considering that the data set varied from zero to 37%. Regarding solvent/non-solvent ratio of 1:5, FUC nanoparticles (503 ± 60 nm and PdI around 0.50) were obtained, associating approximately 25 ± 17% of RFB. In this case, the mean value resulted from a set of values that ranged between 8.2 to 46%. In terms of particle size, these results are comparable with others reported in the literature for the same methodology (283), which was also observed regarding drug association efficiency (284). Nevertheless, the amount of encapsulated drug varied considerably among trials.

Nanoprecipitation is known as an easy and reproducible technique, but many operating parameters must be managed to ensure the production of nanoparticles

with the intended characteristics. These include the choice of solvent, non-solvent type and volume, stirring rate and time, polymer concentration, to name a few. The referred operating conditions definitely have a major impact on the resulting particulate carriers (274).

Overall, the effect of several factors was investigated and the attempt to optimise the methodology was performed in order to achieve a reproducible formulation with uniform size. A crucial requirement of a production method is that it should be reproducible, which was not observed. Furthermore, the tested protocols did not provide proper control of particle polydispersity, which is an important parameter to be considered. Moreover, drug association efficiency could not be replicated over the experiments, which is critical to accomplish the aims of this research.

Conclusion

In summary, an optimal protocol to obtain CS- and FUC-based nanoparticles that efficiently encapsulate INH and RFB was not established. The literature reports a variety of methods to produce polymeric nanoparticles that could have been applied in the present work. Nonetheless, the intention to use a mild and simple technique to produce the nanoparticles in this work should be clear. Unfortunately, the attempts to optimise the methods (polyelectrolyte complexation and nanoprecipitation) did not succeed. All things considered, due to the limited time to accomplish the aims of the PhD plan, it was decided to focus the work on the development of microparticles, which were worked out in parallel and provided more satisfactory results.

This page was intentionally left in blank

Chapter Four

Microparticles: Materials and Methods

This page was intentionally left in blank

4. Microparticles: Materials and methods

4.1 Materials

FUC (*Laminaria japonica*, M_w 598.4 g/mol) and RFB were purchased from Chemos GmbH (Germany). CS (low molecular weight, 75-85% deacetylation degree, 116 kDa), citrate buffer pH 5 (citric acid ~0.096 M, sodium hydroxide ~0.20 M), dimethylformamide (DMF), Dulbecco's modified Eagle's medium (DMEM), lipopolysaccharide (LPS), mannitol (Man), *N*-(3-dimethylaminopropyl)-*N*′-ethylcarbodiimide hydrochloride (EDAC), non-essential amino acids solution and penicillin/streptomycin (10,000 units/mL, 10,000 g/mL), sodium dodecyl sulphate (SDS), Triton X-100, trypsin-EDTA solution (2.5 g/L trypsin, 0.5 g/L EDTA), trypan blue solution (0.4%), INH, and HCl were supplied by Sigma-Aldrich (Germany). Thiazolyl blue tetrazolium bromide (MTT), phosphate buffer saline (PBS) tablets pH 7.4 and Tween® 80 were supplied by Amresco (USA). Dimethyl sulfoxide (DMSO) was provided by VWR (France) and phorbol 12-myristate 13-acetate (PMA) was provided by Cayman Chemicals (USA). A lactate dehydrogenase (LDH) kit was obtained from Takara Bio (Japan) and L-glutamine solution (200 mM) as well as fetal bovine serum (FBS) from Gibco (Life Technologies, USA). RPMI 1640 and Ham's F12 media were supplied by Lonza Group AG (Switzerland). Middlebrook 7H9 (M7H9; 4.7 g/L) and OADC (oleic acid, albumin, dextrose and catalase) were purchased from Remel (USA). Ultrapure water (milliQ, Millipore, UK) was used throughout the studies and other chemicals were reagent grade.

4.2 Preparation of microparticles by spray-drying

4.2.1 Fucoidan

Microparticles based on FUC were obtained from FUC solutions at concentrations of 1% or 2% (w/v), depending on the formulation. FUC solutions were prepared by dissolving the polymer in water under magnetic stirring (MS-3000 Biosan, Latvia). The final volume of the polymeric solutions was 50 mL. The anti-TB drugs INH and RFB were associated with FUC microparticles, either individually or combined. In the end, five formulations were obtained, with the following

denominations: FUC MP (unloaded MP); FUC-Man MP (unloaded MP), FUC-Man/INH (10/1) MP; FUC/RFB (10/0.5) MP; FUC/INH/RFB (10/1/0.5) MP. The values in parenthesis represent the polymer/drug mass ratio (w/w). Mannitol was used in certain formulations to improve flow properties. In those cases, FUC was used at 1% (w/v) and mannitol at 0.5% (w/v). The remaining formulations were obtained from 2% (w/v) FUC solutions and no addition of mannitol.

FUC solutions with no drugs but with mannitol when applicable, were kept under magnetic stirring until complete solubilisation of the polymer and further spray-dried. Regarding the preparation of microparticles containing the drugs, INH was ground in a porcelain mortar, solubilised with water, and added dropwise to the polymeric solution previously prepared. The solution was stirred for 1 h and then spray-dried. The polymer/drug ratio was kept at 10/1 (w/w). For obtaining microparticles loaded with RFB, the drug was previously ground in a glass mortar, solubilised with 4% (v/v) absolute ethanol. Subsequently, it was added dropwise to the polymeric solution which was stirred for 1 h before spray-drying. Final concentration of RFB was such that a polymer/drug mass ratio of 10/0.5 was obtained. Finally, in the case of the formulations containing both drugs in combination, INH was ground and solubilised with water while RFB was ground and solubilised with 4% (v/v) ethanol prior to drug incorporation into the polymeric solutions. Polymeric solutions containing both drugs underwent magnetic stirring for 1 h before spray-drying took place. Final polymer/drug ratios for this formulation was FUC/INH/RFB =10/1/0.5, w/w.

Dry powder formulations were obtained by spray-drying (Büchi B-290 Mini Spray Dryer, Büchi Labortechnik AG, Switzerland), with the equipment operating in an open mode configuration, and compressed air used as fluid. Polymeric solutions were spray-dried on a laboratory scale spray-dryer (Figure 4.1) equipped with a high-performance cyclone. During the process, the solution passes through an atomizer that creates a spray, forming droplets. The droplets are dried when exposed to the hot air in a drying chamber. The drying gas is heated at a defined temperature (inlet temperature) and promotes the rapid evaporation of the solvent present in the droplets. Next, the resultant dried particles enter the cyclone, where they are separated from the air stream by the helicoidal motion of the air flow. Finally, the obtained dry powder accumulates in the powder collector.

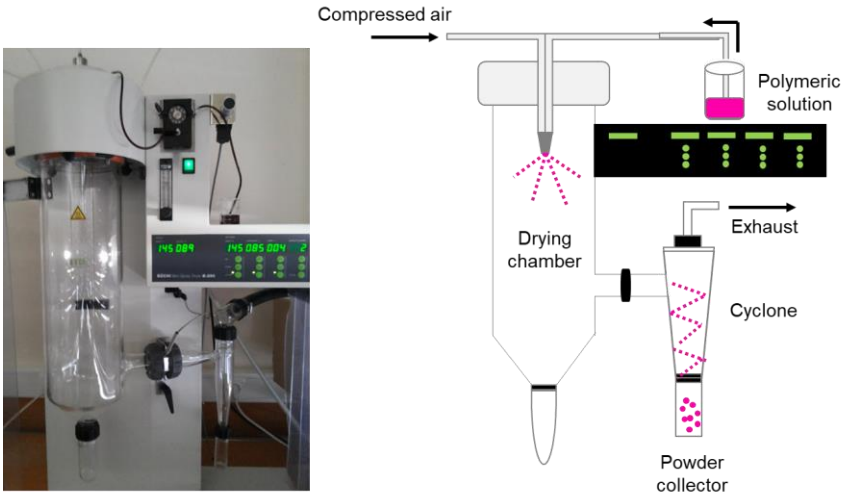

Figure 4.1. Scheme of the spray-drying process.

The spray flow rate was set at 473 L/h and the inlet temperature, the aspirator and the feed flow used to prepare each formulation are displayed in Table 4.1. Each formulation was prepared in triplicate (n = 3) and dry powders were stored in desiccators until further use. The aqueous solutions and the resulting dry powders loaded with drugs were protected from light in every step of manipulation and storage.

4.2.2 Chitosan

Microparticles based on CS were obtained from 2% (w/v) solutions which were prepared by dissolving the polymer under stirring (MS-3000 Biosan, Latvia) in a mixture of 1% (v/v) acetic acid and ethanol absolute (solvent ratio 10/1). The final volume of the polymeric solutions was 50 mL. INH and RFB were associated with CS microparticles, either individually or in combination. In the end, four formulations were prepared, with the denominations described as follows (in parenthesis is indicated the mass ratio between materials: CS MP; CS/INH (10/1) MP; CS/RFB (10/0.5) MP; and CS/INH/RFB (10/1/0.5) MP.

CS solutions with no drugs underwent magnetic stirring until complete solubilisation of the polymer and were then spray-dried. Regarding the preparation of microparticles containing INH only, the drug was ground in a porcelain mortar, solubilised in acetic acid and dropped into the polymeric solution previously prepared. The solution was stirred for 1 h and then spray-dried. The polymer/drug

ratio was kept at 10/1 (w/w). For obtaining carriers loaded with RFB, the drug was previously ground in a glass mortar, solubilised with 10% (v/v) absolute ethanol and added dropwise to the CS solution, which was stirred for 1 h before spray-drying. The final concentration of RFB was such that a polymer/drug mass ratio of 10/0.5 was obtained. Finally, in the case of the formulations containing both INH and RFB in combination, drugs were separately ground and properly solubilised, as described above, prior to drug incorporation into the polymeric solutions. Polymeric solutions containing both drugs were kept under magnetic stirring for 1 h before spray-drying. Final polymer/drug ratios for the referred formulation was CS/INH/RFB = 10/1/0.5, w/w.

CS solutions were then spray-dried, and the obtained dry powders were stored, as described above. The spray-drying parameters for producing CS microparticles are presented in Table 4.1

Table 4.1. Spray-drying parameters (inlet temperature, aspirator and feed rate) used to produce fucoidan- and chitosan-based microparticles and resulting outlet temperature.

Microparticles	Inlet Temp.(°C)	Aspirator (%)	Feed rate (mL/min)	Outlet Temp.(°C)
Unloaded FUC	125 ± 1	80	2.0	69 – 73
Unloaded FUC-Man	145 ± 1	85	1.0	86 – 92
FUC-Man/INH (10/1)	160 ± 1	90	1.0	98 – 102
FUC/RFB (10/0.5)	145 ± 1	85	1.0	86 – 92
FUC/INH/RFB (10/1/0.5)	145 ± 1	85	1.0	88 – 95
Unloaded CS	160 ± 1	80	1.3	96 – 99
CS/INH (10/1)	160 ± 1	80	1.3	98 – 102
CS/RFB (10/0.5)	160 ± 1	80	1.3	96 – 100
CS/INH/RFB (10/1/0.5)	160 ± 1	80	1.3	96 – 99

The production yield of the spray-drying process was calculated for all formulations at the relationship between the solid content in the resulting powder (collected microparticles) and the total solid content in the feed dispersion:

Yield (%) = (Weight of collected MP / Weight of solids (polymer+drug) in the dispersion) x 100 (1)

4.2.3 Preparation of fluorescently labelled microparticles

Fluorescent FUC and CS microparticles (unloaded) were produced to be used in a single assay (macrophage capture – Section 6.5), following the same conditions displayed in Table 4.1

Fucoidan

A fluorescent label was attached to FUC by reacting 1 g of the polymer (commercial powder) with fluorescein sodium salt (24.4 mg dissolved in 4 mL of 96% (v/v) ethanol), in the presence of EDAC (9.6 mg). This was dissolved in 16 mL of milliQ water and added to the solution to activate the fluorescein. The covalent attachment of the dye to the polymer was carried out by adding fluorescein into a 2% (w/v) FUC solution. The reaction was stirred overnight, and then dialysed (2000 Da Mw cut-off) against distilled water, ensuring light protection during the whole process.

In the end, dialysates were frozen, freeze-dried (FreeZone Benchtop Freeze Dry System, Labconco, USA), and stored in desiccators. Finally, the resulting fluorescently-labelled FUC was spray-dried and the dry powder was stored, protected from light, for further use.

Chitosan

Fluorescently-labelled CS was synthesised by reacting 1 g of CS (2%, w/v, dissolved in acetic acid) with fluorescein sodium salt (40 mg). The dye was first solubilised in 15 mL of 96% (v/v*)* ethanol, being then added to CS solution. The covalent interactions of the dye with the polymer occurred in the presence of 31 mg (dissolved in water) of EDAC. The reaction was kept under stirring for 24 h, protected from light, and then dialysed against distilled water. The obtained dialysates were then frozen, freeze-dried and stored, as described above.

4.3 Characterisation of microparticles

4.3.1 Morphology

The morphological examination of the produced microparticles was conducted by field emission scanning electron microscopy (FESEM Ultra Plus, Zeiss, Germany). Generally, dry powders were placed onto metal plates and 5 nm thick iridium film was sputter-coated (model Q150T S/E/ES, Quorum Technologies, UK) on the samples before viewing.

4.3.2 Particle size

The size of microparticles was estimated as the Feret's diameter (distance between two tangents on opposite sides of the particle) and was directly determined with an optical microscope (Microscope TR 500, VWR International, Belgium), The Feret's diameter was estimated as the mean of 300 particles (n = 3). The particle size distribution of drug-loaded microparticles was further determined by laser light scattering (SprayTec, Malvern, UK). Briefly, approximately 15 mg of dry powder were dispersed in 15 mL of 2-propanol and sonicated for 5 min. Data analysis is expressed in terms of median volume diameter of 50% (Dv50) of aerosol droplets. Complementarily, span values were determined to provide an indication of the width of size distribution. Analysis was carried out in triplicate with an obscuration threshold of 10% (285).

4.3.3 Density

Real density (g/cm^3) was determined by helium pycnometry (n = 3; Micromeritics AccuPyc 1330, Aachen, Germany). Bulk and tap densities (g/cm^3) were determined by measuring the volume of a known weight of powder before and after mechanical tapping (30 taps/min, Densipro 250410, Deyman, Spain). The determination of tap density involved tapping the sample until a constant volume was achieved. Measurements were performed in triplicate in all cases. Thus, bulk and tap densities (g/cm^3) were calculated according to the following equations:

Bulk density = Dry powder weight / Initial volume of powder (2)

Tap density = Dry powder weight / Final volume of powder (3)

4.3.4 Dry powder analysis using Powder X-Ray Diffraction (PXRD)

The raw materials, free drugs, and microparticles were analysed by PXRD in a PANalitycal X'Pert Pro diffractometer, using nickel filtered CuKα radiation with a wavelength of 0.154 nm. An X'Celerator detector was used and the operating conditions were 45 kV and 35 mA. The diffractograms were obtained in reflection mode from 5 to 70° 2theta with a step size of 0.05 °and 1500 s per point.

4.3.5 Drug association efficiency and loading

In order to determine the amount of drug associated with each formulation, an established amount of drug-loaded microparticle was solubilised with 10 mL of HCl 0.1M, under magnetic stirring for 20 min. After complete dissolution, samples were filtered (0.45 µm syringe filter) before quantification.

Particularly, to quantify the content of INH and RFB associated with CS microparticles, the formulations CS/INH (15 mg) and CS/RFB (30 mg) were solubilised and analysed by UV-Vis spectrophotometry (Pharmaspec UV-1700, Shimadazu, Japan). Measurements were performed at a wavelength of 268.5 nm and 500 nm to quantify INH and RFB, respectively. In order to determine the drug association efficiency of CS/INH/RFB (10/1/0.5) microparticles, the dry powder (30 mg) was properly dissolved and samples were spectrophotometrically analysed at both 268.5 nm and 500 nm. The analysis at 500 nm provided a direct measure of the RFB amount present in the CS microparticles associating the drugs in combination. In turn, the measurement performed at 268.5 nm required a 1:10 dilution and represents the sum of INH and RFB contents. Next, the amount of INH was calculated by subtracting the absorbance obtained at 500 nm (RFB) from that acquired at 268.5 nm (RFB + INH). In general, the drug content of CS microparticles was determined after establishing calibration curves, which were performed in an adequate media (counting on any effect from the polymer). A screening of the matrix material (CS) revealed no interference of this polymer at the selected wavelengths.

Differently, the polymeric matrix based on FUC presented some interference at the wavelength 268.5 nm. Therefore, the drug content of FUC formulations was determined by high-performance liquid chromatography (HPLC – Agilent 1100 series, Germany). A LiChrospher® 100 RP-18 (4.6 µm) column of 4 mm i.d. x 250 mm length with security guard cartridge was used. The analysis conditions were established as follows: 20 µL injection volumes, and flow rate of 1.0 mL/min. Detection was performed by a diode array detector set at a wavelength of 275 nm. The chromatographic analysis was achieved by using a gradient system, in which the mobile phase consisted of phosphate buffer 20 mM pH = 7 (A) and acetonitrile (B). The elution was conducted with a gradient starting with A/B = 95:5 kept for 5 min, followed by 3 min step gradient, until a 30:70 A/B ratio was reached, which was then kept for 19 min.

Overall, to determine the drug content of FUC microparticles, 20 mg of dry powder were accordingly solubilised (HCl 0.1M) and aliquots (20 µL) were analysed by HPLC. Under the conditions previously described, INH and RFB were eluted at 5.0 and 20 min, respectively. Calibration curves (10 – 400 mg/mL) were obtained using INH and RFB analytical standard dissolved in HCl 0.1M.

In the end, drug association efficiency (AE) and microparticle loading capacity (LC) were estimated (n = 3) by the following equations (286,287):

$$AE\ (\%) = (\text{Real drug content} / \text{Theoretical drug content}) \times 100 \quad (4)$$

$$LC\ (\%) = (\text{Real amount of drug} / \text{Weight of MP}) \times 100 \quad (5)$$

4.4 Evaluation of aerodynamic properties

The evaluation of aerosolisation properties of the produced dry powders was performed upon assessment in the Andersen cascade impactor (ACI, Copley Scientific Ltd., UK). The *in vitro* aerosol performance was determined by filling HPMC size 3 capsules (Quali-V-I, Qualicaps, Spain) with 30 mg of powder. The content of three capsules was discharged in each aerodynamic test using an RS01 dry powder inhaler (Plastiape Spa, Italy). The ACI was operated at 60L/min, a flow rate that corresponds to a pressure drop of 4 kPa over the device. The system was activated for 4 seconds, a duration consistent with 4L of air drawn through the inhaler. The apparatus was assembled using the appropriate adaptor kit for the 60

L/min air flow test, thus establishing the cut-offs of the stages from -1 to 6 as following: 8.60, 6.50, 4.40, 3.20, 1.90, 1.20, 055, 0.26 µm.

In order to prevent particle bounce, the collection plates were previously coated with 0.1% (v/v) Span® 85 in cyclohexane solution. Moreover, a glass fibre filter (Whatman, UK) was placed in the filter (F) part of the equipment to collect particles with a diameter lower than that of stage 6 cut-off. The powder was recovered from the apparatus with a water/acetonitrile mixture (50/50, v/v), samples were sonicated for 5 min, filtered (0.45 µm, RC, Sartorius, US) and analysed. The drug mass deposited in the impactor was determined by HPLC (Agilent 1200 series, Germany), following the analytical protocol described above (Section 4.3.5). Three samples were analysed, and mean value as well as standard deviation calculated.

The mass of drug deposited inside the impactor and the inhaler allows the calculation of a number of different deposition parameters. The metered dose (MD) is the mass of drug recovered and quantified by HPLC and is calculated by summing the drug recovered from the inhaler (device and capsule) and the impactor (induction port, pre-separator, stages -1 to 6 and filter). The emitted dose (ED) was considered as the amount of drug leaving the device and reaching the impactor. The mass median aerodynamic diameter (MMAD) was determined by plotting the cumulative percentage of mass against ACI cut-off diameters on a probability scale *versus* aerodynamic diameter of the stage on a logarithmic scale. Fine particle dose (FPD) was defined as the mass of drug particles with size <5µm (calculated from log-probability plots), and the fine particle fraction (FPF) was calculated as the percentage ratio between FPD and ED.

4.5 *In vitro* drug release profiles

The release profiles of INH and RFB from the produced microparticles were determined in phosphate buffered saline (PBS, pH 7.4, VWR, USA) and in citrate buffer (pH 5), both containing 1% (v/v) Tween® 80. The former represents the local pH of the lung, while the latter simulates the pH found in macrophage cells. In addition, Tween® 80 not only represents the lung surfactant present in the lung lining fluid, but also facilitates the solubilisation of RFB, which is barely soluble in the referred buffers.

4.5.1 Fucoidan microparticles

Twenty mililigramas of drug-loaded FUC microparticles were suspended in a test tube containing 10 mL of release medium, which was kept under mild shaking (100 rpm; Orbital Shaker OS 10, Biosan, Latvia) at 37 ºC (Dry line; VWR, USA). To determine the drug release over time, test samples were withdrawn (1 mL) at pre-established time intervals (5, 10, 15, 30 min), centrifuged (16000 *xg*, 15 min; Heraeus Fresco 17 Centrifuge, ThermoScientific, USA), and filtered (0.45 µm syringe filter). The drug content was determined in the supernatant by HPLC, using the protocol described in section 4.3.5. Calibration curves were obtained dissolving the drug analytical standards in the corresponding release medium.

4.5.2 Chitosan microparticles

Specifically, 15 mg of CS/INH (10/1) microparticles were incubated with release media (10 mL) and samples (1 mL) were collected, diluted (1:10) and spectrophotometrically measured at 268.5 nm to determine INH content. Similarly, aliquots (1 mL) obtained from the incubation of 30 mg of CS/RFB (10/0.5) microparticles with the release media (10 mL) were analysed at 500 nm. For analysing carriers containing the two drugs in combination, 15 mg of CS/INH/RFB (10/1/0.5) microparticles were accordingly incubated and the collected samples (1 mL) were measured at a wavelength of 500 nm to determine RFB content. Next, a 1:10 dilution was performed, and a further measurement was made at 268.5 nm in order to determine the drug content representing the sum of INH and RFB. At last, the amount of INH was obtained by subtracting the absorbance value at 500 nm from that of 268.5 nm.

Overall, tested samples were withdrawn at specific time intervals (15, 30, 45, 60, 120 min), centrifuged (16000 g, 15 min) and the supernatant filtered (0.45 µm syringe filter) before analysis. Adequate calibration curves were established by dissolving drug standards in the media, resulting from the incubation of unloaded CS microparticles with the referred medium (under the same conditions described above), followed by centrifugation (4000 rpm, 20 min; Centrifuge MPW 223e, Poland) and filtration (0.45 µm syringe filter).

Each drug release experiment was performed in triplicate. The percentage (%) of drug released over time was determined based on the following equation:

$$\text{Drug release (\%)} = (\text{Quantified drug at each time point} / \text{Initial drug content}) \times 100 \quad (6)$$

4.6 *In vitro* biocompatibility studies

4.6.1 Cell cultures

Cell lines representing the human alveolar epithelium (A549) and rat alveolar macrophages (NR8383) were purchased from the American Type Culture Collection (ATCC, UK) and used between passages 25–36 (A549) and 9–18 (NR8383). Particularly, A549 cells were maintained in DMEM, supplemented with 10% (v/v) FBS, 1% (v/v) L-glutamine solution 200 mM, 1% (v/v) non-essential amino acids and 1% (v/v) penicillin/streptomycin. For the assays, the adherent A549 cells were harvested using trypsin-EDTA solution. In turn, the semi-adherent NR8383 cells were grown in Ham's F12 containing 15% (v/v) FBS, 1% (v/v) L-glutamine and 1% (v/v) penicillin/streptomycin. After incubation, the non-adherent fraction of NR8383 cells was removed, adherent cells were scraped and used to perform the assays.

THP-1 human monocytic cells were obtained from the Leibniz-Institut DSMZ (Braunschweig, Germany) and used between passages 10–17. This cell line was cultured in suspension at a density of 0.2 – 0.8 x 10^6 cells/mL in RPMI 1640 medium, supplemented with 10% (v/v) FBS, 1% (v/v) L-glutamine and 1% (v/v) penicillin/streptomycin. THP-1 cells were differentiated to acquire the macrophage phenotype by treatment with phorbol 12-myristate 13-acetate (PMA, 50nM; 0.2 x 10^6 cells/mL, 48 h exposure) before performing the experiments.

A549 and NR8383 cell lines were grown using 75 cm^2 flasks for adherent cells whereas THP-1 cells were cultured in flasks for cells in suspension (75 cm^2). In general, cell cultures occurred in a humidified 5% CO_2 / 95% atmospheric air incubator at 37 ºC (HerAcell 150, Heraeus, Germany).

4.6.2 Assessment of metabolic activity by MTT test

The cytotoxic effect of microparticles was assessed on both A549 and macrophage-differentiated THP-1 cells using the tetrazolium reduction assay, known as the MTT test. The experiment is based on the ability of the compound (3-(4,5-dimethylthiazol-2-yl)-2,5-diphenyltetrazolium (MTT) to be enzymatically reduced by viable cells. The reaction induces a change in the colour of the reagent from yellow to purple. To perform the assay, A549 cells (1.0 x 10^4 cells/well) and macrophage-differentiated THP-1 cells (0.35 x 10^6 cells/well) were separately seeded onto 96-well plates (Orange Scientific, Belgium). Each well was filled with 100 µL of the respective cell culture medium (CCM) and the cells were allowed to attach for 24 h (37 ˚C and 5% CO_2 atmosphere). After this time, the cells were exposed to solutions of the polymers (FUC and CS as raw materials), unloaded and drug-loaded microparticles, for 3 and 24 h. The test solutions were previously prepared by dissolving the samples with the specific CCM (37 °C) without FBS at the concentrations of 0.1, 0.5 and 1.0 mg/mL. INH and RFB were also tested as free drugs at concentrations equivalent to their theoretical loading in the microparticles, i.e. respecting the polymer/drug mass ratio of 10/1 in the case of INH (0.01; 0.05 and 0.1 mg/mL) and 10/0.5 for RFB (0.005; 0.025 and 0.05 mg/mL). CCM and SDS (2%, w/v) were used as positive and negative controls of cell viability, respectively.

After the exposure time, 30 µL of MTT solution (0.5 mg/mL in PBS, pH 7.4) were added to each well and allowed to incubate for a period of 2 h at 37 ˚C. Thereafter, formazan crystals, formed during tetrazolium metabolisation, were solubilised with 50 µL of DMSO (A549 cells) or 70 µL of 10% (w/v) SDS in a 1:1 mixture of DMF:water (THP-1 cells). Finally, absorbance was determined by spectrophotometry (Infinite M200, Tecan, Austria) at 540 nm and corrected for background absorbance at 640 nm (288). Cell viability of treated cells was expressed as a percentage of that observed for the positive control. The assay was performed at least three times, with six replicates at each concentration of test solutions, including controls. Relative cell viability was calculated as follows:

$$\text{Cell viability (\%)} = (A - S) / (CM - S) \times 100 \quad (7)$$

where A is the absorbance obtained for each of the concentration of test solutions, CM is the absorbance observed for untreated cells (incubated with cell culture medium only) and S is the absorbance obtained for negative control of cell viability.

4.6.3 Evaluation of cell membrane integrity

The integrity of cell membrane was assessed on both cell lines (A549 and macrophage-differentiated THP-1 cells) by the quantification of lactate dehydrogenase (LDH) released upon exposure to the proposed formulations. Leakage of enzymes such as LDH is a well-known marker of cytotoxicity. The cytotoxicity of the produced microparticles was evaluated in parallel with the MTT assay described above. For the assay, A549 cells (1.0×10^4 cells/well) and macrophage-differentiated THP-1 cells (0.35×10^6 cells/well) tested in the MTT assay for 24 h with the formulations used at the highest concentrations (i.e.1 mg/mL) were assessed. After the exposure time, aliquots (100 µL) of cell supernatants were placed into eppendorfs and centrifuged (16000 *xg*, 5 min). The supernatant (75 µL) obtained upon centrifugation was transferred to a new 96-well plate and processed using a commercial LDH kit (Takara Bio, Japan). The absorbance was measured by spectrophotometry (Infinite M200, Tecan, Austria) at a wavelength of 490 nm (background correction at 690 nm). Cells incubated with CCM only were considered the negative control; those treated with Triton X-100 (10%, v/v) were used as the positive control, the latter being assumed as 100% of LDH release. Thus, measurements were performed in triplicate and the percentage of released LDH was determined based on the following formula:

$$\text{Released LDH (\%)} = (\text{Abs value} / \text{Abs T}) \times 100 \quad (8)$$

where Abs represents the absorbance obtained for the LDH release by the cells exposed to the test samples and Abs T is the absorbance obtained for cells treated with Triton X-100 (positive control).

4.7 Macrophage activation induced by microparticles

In order to evaluate the capability of microparticles to activate macrophage-like cells, differentiated THP-1 cells (0.35 x 10^6 cells/well) were incubated with dual drug-loaded microparticles, as well as with the polymers (commercial powders) at a concentration of 1 mg/mL. After a period of exposure of 24 h, cell-free supernatants were collected and cytokine content in the samples was measured using Quantikine® HS ELISA kits (R&D Systems, USA). TNF-α and IL-8 levels were quantified as the most relevant pro-inflammatory cytokines. The amount of each cytokine was expressed in *pg/mL* based on reference standard curves. The level of cytokines obtained from LPS- and CCM-treated cells was used as control. The absorbance of samples was determined at 450 nm in a microplate reader (Infinite M200; Tecan, Austria) and corrected for background absorbance at 540 nm.

4.8 Preliminary evaluation of microparticle uptake by macrophages

The uptake of the produced microcarriers by macrophage-like cells was evaluated by flow cytometry (FacScalibur cell analyser, BD Biosciences, Belgium), which required the exposure of cells to fluorescently-labelled particles (production detailed in section 4.2.3).

The assay was performed using macrophage-differentiated THP-1 and rat alveolar macrophage (NR8383) cells. For the assay, phorbol-differentiated THP-1 (0.35 x 10^6 cells/mL) and NR8383 (0.2 x 10^6 cells/mL) cells were seeded (5 mL/well) into 35 mm-Petri dishes containing 5 mL of the respective complete medium. Cells were incubated for 24 h to ensure the adhesion of 50 – 75% of the original population. Next, fluorescent microparticles (50 and 200 µg/cm^2) were aerosolised onto the macrophage layer using a Dry Powder Insufflator™ (Model DP-4, Penn-Century™, USA). Cells that were not submitted to the contact with fluorescent microparticles were considered as negative control. The phagocytic process occurred upon incubation for 2 h at 37 ºC and was stopped by the addition of a cold solution of PBS.3% FBS (5 mL, two applications). Then, cells were scraped, re-suspended in 3 mL of PBS.3% and centrifuged (1500 rpm, 2 min, room temperature, centrifuge MPW-223e, MedInstruments, Poland). The centrifuged cells were washed with PBS.3% (5 mL) thrice and, finally, re-suspended in 1 mL buffer for flow

cytometric analysis (BD Biosciences FACSCalibur, Belgium). For this purpose, side scatters light was used to distinguish the viable cell population, whereas FSC-H and SSC-H channels were applied to measure size and granularity of cells, respectively. A total of 10000 events was counted within a gated region and the data were presented as mean fluorescence (FL) intensity. The number of cells associated with fluorescence was considered the definition for uptake. The assay was replicated at least three times for each dose.

4.9 *In vitro* antibacterial activity

4.9.1 Culture of mycobacteria

The therapeutic efficacy of microparticles was evaluated *in vitro* against *Mycobacterium bovis* BCG (DSMZ 43990). This was provided, as a gift, by Centro de Estudos de Doenças Crónicas da Faculdade de Ciências Médicas da Universidade Nova de Lisboa (CEDOC/FCM-UNL). The stocks of mycobacteria were preserved and stored in -80ºC ultra-low temperature freezers (U725 Innova New Brunswick Scientific, USA). Mycobacteria were cultivated in M7H9 broth, supplemented with 10% (v/v) OADC and 0.05% (v/v) of Tween® 80. Mycobacteria were handled inside a laminar flow hood (Bio48 Faster, Italy), respecting the guidance and safety requirements to prevent contamination. That includes autoclave sterilisation (Uniclave88, Portugal) of infectious materials.

4.9.2 Determination of minimum inhibitory concentration (MIC)

The lowest concentration of free antibiotics required to inhibit mycobacteria growth was determined by the MTT assay (289). Firstly, stock solutions of INH (1 mg/mL) and RFB (1 mg/mL) were prepared by dissolving the drugs in the M7H9 supplemented medium. It is important to mention that RFB was previously solubilised in ethanol and only thereafter diluted with M7H9 broth. Stock solutions were filtered (0.22 µm sterile syringe filter) and mixed at concentrations proportional to the drug mass ratio contained in the microparticles. The microparticle formulations undergoing this assay were those containing the combination of drugs (FUC/INH/RFB and CS/INH/RFB = 10/1/0.5, w/w). Therefore, drug solutions were

mixed respecting these ratios. The susceptibility of *M. bovis* strain was then evaluated by incubating mycobacteria with a drug solution combining INH-RFB, followed by serial dilutions.

Similarly, the growth inhibition of mycobacteria promoted by the produced dual drug-loaded microparticles was also assessed. Dry powder was dissolved with broth (1 mg/mL) and then diluted, based on the calculations to meet the desired drug concentrations. Generally, 96-well flat-bottom microplates (Orange Scientific, Belgium) were filled with test samples, according to the scheme displayed in Figure 4.2. Three bacterial suspensions were prepared, and the assays were conducted after achieving an optical density value (OD_{nm}) of approximately 0.2, measured by spectrophotometry (600 nm, Infinite M200, Tecan, Austria). For the experiment, solutions (180 µL) of free drugs or microparticles were added into the wells (column 4), making continuously serial two-fold dilutions with M7H9 supplemented broth (columns 5 – 11). Next, 20 µL of bacterial suspension were added into the respective well, completing the final volume of 200 µL per well. Wells (column 2) filled with only M7H9 supplemented medium (200 µL) were used as negative controls. Similarly, bacterial suspensions (20 µL) were introduced in wells (column 3) containing M7H9 medium (180 µL) in the absence of free drugs/microparticles, which were assumed as positive controls. Bacterial growth of each suspension 1, 2 and 3 was evaluated in B-C, D-E, and F-G rows, respectively. Assays were performed in triplicate.

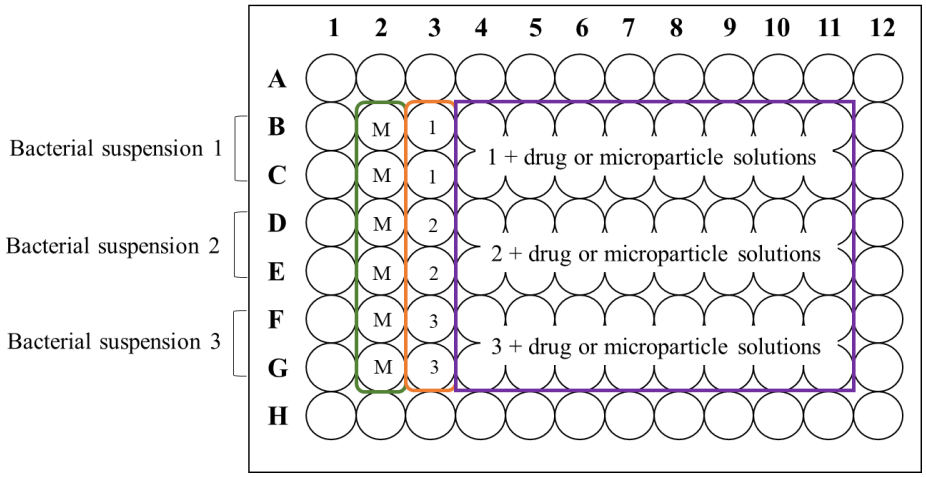

Figure 4.2. Scheme of the 96-well microplate showing columns 4-11 filled with solutions of free drugs or microparticles serially diluted with M7H9 broth, containing mycobacteria in triplicate: lines B-C (suspension 1), lines D-E (suspension 2) and lines F-G (suspension 3). Contents of column 2 (only M7H9 medium) and column 3 (bacterial suspensions in broth) were considered negative and positive control, respectively.

The outside lane of wells (a frame-like) was filled with sterile distilled water to avoid the evaporation of microplate content. The plates were covered with the lid, sealed with parafilm, and incubated at 37 °C (Binder, USA) for 7 days. After the incubation time, 30 µL of MTT sterile solution were added to each well, followed by 1 h of incubation at 37 °C. Then, 50 µL of DMSO were added into the wells, resulting in a colour change from yellow to dark gold, proportional to the growth rate of mycobacteria. The absorbance was measured by spectrophotometry (Infinite M200, Tecan, Austria) at 540 nm.

4.10 Preliminary *in vivo* studies

Male BALB/c mice were obtained from the Gulbenkian Institute of Science (Oeiras, Portugal). The animals were maintained under standard pathogen-free conditions and were fed commercial chow and given free access to acidified drinking water. The experimental procedures were approved by the local ethical committees of the Faculty of Pharmacy and of the Institute of Molecular Medicine in accordance with the European Union Directive (201/637EU) and Portuguese laws (DR 113/2013, 2880/2015 and 260/2016.

Animals (aged 6 – 8 weeks) weighing 18 – 31 g received unloaded FUC or CS microparticles via pulmonary administration, using the method described by Gaspar et. al. (290). Briefly, the dry powder was administered by using a simple apparatus based on a 15-mL conical centrifuge tube in which the dry powder was inserted. A small hole was made at the bottom of the tube allowing the powder delivery to the mouse. A manual pump connected to the upper part of the tube allowed the production of a turbulent air stream for fluidising the powder. Each mouse was restrained in a 50-mL conical tube which had a small hole made at the bottom. The lower part of the tube was connected to the 15-mL tube through a baby bottle teat. Dry powder (60 mg) were inserted in the device and each mouse (four mice per group) received unloaded microparticles by inhalation upon 2 min, once a day, for two weeks. A control group of mice received no treatment.

On the first day of treatment, before powder inhalation, blood samples (100 – 200 µL) were collected from the tail vein into tubes with no anticoagulant. Following centrifugation, serum aliquots (30 – 50 µL) were prepared and stored at -30 °C. After 2-weeks of treatment, mice were anaesthetised with isoflurane, samples of blood were collected from the retinal blood vessels and a few drops of peripheral blood were used to prepare blood smears (three slides per mouse). Moreover, the remaining blood samples were then centrifuged to separate the serum, which were stored at -30°C for further analysis to detect serum immunoglobulin E (IgE).

4.10.1 Eosinophil count on blood smears

Slides with blood smears were stained by Wright–Giemsa staining method (291). A total of 100 leucocytes were counted in each blood smear with the use of a light microscope (Microscope TR 500, VWR International, Belgium). Twelve slides (blood smears) were included in the count, considering three slides per mouse in each of the group (n=4).

4.10.2 Ouchterlony double immunodiffusion to detect serum immunoglobulin E (IgE).

Ouchterlony double immunodiffusion technique was performed to determine if IgE was present in sera from mice treated with unloaded FUC and CS microparticles (292). To obtain positive control samples, C57BL/6J mice (Charles River, France) were sensitised to OVA (0.1 mg/mL in PBS). The intraperitoneal injection of OVA (200 µL) was performed twice with an interval of 2 weeks between administrations. Polyclonal IgE antiserum (Nordic Immunology, Netherlands) was used as the primary antisera to detect IgE in the serum samples. The antisera was diluted (1:2) with Tris-base (Nzytech, Portugal). A pool of mouse serum (8 µL) was prepared by combining the sera collected from the OVA-sensitised animals. Likewise, equal volumes of serum collected from the treated mice of each group were combined to prepare a pool (8 µL).

For the Ouchterlony assay, agar gel/phosphate saline buffer 1.5% (w/v) was poured to a depth of 3 mm onto glass slides (25 x 75 mm) that were coated with dried 1% (w/v) agar gel/water. Wells were made using a template and gel punch; the agar plugs were removed from wells using a water vacuum pump. The assay format consisted of a central well surrounded by three equidistant wells.

The antisera solution (8 µL) was placed in the central well and the peripheral wells were filled with the pools of treated mouse sera and the positive control (8 µL). Slides were set on a horizontal surface and incubated in a moist chamber at 4°C for two days. Afterwards, they were washed with PBS buffer several times and stained with Coomassie Brilliant Blue G 250 (Serva, Germany). The slides were destained in 10% methanol (v/v) / 10% acetic acid (v/v) for 5 min and then washed with distilled water. Results were scored based on the observation of a visible line of precipitation.

4.11 Statistical analysis

Statistical significance was determined with student t-test and one-way analysis of variance (ANOVA) with the pairwise multiple comparison procedures (Holm-Sidak method), which were performed to compare two or multiple groups. Analysis was run using the Sigmaplot software (version 12.5, Systat Software Inc., UK). and differences were considered significant at a *p*-value of less than 0.05.

This page was intentionally left in blank

Chapter Five

Fucoidan Microparticles: Results and Discussion

The information presented in this chapter was partially published in the following publications:

1. Ludmylla Cunha, Ana M. Rosa da Costa, João P. Lourenço, Francesca Buttini and Ana Grenha. Spray-dried fucoidan microparticles for pulmonary delivery of antitubercular drugs. *Journal of Microencapsulation* ***2018***, 35(4),392-405; doi: 10.1080/02652048.2018.1513089
2. Ludmylla Cunha, Susana Rodrigues, Ana M. Rosa da Costa, M. Leonor Faleiro, Francesca Buttini and Ana Grenha. Inhalable fucoidan microparticles combining two antitubercular drugs with potential application in pulmonary tuberculosis therapy. *Polymers* ***2018***, 10(636),1-19; doi: 10.3390/polym10060636

This page was intentionally left in blank

5. Fucoidan microparticles: Results and discussion

5.1 Preparation and characterisation of fucoidan microparticles

The rationale of selecting FUC as matrix material of inhalable microparticles, aimed at tuberculosis therapy, relies on its chemical composition, which includes moieties that enable macrophage targeting. For this reason, FUC-based microparticles reported herein were produced with a higher amount of polymer, comparing with drugs, to provide the means for polymer interaction with macrophages, and therefore to favour microparticle uptake (36). Moreover, drug concentrations were selected to produce microparticles that, when used in *in vivo* studies, permit a reduction of the dose administered by inhalation in comparison with oral delivery.

FUC microparticles associating each drug separately were successfully obtained by spray-drying and were recovered with yields of 74% – 78% (Table 5.1). As well, spray-dried FUC microparticles loaded with a combination of the two first-line anti-TB drugs (INH and RFB) were produced with high yield (81%) indicating the effectiveness of the technique. The use of the high-performance cyclone instead of the conventional cyclone separator certainly contributed to the high yields, an effect that was previously reported (72) and further observed in other works of our research group (293).

Table 5.1. Spray-drying yield, drug association efficiency, loading capacity, Feret´s diameter, median volume particle size (D_v50) and density values of fucoidan (FUC)-based microparticles (mean ± SD, *n* = 3). INH: isoniazid; Man: mannitol; RFB: rifabutin.

Microparticles	Production yield (%)	Association efficiency (%)	Loading capacity (%)	Feret´s diameter (µm)	D_v50 (µm)	Span	Density (g/cm^3)		
							Real	Bulk	Tap
Unloaded FUC	85 ± 1	–	–	1.62 ± 0.80	–		1.78 ± 0.01	0.45 ± 0.06	0.77 ± 0.19
Unloaded FUC-Man	79 ± 1	–	–	1.60 ± 0.93	–		1.66 ± 0.01	0.26 ± 0.04	0.51 ± 0.07
FUC-Man/INH (10/1)	74 ± 6	95 ± 1	8.6 ± 0.4	1.90 ± 0.98	3.97 ± 0.11	1.76 ± 0.05	1.51 ± 0.01	0.22 ± 0.02	0.43 ± 0.04
FUC/RFB (10/0.5)	78 ± 5	81 ± 3	3.9 ± 0.3	1.40 ± 0.70	2.51 ± 0.02	1.99 ± 0.05	1.77 ± 0.01	0.17 ± 0.01	0.33 ± 0.02
FUC/INH/RFB (10/1/0.5)	81 ± 2	97 ± 4 (INH) 95 ± 4 (RFB)	8.5 ± 0.4 (INH) 4.1 ± 0.2 (RFB)	1.43 ± 0.75	2.77 ± 0.03	2.91 ± 0.07	1.74 ± 0.01	0.17 ± 0.01	0.35 ± 0.02

Considering the carriers loaded with one antibiotic, drug association efficiencies were 81% for RFB and 95% for INH, resulting in loading capacities of 3.9% (RFB) and 8.6% (INH) (Table 5.1), values close to the theoretical drug loadings (9.1% for INH and 4.8% for RFB). When combined in the same formulation (FUC/INH/RFB MP), drugs were also efficiently associated to microparticles, with INH registering 97% and RFB 95% of association efficiency. In this case, loading capacities reached 8.5% (INH) and 4.1% (RFB), again close to the theoretical values. In all formulations, the selected theoretical drug loadings are similar to those reported in other works (294). The fact that both drugs were associated with similar efficiencies demonstrates that the process was independent of their aqueous solubility (125 mg/mL for INH and 0.19 mg/mL for RFB) (135,295). In general, the obtained values of drug association are considered high, which is tipical of spray-dried microparticles, as the method is frequently reported to lead to high association of drugs (296). Furthermore, the approach of associating anti-TB drugs in a single formulation meets the recommendations of the WHO regarding the need to establish a combined therapy for TB (261). It is worth mentioning that INH is present in a higher amount than RFB, because the latter is a more potent drug (297), and also has a more toxic profile, as will be demonstrated later on in Section 5.7 (Chapter 5).

In general, particles presented a spherical or approximately spherical shape, although with distinct surface features. The morphological analysis performed with electronic microscopy revealed that the unloaded microparticles exhibited a slightly convoluted shape but smooth surface (Figure 5.1a). However, the incorporation of drugs in the microparticles produced important modifications on their morphology, which became more irregular and acquired corrugated surfaces (Figure 5.1b,c), particularly the two formulations containing RFB. This morphology is possibly the result of uneven shrinkage forces occurring during the drying of droplets, depending on the feed composition and process conditions (95). In these cases, the presence of RFB may have contributed to the morphological alterations perceived on the produced microparticles, as the observed surface irregularities have been reported for other spray-dried microparticles loaded with this drug (239). The irregular surface can also be thought as a result of the drying process, in which the removal of ethanol from the microparticles' surface occurs faster than water evaporation. The higher volatility of ethanol induces the formation of a primary shell that collapses as the water content in the core evaporates (298).

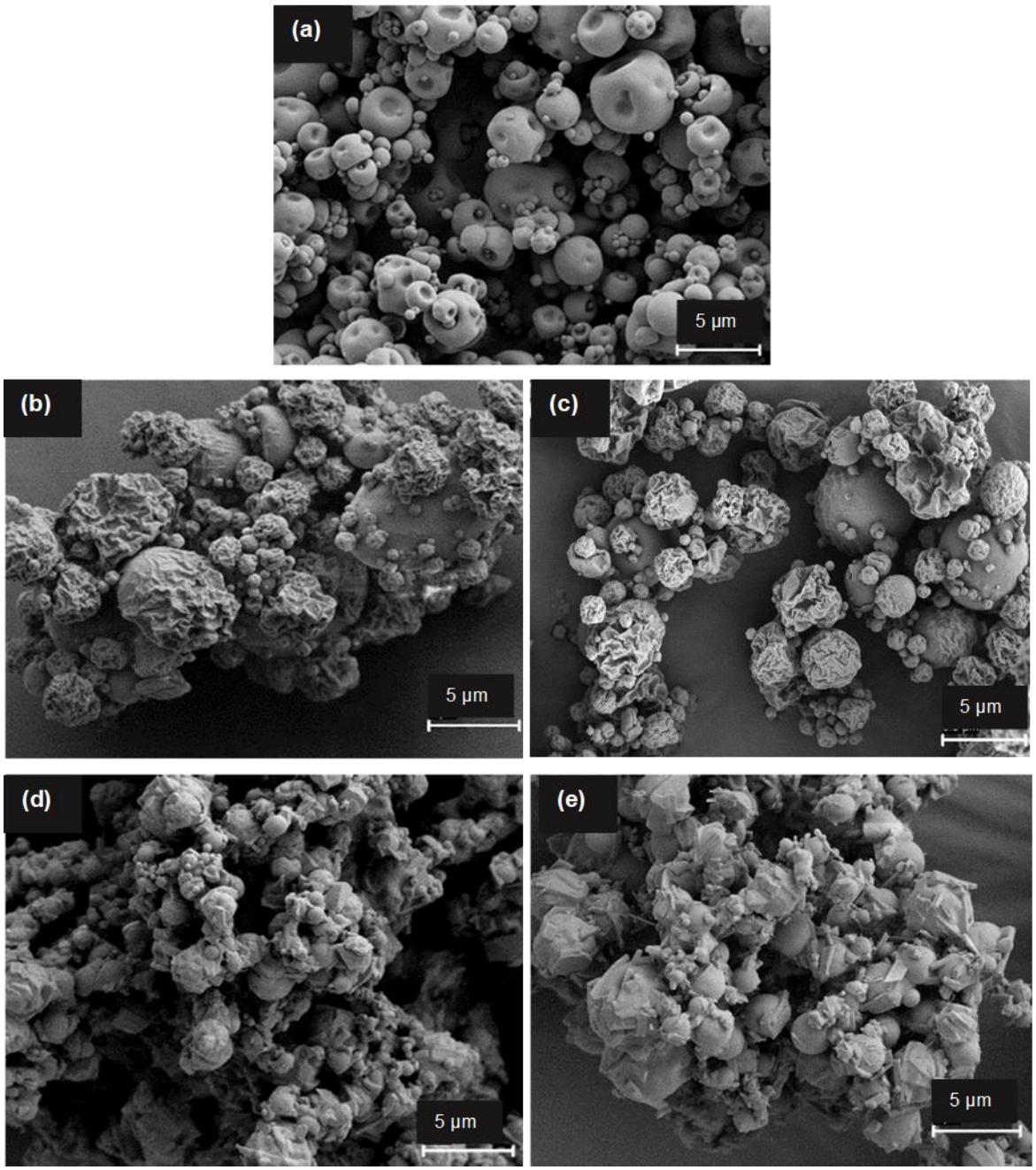

Figure 5.1. Scanning electron microphotographs of fucoidan (FUC)-based microparticles: (a) unloaded FUC microparticles, (b) FUC/RFB = 10/0.5 (w/w) microparticles; (c) FUC/INH/RFB = 10/1/0.5 (w/w) microparticles; (d) unloaded FUC-Man microparticles; (e) FUC-Man/INH = 10/1 (w/w) microparticles. INH: isoniazid, Man: mannitol, RFB: rifabutin.

As previously mentioned in the methodology, Man (0.5%, w/v) was incorporated in the formulation associating only INH, as producing microparticles only with FUC and INH, led to large aggregates clearly observed in the collecting

vessel. Their formation could not be avoided by simple optimisation of spray-drying parameters. The incorporation of Man produced significant and visible changes in microparticle morphology. As depicted in Figure 5.1d, Man has apparently deposited over microparticles surfaces as crystals of different forms (acicular, hexagonal, etc.), which is also observed in Figure 5.1e, depicting FUC-Man microparticle further associating INH. The formation of the referred crystals is possibly related to the outlet temperature of the spray-drying process, as the appearance of small crystals is favoured by the rapid drying of the droplets due to high temperatures (299). Further associating INH did not induce morphological alterations comparing with FUC-Man microparticle (Figure 5.1d).

Drug-loaded microparticles were found to have Feret's diameter ranging from 1.40 to 1.90 µm, as displayed in Table 5.1. No significant differences in microparticle size were noticed after drug incorporation (around 1.6 µm for unloaded FUC microparticles), which was expected considering the relatively low theoretical loading. Additionally, the particle size distribution of drug-loaded formulations was further measured as volume diameter by laser light scattering and showed median diameters (Dv50) varying between 2.51 and 3.97 µm (Table 5.1). In addition, span values ranged from 1.8 to 2.9 µm. The particle size distribution reflects the productive efficiency of spray-drying to provide dry powders with favourable aerodynamic properties for inhalation purposes (300). In this sense, the obtained results indicate that the produced microparticles present a suitable size for pulmonary deposition (301). To the best of our knowledge, no study to date has reported the production of inhalable microparticles based only on FUC with potential application in pulmonary TB therapy. Moreover, this is the first study describing the use of spray-drying to produce respirable FUC-based microparticles loaded with one or two first-line anti-TB drugs.

Real, bulk and tap densities were determined (Table 5.1), considering that the density of particles is an important factor for successful application in inhalation because it strongly influences the sedimentation and dispersion properties of inhalable dry powders (66). Real densities of spray-dried powders ranged from 1.51 to 1.78 g/cm^3, high values that could suggest that particles have a matrix dense core. Because of the method of determination, bulk densities had decreased values, varying between 0.17 and 0.45 g/cm^3, while tap densities were in the range of 0.33

– 0.77 g/cm^3. These results are similar to others reported for spray-dried microparticles (302,303). In this case, the dry powders with the lowest apparent particle density are those containing RFB. Generally, low tap density powders are considered good for dispersibility, which may be the result of the airiness produced by the irregular and wrinkled surfaces (304), such as observed for both FUC/RFB and FUC/INH/RFB formulations. It is important to stress that, from an eye observation, the presence of RFB seemed to improve microparticle dispersibility, as verified in other studies with polymeric microparticles (135). In fact, experimental determination of aerosolisation properties has been performed to reinforce this observation, as is discussed later on.

5.1.1 Dry powder analysis using Powder X-Ray Diffraction (PXRD)

The produced dry powders were analysed by X-Ray diffraction in order to qualitatively determine the phases present in the samples. Figure 5.2 presents the corresponding diffractograms. The presence of sharp peaks of free INH demonstrate its crystalline nature, which is slightly altered after its association with the microparticles (Figure 5.2b). This indicates a phase transition resulting from a new arrangement of atoms, that can lead to the appearance or disappearance of new diffraction peaks, according to the symmetry of the new phase (305). Spray-drying had much stronger impact on the structure of RFB, since the drug apparently acquires an amorphous form after undergoing the process. Another explanation for such modification would be the formation of small RFB crystals during spray-drying in such a way that prevents their detection by the XRD equipment (Figure 5.2c). Nevertheless, the technique is in fact reported to modify the crystalline form of both drugs (306,307). This may have implications on physicochemical properties such as solubility, release profile, stability, and therapeutic efficacy of drugs (308). Indeed, amorphous state increases the aqueous solubility, which reflects on drug release profile, as will be further discussed in this chapter. Nonetheless, such modifications had no impact on drug antibacterial activity, as it will be demonstrated in section 5.7. Long-term stability is a matter of concern though, since amorphous materials are inherently unstable and tend to recrystallise upon storage (309).

As aforementioned, the incorporation of Man in microparticles apparently resulted in a deposition of crystals of different forms (acicular, hexagonal, etc.) over the surfaces of FUC-Man (unloaded) and FUC-Man microparticles associating INH. In both cases the formation of a crystalline phase was observed by XRD (Figure 5.2a). Data suggest the existence of different polymorphs of Man in the two samples, although further structural testing is needed to confirm these observations.

Fucoidan diffractogram shows that there are no reflection peaks, indicating that the polymer is amorphous in nature, displaying similar diffraction patterns after being spray-dried to produce the microparticles (Figure 5.2a). The diffractograms of drug-loaded FUC microparticles evidenced the absence of drug crystalline peaks, which indicates amorphisation or reduction of drug crystallite size (310). Drug amorphisation is also an evidence of the drug-polymer interaction, demonstrating successful incorporation into the polymeric matrix.

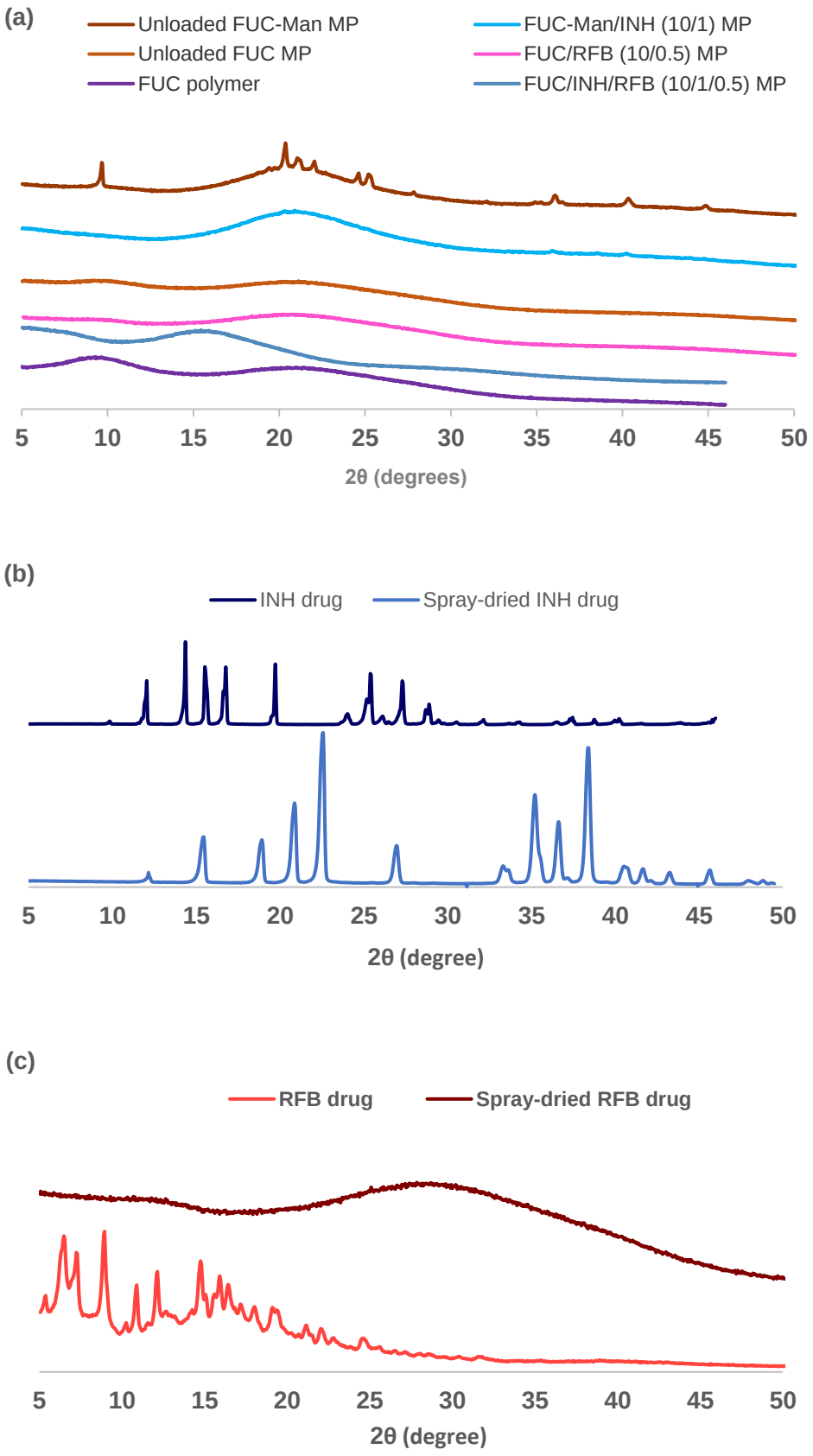

Figure 5.2. Diffractograms of (a) fucoidan (FUC) polymer, unloaded and drug-loaded FUC microparticles; (b) free isoniazid (INH) before and after spray-drying, (c) free rifabutin (RFB), before and after spray-drying.

5.2 Evaluation of aerodynamic properties

The design of inhalable microparticles requires adequate flowability to promote lung deposition. In light of this, the *in vitro* aerosol performance was assessed in the ACI by using an RS01 dry powder inhaler. The obtained data are presented in Table 5.2.

Table 5.2. Aerodynamic properties of fucoidan (FUC) microparticles loaded with isoniazid (INH) and/or rifabutin (RFB). Loaded amount of powder in the capsule was 30 mg, corresponding to approximately 2.6 mg of INH and 1.4 mg of RFB, according to the drug content found in each formulation (*n* = 3, mean ± SD). FPD: fine particle dose; FPF: fine particle fraction; Man: mannitol; MMAD: mass median aerodynamic diameter.

Microparticles (Polymer/drug ratio, w/w)		Metered dose (mg)	Emitted dose (mg)	MMAD (µm)	FPD <5 µm (mg)	FPF <5µm (%)
FUC-Man/INH (10/1)		2.02 ± 0.06	1.98 ± 0.05	3.78 ± 0.14	0.78 ± 0.01	39.1 ± 1.1
FUC/RFB (10/0.5)		1.15 ± 0.01	0.97 ± 0.01	1.99 ± 0.01	0.53 ± 0.01	55.0 ± 0.1
FUC/INH/RFB (10/1/0.5)	**INH**	1.91 ± 0.26	1.64 ± 0.23	3.90 ± 0.01	0.82 ± 0.02	50.2 ± 2.4
	RFB	1.29 ± 0.03	1.10 ± 0.02	3.64 ± 0.32	0.53 ± 0.01	45.4 ± 1.4

Regarding the formulations that associate only one antibiotic, the results demonstrated that 98% of the loaded INH and 84% of RFB were emitted from the device, indicating the suitability of FUC to be used as a matrix material in spray-dried inhalable microparticles. The better flowability of FUC-Man/INH microparticles may be related to the incorporation of Man in the formulation. Man is a non-hygroscopic sugar (311) and the visible deposition of crystals on the surface conferred roughness, thus avoiding microparticle aggregation. Similarly, the irregular surfaces observed in FUC/RFB microparticles have possibly contributed to the good dispersibility and flow properties of the formulation, as surface irregularities can reduce the contact between microparticles, thus decreasing agglomeration (78).

With respect to the formulation containing both INH and RFB, the results demonstrated that more than 85% of the drugs were emitted from the device, also indicating good dispersibility of the produced dry powder. In the sequence of the previous comments, the adequate flowability is possibly a result of the wrinkled surfaces observed in the produced microparticles. Surface irregularities are

expected to reduce the interparticulate cohesive forces that lead to agglomeration, enhancing powder dispersibility, as well as improving the respirable fraction of the formulation (78,298). This aspect is crucial when a lactose carrier (or other) is not included in the formulation, and spray-dried microparticles are aerosolised alone (312). As depicted in Table 5.2, the produced powders showed FPF (≤5 μm) ranging within 39–55%, which represents the fraction of microparticles with potential ability to reach the respiratory zone. Overall, the results are in agreement with the *in vitro* respirability usually exhibited by dry powder inhaler formulations (301). Additionally, the use of the RS01 device may have contributed to the maximisation of the performance, as it is described that the spinning capsule rotation provided by this inhaler is more efficient in powder disaggregation compared with other capsule motion profiles (313,314).

Figure 5.3 illustrates the stage-by-stage deposition profiles of INH and RFB in the ACI after aerosolisation of different microparticle formulations. The drug recovery varied between 82 and 99%, being in accordance with the values established by the European Pharmacopeia (75). Observing the distribution, it is visible that FUC-Man/INH microparticles deposited more in the upper part stages, while FUC/RFB microparticles were able to deposit on stages 3–4 (Figure 5.3a), which collect particles <3.2 μm, potentially capable to reach the deep zones of the lung. According to drug mass deposition on ACI stages, the MMAD of drug particles was estimated as 3.78 μm and 1.99 μm for FUC-Man/INH and FUC/RFB, respectively, which certainly justifies the previous observation.

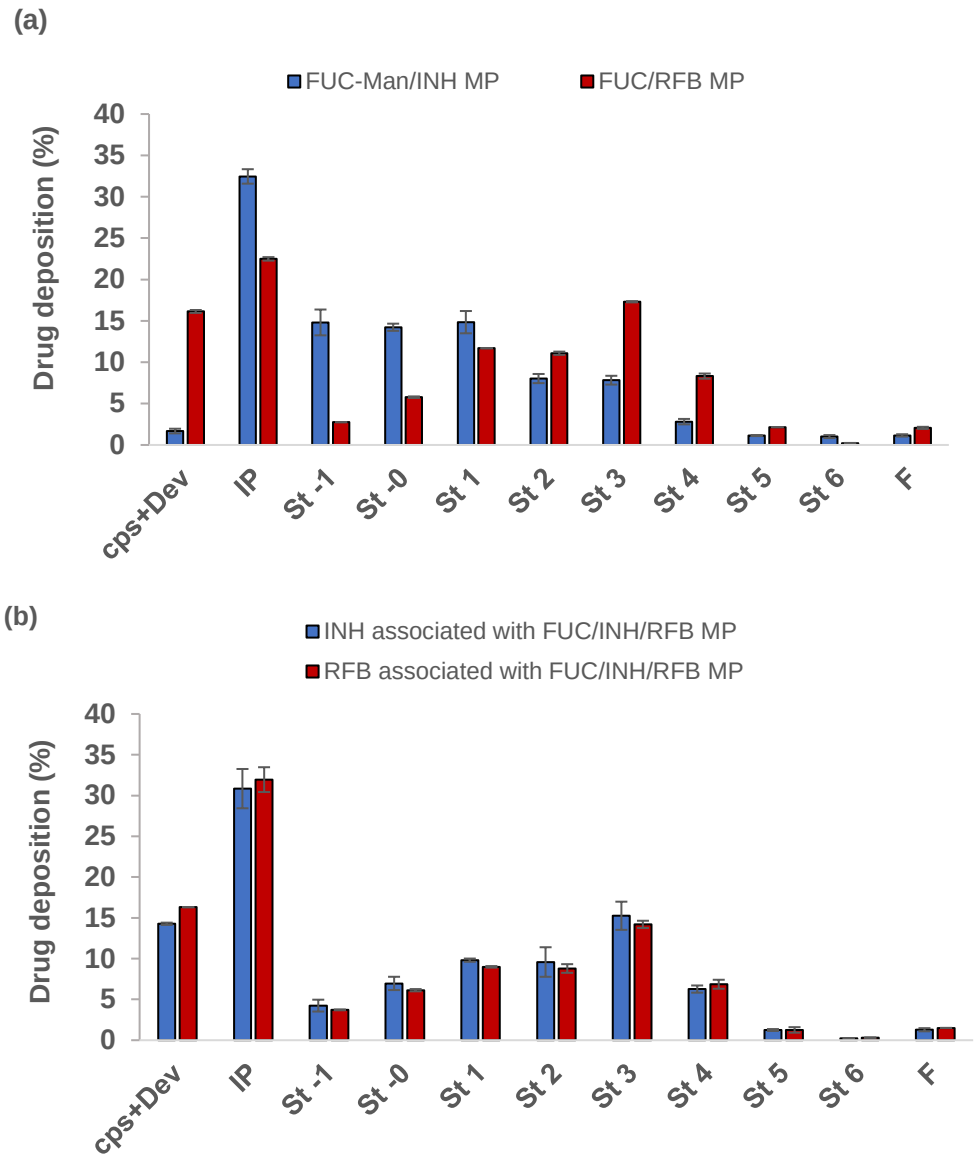

Figure 5.3. *In vitro* aerodynamic deposition of antitubercular drugs (isoniazid – INH and rifabutin – RFB) in the Andersen cascade impactor. Drugs associated with fucoidan (FUC) microparticles (MP) either individually (a) or together in a single formulation (b). Values are mean ± SD, *n* = 3. Cps: capsule; Dev: inhaler device; IP: induction port; F: filter; Man: mannitol; St: stage.

Differently, the dry powder associating simultaneously the two antibiotics, displayed uniformly drug deposition (Figure 5.3b). The similarity between the profiles of both drugs demonstrates that INH and RFB were equally co-deposited on the several stages, thus supporting the decision of developing a delivery system with a combination of the two drugs. Furthermore, this indicates that the drugs have even distribution within the microparticles. For this formulation, drug mass

deposition on ACI stages resulted in MMAD values of 3.6 – 3.9 µm, also suggesting a suitable size for deep lung deposition. In fact, particles with an aerodynamic diameter within the range of 1–5 µm display a greater tendency for reaching the respiratory zone and, if with extrafine size (<2 µm), they have more peripheral deposition within the area (315).

In summary, the produced FUC-based microparticles were demonstrated to have adequate aerodynamic characteristics for the pulmonary delivery of anti-TB drugs with great propensity to reach the respiratory zone, possibly with better respirability being expected for microparticles associating RFB as single drug. Additionally, the developed microparticles also displayed particle sizes in the range expected to potentiate phagocytosis by alveolar macrophages (1–6 µm), the target cells (104).

5.3 *In vitro* drug release profiles

The *in vitro* release of drugs was evaluated in PBS (pH 7.4) with the addition of 1% (v/v) Tween® 80, resembling the lung lining fluid in terms of pH and the presence of surfactant (316,317). The latter also enables the dissolution of RFB, which is sparingly soluble in aqueous media. Considering that alveolar macrophages are the target cells in this study, drug release studies were also conducted in citrate buffer (pH 5), simulating the phagolysosomal environment (318). The obtained results are shown in Figure 5.4.

Figure 5.4a comprises the release profile of INH and RFB from formulations containing each drug separately (thin lines). The dissolution profiles of free drugs are also presented (dashed lines). As can be observed, at pH 7.4, the release of INH and RFB from microparticles was very rapid, drugs being completely released after 15 min (Figure 5.4a). The rapid release of INH was expected, owing to the high solubility of the drug. However, the release of RFB followed a similar pattern at all time points and no significant differences were perceived comparing the release profiles of the two antibiotics. Assuming that macrophage uptake will occur in the sequence of the application of these microparticles, drug release studies were also conducted in citrate buffer (pH 5), simulating the phagolysosomal environment, as referred above. As depicted in Figure 5.4b, drugs were released in similar fast

manner and no significant differences were observed between the two media, indicating that the release of drugs was not influenced by pH, in this case.

Likewise, the two drugs were rapidly released from the microparticles associating INH and RFB simultaneously. In this case, INH is completely available after 10 min, disregard the pH of the release medium (Figure 5.4c,d). At pH 5, RFB released precisely at the same rate as INH (Figure 5.4d). In turn, at pH 7.4, the release was a little bit slower, although not to a statistically significant level (Figure 5.4c). At pH 7.4, approximately 75% of the RFB was released within 10 min, and 100% was released within 30 min (Figure 5.4c). The faster release in acidic medium is possibly a consequence of a certain protonation of the drug, which increases its solubility. However, no significant difference was perceived at any time point, demonstrating once more that the release of the two drugs from the formulation was not significantly influenced by pH.

Importantly, the release of drugs from the produced microparticles did not show significant differences from the respective drug dissolution profiles (Figure 5.4a-d). It should be noticed that the spray-drying process modifies the crystalline form of both drugs, especially RFB, as reported in the literature (306,307) and was also verified in the present study (section 5.1.1). As a result, the aqueous solubility of drugs is increased due to the conversion into amorphous form or alterations in the regular ordered arrangement (319).

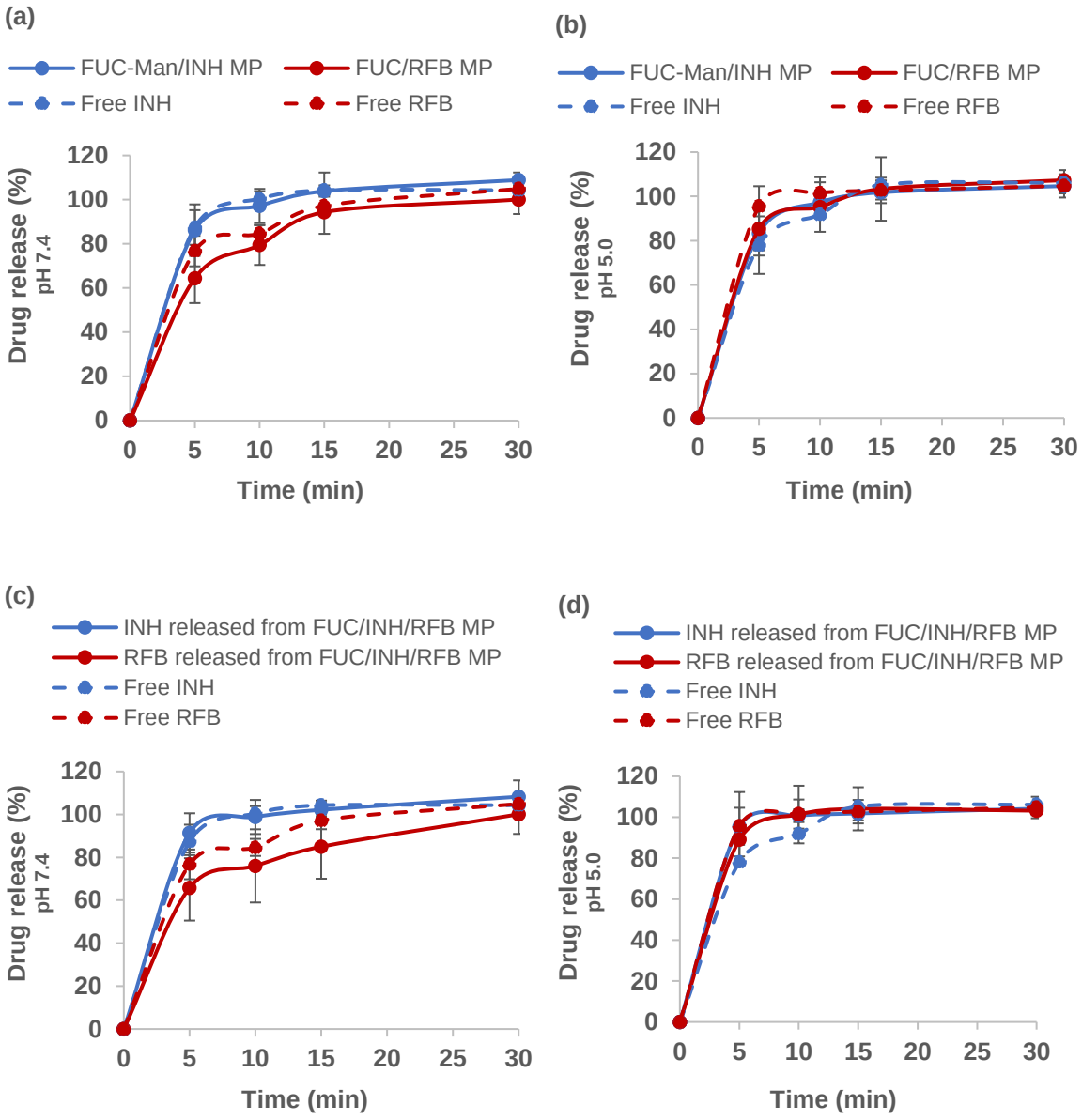

Figure 5.4. Drug dissolution and *in vitro* release profiles of isoniazid (INH) from FUC-Man/INH (10/1, w/w) microparticles and of rifabutin (RFB) from FUC/RFB microparticles (10/0.5, w/w), in (a) PBS pH 7.4-Tween® 80 and (b) citrate buffer pH 5.0-Tween® 80, at 37 °C. Drug dissolution and *in vitro* release profile of INH and RFB from FUC/INH/RFB (10/1/0.5, w/w) microparticles in (c) PBS pH 7.4-Tween® 80 and (d) citrate buffer pH 5.0-Tween® 80, at 37 °C. FUC: fucoidan; Man: mannitol; mean ± SD, *n* ≥ 3.

These results are in agreement with other studies reporting rapid release profiles of INH and RFB from spray-dried polysaccharide microparticles (135,306). The rapid release could be explained by two main factors: the surface irregularities, which increase the contact with the medium, and the high solubility of the polymeric

matrix. FUC is very soluble in the media, thus easily releasing the drugs. However, it is worth mentioning that the observations of this study do not precisely predict *in vivo* occurrences, considering that a lower amount of liquid is present in the alveoli compared with that involved in the assays. It is well known that the alveolar epithelium is covered by a thin layer (0.01–0.1 μm) of lung lining fluid, and thus microparticles are expected to be only partially in contact with this fluid, and not immersed in it (320,321). Consequently, *in vivo* drug release will probably occur more slowly, allowing microparticle internalisation by macrophage cells before particle dissolution and complete drug release.

5.4 *In vitro* biocompatibility studies

5.4.1 Assessment of metabolic activity by MTT test

The metabolic assay MTT was performed to evaluate the effect of the produced microparticles on cell viability, upon 3 h and 24 h exposure. Considering the environment underlying tuberculosis pathogenesis, alveolar epithelial cells (A549) and macrophage-differentiated THP-1 cells were used. For the purpose of this discussion, it was considered that a material has cytotoxic potential when it reduces the cell viability below 70%, as designated by ISO 10993-5 (322).

Figure 5.5 shows the results obtained for A549 cells. Overall, cell viability remained over 75%, except upon exposure to RFB as a free drug, at the highest tested concentration (0.05 mg/mL). In this case only, time- and concentration-dependent effects were observed ($p < 0.05$) for RFB, decreasing cell viability below 70%. For this drug, exposure to 0.05 mg/mL induced 69% cell viability at 3 h and 49% at 24 h (Figure 5.5d). However, the microencapsulation of RFB seemed to reverse this behaviour, eliciting cell viabilities between 74 and 97% (Figure 5.5a,b) for RFB-loaded microparticles (single drug formulations); and 76% – 98% for microparticles combining the two drugs (FUC/INH/RFB formulations). This indicates that microencapsulation had a beneficial impact on drug toxicity, providing its decrease, particularly at the highest tested concentration at both time points ($p < 0.05$).

In the same way, the microencapsulation of INH seemed to have favoured cell tolerance to INH after 24 h exposure to all tested concentrations. Although the

free drug did not present any cytotoxicity (Figure 5.5c), the viability of A549 cells exposed to INH-loaded microparticles (single drug formulation) (Figure 5.5a,b) was higher than that observed for cells treated with free INH ($p < 0.05$). This apparent cytoprotective effect of microparticles was, however, not observed at 3 h. The formulation combining the two antibiotics showed no significant differences in comparison with free INH in terms of cell viabilities, considering all conditions.

It is important to notice that the produced drug-loaded FUC microparticles showed different effects on the viability of A549 cells. For instance, upon 24 h exposure, microparticles loaded with INH only, had significantly less impact on cell viability than microparticles containing RFB, either alone or in combination ($p < 0.05$), considering all tested doses. The stronger effect of RFB-containing formulations is attributed to the presence of the proper drug, which is a potent antibiotic (297) and may be cytotoxic, depending on the dose, as is further discussed in this section.

.

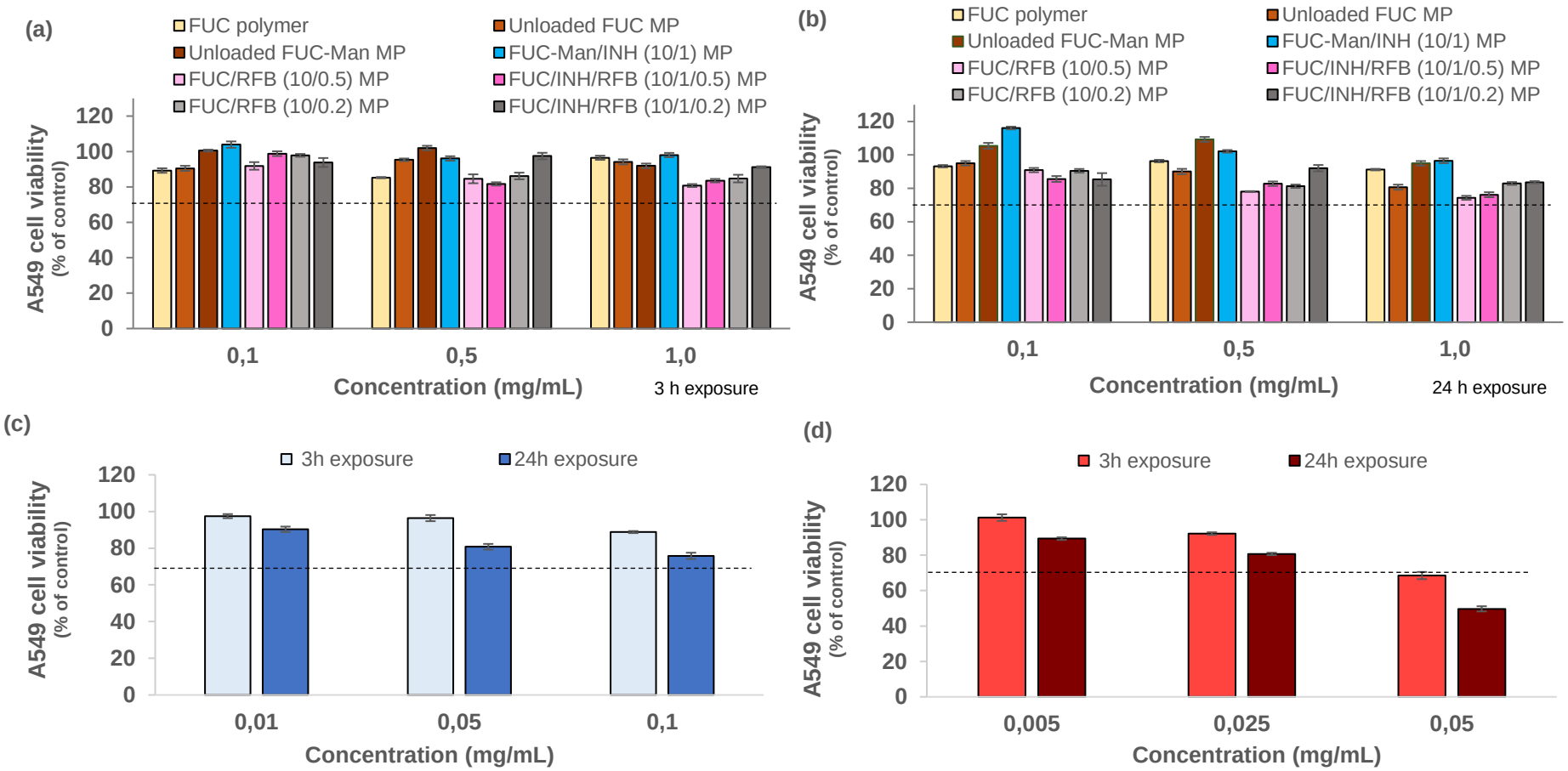

Figure 5.5. A549 cell viabilities upon (a) 3 h and (b) 24 h of exposure to fucoidan (FUC) polymer, unloaded and drug-loaded FUC microparticles; (c) exposure to INH as a free drug; and (d) exposure to RFB as a free drug. Cell viability was calculated as a percentage of positive control (untreated cells). Data represent mean ± SEM (*n* = 3, six replicates per experiment at each concentration). Dashed line indicates 70% cell viability. INH: isoniazid; Man: mannitol; MP: microparticles; RFB: rifabutin.

Taking into consideration that FUC is herein proposed as the matrix of spray-dried microparticles, the raw material (commercial powder) and unloaded microparticles were also evaluated to disclose any effect of the carrier itself. Overall, no cytotoxicity was observed, with cell viabilities remaining over 80% in all conditions (Figure 5.5a,b). Nevertheless, the literature reports opposite effects, describing FUC as an inhibitor of cell viability (A549 cells) in time- and dose-dependent manner (323,324). These differences are possibly explained by varied FUC composition, as this is highly dependent on the source of the polymer (161). As such, other carrier systems based on FUC, developed for pulmonary delivery of antibiotics, have exhibited no toxic effect on A549 cells (120), as observed in the present study. Additionally, although FUC has been shown to reduce A549 cell viability due to its antitumor activity, the pharmacological effect of FUC varies with its molecular weight (325). In this work, the absence of cytotoxicity of FUC was also evidenced in its microparticulate form.

Figure 5.6 exhibits the results obtained for macrophage-differentiated THP-1 cells. These cells responded in a relatively similar manner comparing with A549 cells, although perhaps with higher sensitivity. In fact, RFB showed again cytotoxic effect as a free drug, but in this case, this was observed at the concentrations of 0.025 and 0.05 mg/mL, and at both time-points (Figure 5.6d). At 24 h, 57% and 49% cell viability were registered, respectively. This indicates higher susceptibility of macrophage-like THP-1 cells when compared to A549 cells, differing from reports that demonstrate higher resistance of differentiated THP-1 cells (293,326). RFB-loaded microparticles (FUC/RFB MP) slightly decreased cell viabilities below 70% in all conditions, considering both time-points, except at the lowest concentration (0.1 mg/mL). Moreover, both concentration- and time-dependent effects were observed for this formulation, although with stronger contribution from the former ($p < 0.05$). Similarly, macrophage-differentiated THP-1 cells were slightly sensitive to the contact with microparticles of FUC/INH/RFB (10/1/0.5) after long-time exposure. In fact, at 24 h, cell viability decreased to 65% upon exposure to the highest dose of microparticles (1.0 mg/mL) (Figure 5.6a,b). Comparatively, A549 cells have shown 76% viability in the same conditions ($p < 0.05$). Concerning macrophage-like THP-1 cells, no significant time-dependent or dose-dependent effects were observed for FUC/INH/RFB = 10/1/0.5 (w,w) microparticles.

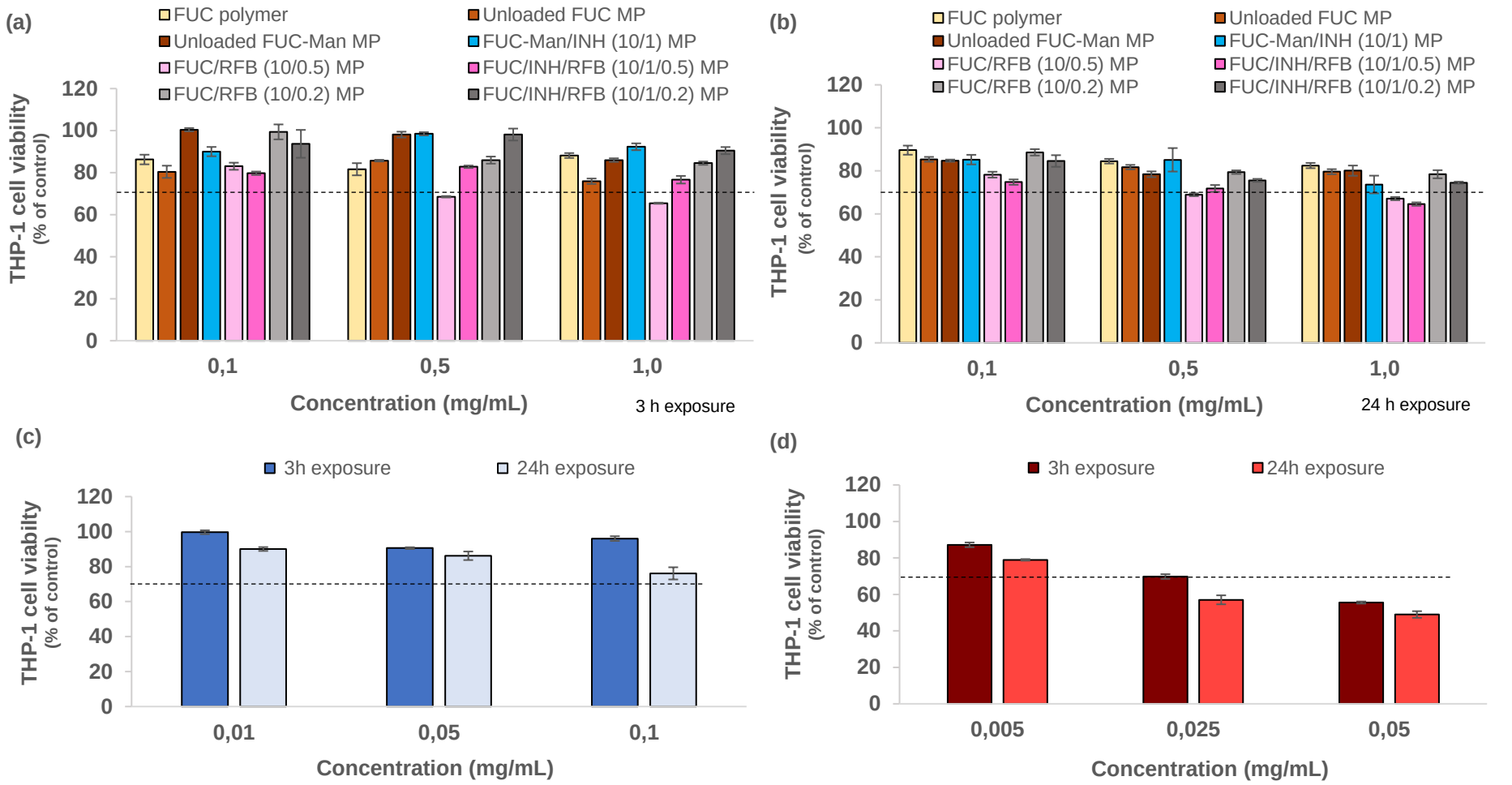

Figure 5.6. Macrophage-differentiated THP-1 cell viabilities upon (a) 3 h and (b) 24 h of exposure to fucoidan (FUC) polymer, unloaded and drug-loaded FUC microparticles; (c) exposure to INH as a free drug; and (d) exposure to RFB as a free drug. Cell viability was calculated as a percentage of positive control (untreated cells). Data represent mean ± SEM (*n* = 3, six replicates per experiment at each concentration). Dashed line indicates 70% cell viability. INH: isoniazid; Man: mannitol; MP: microparticles; RFB: rifabutin.

The mild toxicity observed in THP-1 cells is clearly due to the RFB content, a drug that has already showed toxicity *in vivo* (327,328). In order to further confirm this, microparticles loaded with RFB, either alone or in combination, were produced with lower amounts of RFB to be purposely tested regarding cytotoxicity. These formulations are referred to as FUC/RFB (10/0.2) and FUC/INH/RFB (10/1/0.2) microparticles. No cytotoxicity was registered for these particles (Figure 5.6a,b), demonstrating that the decrease in RFB content resulted in the viability of differentiated THP-1 cells over 75% in all conditions. This observation confirms that the cytotoxic effect is due to RFB content. As well, the referred formulations showed no cytotoxicity on A549 cells.

Despite THP-1 sensitivity, no cytotoxic effect was observed upon exposure to free INH (cell viability of 76% – 99%) and INH-loaded microparticles (cell viability of 73% – 98%), reinforcing the general absence of toxicity of INH in this assay (Figure 5.6c). In addition, unloaded FUC microparticles and the polymer itself (commercial powder) were also tested as control in this cell line (Figure 5.6a,b), resulting in cell viability above 76% in all cases, thus evidencing the absence of detrimental effects of the polysaccharide under the tested conditions.

Overall, it can be considered that both A549 and macrophage-differentiated THP-1 cells tolerated well the exposure to FUC-based microparticles. A mild cytotoxic effect was registered in macrophage-like THP-1 cells when exposed to microparticles containing RFB, either alone or in combination, especially at the highest tested concentration (1.0 mg/mL), with the toxicity being attributed to the RFB content. However, it should be highlighted that the highest tested dose is much higher than the one that is expected to occur *in vivo*, as after the delivery, the dry powder will be distributed through a large surface. Therefore, the effects will probably be more similar to those of the lower dose (0.1 mg/mL) than to those of the highest dose or even that of 0.5 mg/mL. Unfortunately, it was not possible to find the ways that permitted weighing such a low amount of dry powder that could better resemble the *in vivo* conditions.

5.4.2 Evaluation of cell membrane integrity

As a complement to the MTT assay, the amount of the cytoplasmic enzyme LDH released upon 24 h exposure to the highest concentrations of raw material,

microparticles, and free drugs was also determined. The results are displayed in Figure 5.7. The incubation with CCM only was considered the condition inducing the release of a standard amount of LDH and was, thus, used for comparisons.

The results essentially confirmed those of MTT, with free RFB having a more intense effect on the release of LDH. The incubation with CCM induced 21% of LDH release in A549 cells (Figure 5.7a) and 34% in macrophage-differentiated THP-1 cells (Figure 5.7b). The exposure to free RFB significantly increased these values to 42% and 56%, respectively ($p < 0.05$), corroborating the observations of RFB cytotoxicity. Despite RFB cytotoxicity, FUC/INH/RFB microparticles generated similar LDH release compared with CCM in both cell lines, which reinforces the beneficial effect of microencapsulation regarding RFB cytotoxicity. Additionally, microparticles of FUC/RFB (10/0.5, w/w) induced significantly lower release of LDH from A549 cells, comparing with the free drug ($p < 0.05$), demonstrating once more the influence of microencapsulation on the cytotoxic effect of RFB. Despite that, the formulation generated greater amounts of LDH (29%) compared to control CCM ($p < 0.05$), showing a certain level of cytotoxicity.

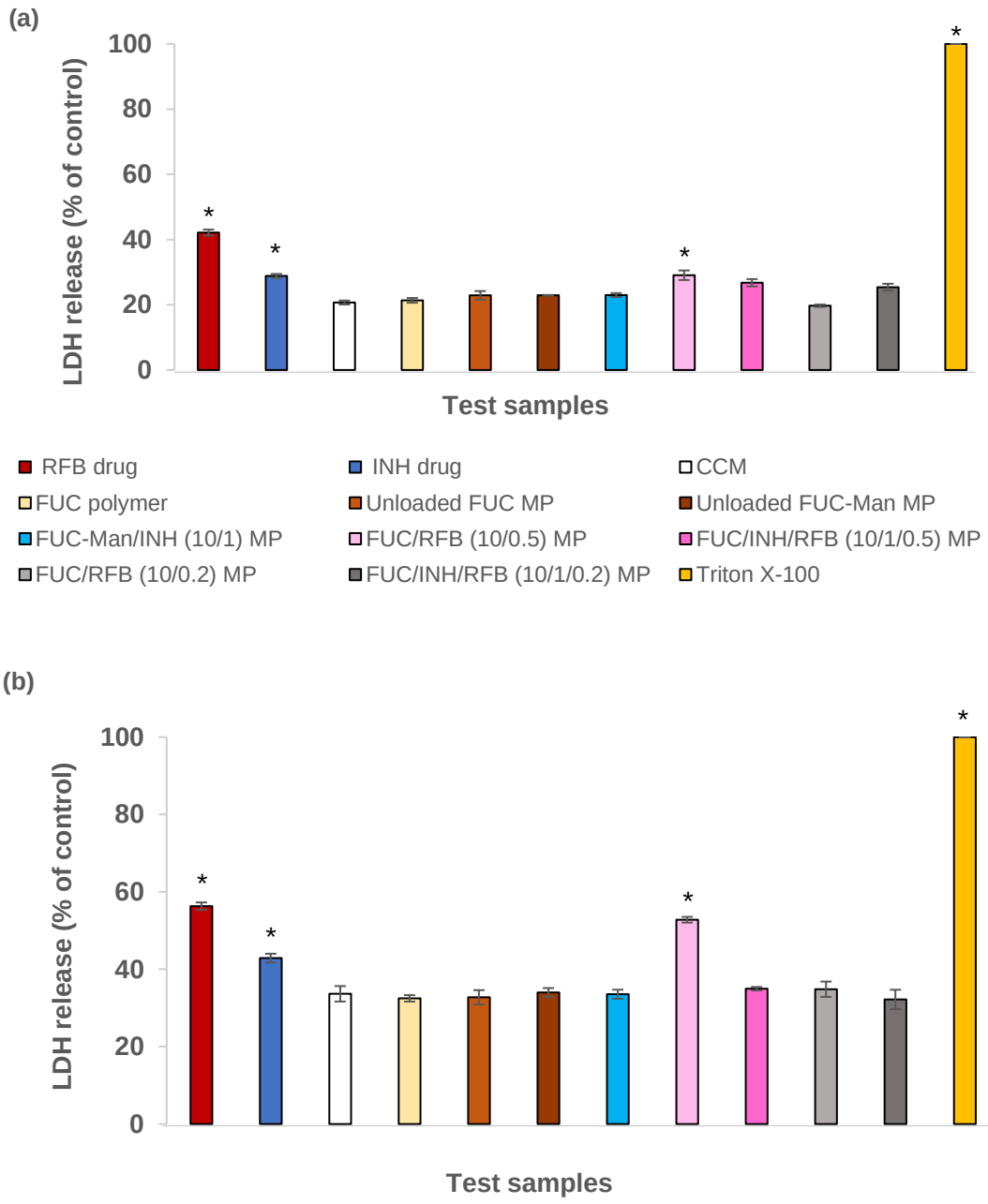

Figure 5.7. Release of lactate dehydrogenase (LDH) from (a) A549 cells and (b) macrophage-differentiated THP-1 cells exposed to fucoidan (FUC) polymer, FUC-based microparticles (1.0 mg/mL), free rifabutin (RFB, 0.05 mg/mL), and free isoniazid (INH, 0.1 mg/mL). Cell culture medium (CCM) and Triton X-100 were used as negative and positive controls, respectively. The released LDH was calculated based on 100% assumed for positive control. Data represent mean ± SEM (*n* = 3, six replicates per experiment at each concentration). * p < 0.05 compared to CCM.

Curiously, free INH also induced the release of a significantly higher amount of LDH compared with the control CCM (29% for A549 cells and 43% for

macrophage-differentiated THP-1 cells, $p < 0.05$). This indicates a certain degree of toxicity of the drug that was not observed in the MTT assay. However, microencapsulation apparently reverted the toxicological effect ($p < 0.05$), as microparticles loaded with INH, either alone or in combination, induced LDH at levels close to CCM in both cell lines. For instance, INH-loaded microparticles (single drug formulation) elicited a significant decrease in the release of LDH (23% for A549 and 34% for differentiated-THP-1 cells), comparing with free INH ($p < 0.05$), corroborating the assumption that microencapsulation of drugs favours their toxicological profile. In microparticles associating RFB as single drug, a concentration-dependent effect was observed, as FUC/RFB (10/0.5, w/w) microparticles generated, in A549 cells, around 29% of LDH release while FUC/RFB (10/0.2, w/w) microparticles induced 20% release ($p < 0.05$). Regarding differentiated-THP-1 cells, the reduction of RFB content decreased the release of LDH from 53% to 35% ($p < 0.05$).

As expected, the results of macrophage-like THP-1 cells (Figure 5.7b) evidenced higher sensitivity of these cells comparing with A549 cells (Figure 5.7a). In fact, Figure 5.7b generally shows higher values of LDH release upon exposure to all samples. The incubation with CCM generated 34% LDH release, which is itself 50% higher than that observed in A549 cells. The trend of the results is however very similar to that found in A549 cells, with only the free drugs and FUC/RFB = 10/0.5 (w/w) microparticles generating significantly higher LDH release comparing with the control CCM ($p < 0.05$).

Unloaded FUC microparticles also evidenced an absence of effect on LDH release. The overall evaluation of *in vitro* cytotoxicity indicates a very acceptable toxicological profile of FUC-based microparticles. Nevertheless, it is considered beneficial to widen the toxicological studies of these microparticles to certify their applicability for the proposed objective.

5.5 Macrophage activation

As the dual drug-loaded microparticles provide better compliance with the combined therapy recommended for TB, this formulation was selected for the assay of macrophage activation. The ability of FUC/INH/RFB (10/1/0.5) microparticles to induce macrophage activation was then assessed by determining the amount of

TNF-α and IL-8 secreted by macrophage-like THP-1 cells upon contact with the formulation. The referred cytokines are two pro-inflammatory molecules released by human alveolar macrophages upon infection with *M. tuberculosis* (329,330). The synthesis of pro-inflammatory cytokines such as TNF-α and IL-8 by macrophages contributes to the effective control of the proliferation and dissemination of pathogens (331). The quantity of secreted cytokines was compared with the levels produced upon stimulation with LPS (positive control) and untreated cells (negative control).

Figure 5.8 depicts the obtained results. The contact with drug-loaded FUC microparticles induced TNF-α concentrations of 1.5×10^3 pg/mL (Figure 5.8a), which did not differ statistically from the value registered upon LPS stimulation, although the nominal value was higher in that case (2.5×10^3 pg/mL). This observation is in agreement with a recent report showing that FUC induces TNF-α secretion from macrophage-differentiated THP-1 cells (332). FUC was also tested as a solution, which gives an indication of the effect of the polymer itself. It was shown to induce the production of TNF-α (1.9×10^3 pg/mL), which is not statistically different from the effect of microparticles. Importantly, when comparing with CCM, the induced TNF-α production was higher for both FUC microparticles and FUC solution ($p < 0.05$).

Similar effects were observed regarding the production of IL-8 (Figure 5.8b). Although in this case, LPS generated a significantly higher amount of cytokine (26×10^3 pg/mL, $p < 0.05$), drug-loaded FUC microparticles also revealed an ability to induce its secretion, which reached 14.7×10^3 pg/mL, more than half of the amount corresponding to LPS. Moreover, IL-8 secretion stimulated by the produced microparticles and raw material were much higher than that of the control CCM ($p < 0.05$).

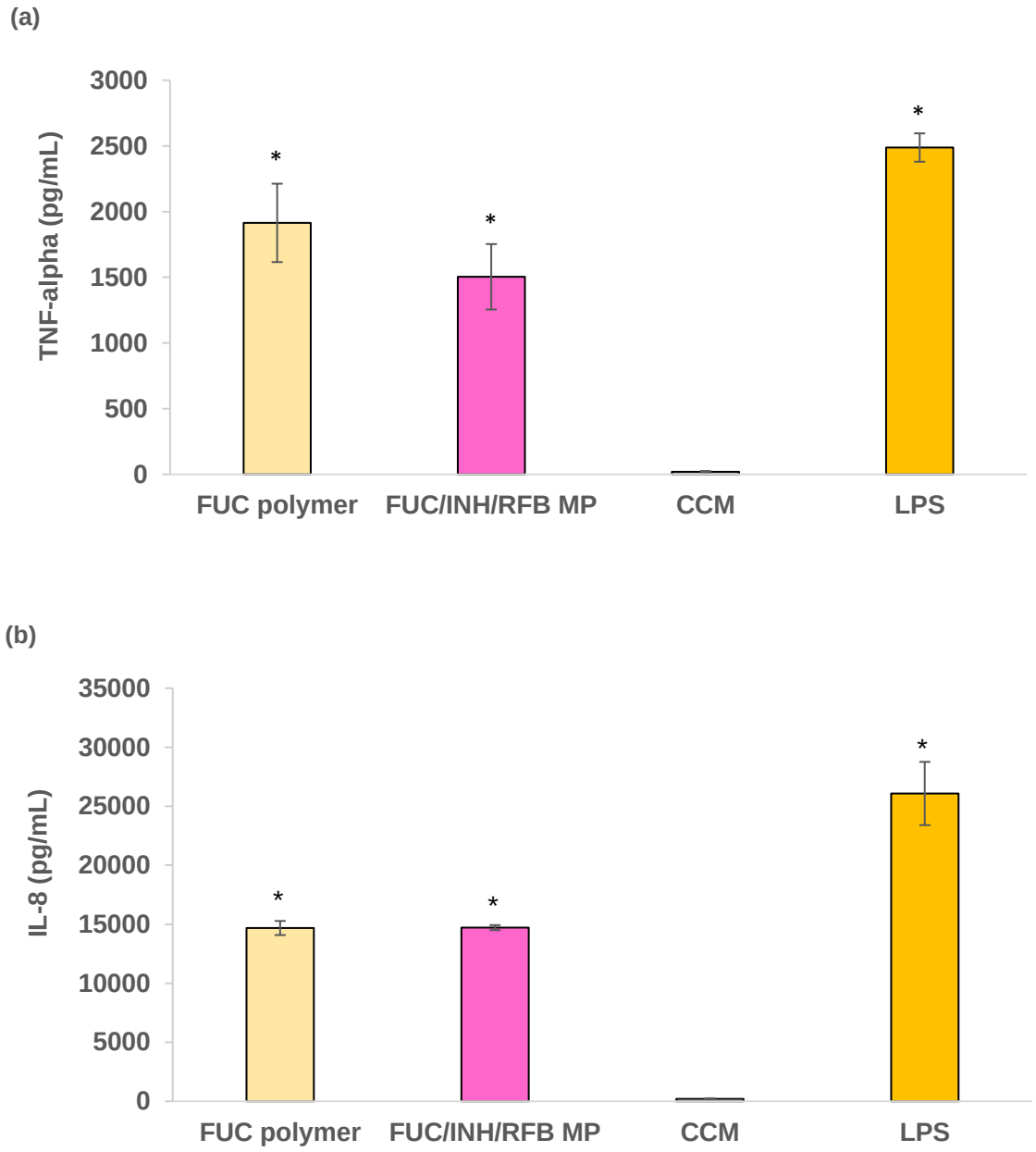

Figure 5.8. TNF-α (a) and IL-8 (b) secretion by macrophage-differentiated THP-1 cells upon 24 h exposure to FUC/INH/RFB (10/1/0.5) microparticles (MP) and FUC as raw material. Cell culture medium (CCM) and lipopolysaccharide (LPS) were used as negative and positive controls, respectively. FUC: fucoidan; INH: isoniazid; RFB: rifabutin. Data represent mean ± SEM (*n* = 3). * p < 0.05 compared to CCM.

Overall, no significant differences were observed in the production of each interleukin upon stimulation by dual drug-loaded microparticles and the raw material FUC. In this way, the results suggest that FUC is the agent responsible for the observed activation of macrophage-like cells. Actually, the immune modulatory activity of FUC has been already reported, and is mediated through the regulation

of immune cells, including macrophages (333,334). Although FUC has been shown to induce the production of TNF-α (332,335) and IL-8 (336) from macrophages and other immune cells (337), the polymer seems to be endowed with anti-inflammatory activity as well (338,339). In truth, the mechanism of action of FUC as a bioactive agent is yet to be unveiled, and this area worths further research.

5.6 Preliminary evaluation of microparticle uptake by macrophages

Taking into consideration the intended application of the developed microparticles, the ability of macrophage cells to internalise the carriers was deemed as an aspect of relevant interest and was, thus, assessed by flow cytometry. Macrophage-differentiated THP-1 cells and rat alveolar macrophages (NR8383) were exposed to two different doses of fluorescently-labelled unloaded FUC microparticles.

As depicted in Figure 5.9, the percentage of THP-1 cells taking up FUC microparticles was around 23% (50 μg/cm^2) and 87% (200 μg/cm^2), demonstrating a dose-dependent uptake ($p < 0.05$). Similarly, the uptake of carriers by rat macrophages varied between 68 and 86% as the concentration raised from 50 to 200 μg/cm^2, also revealing a dose-dependent effect ($p < 0.05$). Significant differences ($p < 0.05$) were observed in the uptake ability evidenced by both cells, particularly at the lowest tested dose (50 μg/cm^2). In this case, 23% and 68% of FUC microparticles were taken up by THP-1 cells and NR8383 cells, respectively. Therefore, the obtained results are a preliminary demonstration of the macrophage's ability to uptake FUC microparticles at a considerable level, depending on the dose. Considering that FUC exhibits in its structure chemical motifs (sulphate groups and fucose units) that can be specially recognised by macrophage surface receptors (36), a more accurate determination of preferential macrophage phagocytosis would be provided by comparing the uptake of FUC microparticles with a material devoid of recognisable moieties. Additionally, complementing cytometry data with confocal microscopy images would be beneficial in corroborating the data obtained so far.

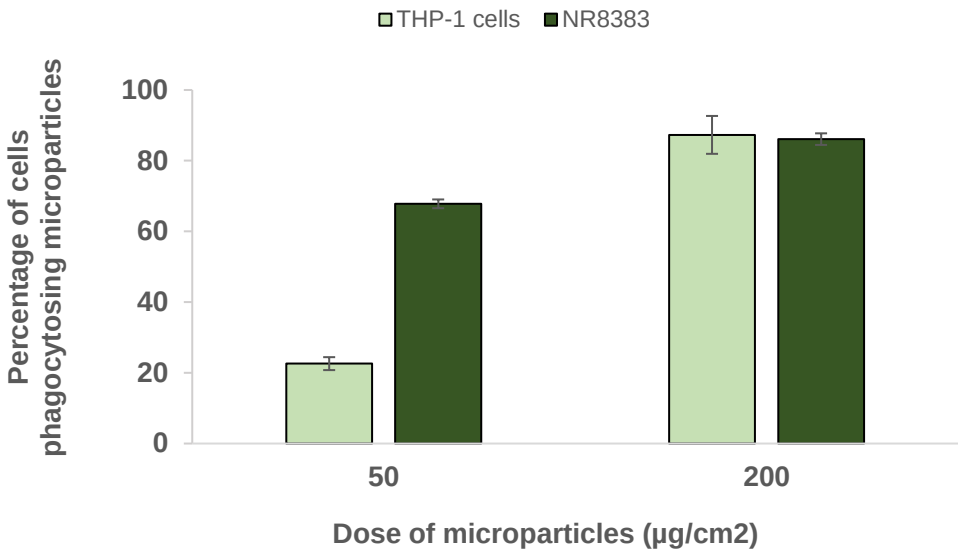

Figure 5.9. Uptake of fluorescently-labelled unloaded fucoidan microparticles by human macrophage-differentiated THP-1 cells and rat alveolar macrophages (NR8383 cells) upon exposure to 50 µg/cm^2 and 200 µg/cm^2, for a period of 2 h. Results are expressed as mean ± SEM (n ≥ 3).

5.7 Determination of minimum inhibitory concentration (MIC)

In order to measure the MIC of the produced systems, *M. bovis* cells were treated with free drugs and microparticles loaded with both INH and RFB (FUC/INH/RFB = 10/1/0.5, w/w). This formulation was selected since it complies with WHO recommendations for combined TB therapy, as previously mentioned. The viability of mycobacteria upon exposure to tested samples was calculated as a percentage of bacterial culture (control), which was considered as 100% of bacterial growth.

The MIC value determined for INH as free drug was 0.125 µg/mL, which is in the value range reported in the literature (340,341). Comparatively, free RFB at a concentration of 0.004 µg/mL was sufficient to inhibit the growth of *M. bovis*, suggesting that RFB is a stronger antimycobacterial agent than INH, probably due to the higher lipophilicity that facilitates its internalisation through the cell membrane (342,343). The literature reports variable MIC values of RFB, depending on the strain of *M. bovis* and on the method of susceptibility testing (344,345). By combining both INH and RFB as free drugs in a single solution, the determined MIC values were 0.008 µg/mL (INH) and 0.004 µg/mL (RFB). It is worth noticing that the

MIC of INH reduced from 0.125 to 0.008 µg/mL when combined with RFB. Differently, either alone or in combination, RFB displayed the same MIC value (0.004 µg/mL). This indicates that the *in vitro* susceptibility of mycobacteria to INH is potentiated when the two anti-TB drugs were applied together.

By exposing *M. bovis* to 0.08 µg/mL of FUC/INH/RFB microparticles, the viability of mycobacteria decreased to the minimum level, therefore being the MIC value of the produced systems. It is important to highlight that, at this microparticle concentration, the drug content, considering the respective association efficiencies, is approximately 0.008 µg/mL (INH) and 0.004 µg/mL (RFB). These concentrations correspond to the MIC values determined for the two drugs when tested in combination (as free drugs). Therefore, the inhibition effect on the growth of *M. bovis* was very similar when comparing dual drug-loaded FUC microparticles and the mixed solution of INH/RFB as free drugs. This observation indicates that the microencapsulation process had no effect on the antibacterial activity of the drugs. In summary, *in vitro* susceptibility of *M. bovis* has been observed towards drug-loaded FUC microparticles with considerable growth inhibition, as expected.

5.8 Preliminary *in vivo* studies

Safety is a matter of utmost importance, considering the pharmaceutical application of the developed carriers. *In vivo* assays performed after product development should not only include the assessment of the therapeutic potential of formulations, as a proof-of-concept, but also address more basic knowledge, comprising tests of the impact of administering novel materials into the lungs. In fact, the area of lung delivery is in strong need of new materials that offer an alternative to the very narrow list of approved excipients, that is led by lactose and mannitol. However, new materials require safety evaluation, which comprises many aspects. Unlike CS, FUC is a polysaccharide that has been poorly investigated as biomaterial, particularly, for pulmonary delivery. In this sense, it was decided to perform an *in vivo* assessment that focused on the material used as the drug vehicle.

To perform the assay, BALB/c mice were submitted to the contact with unloaded FUC microparticles by inhalation. Two parameters were considered to establish if immunological reactions occurred: i) eosinophilia of the peripheral blood smears, and ii) serum IgE detection. The characteristics of airway diseases include

pulmonary eosinophilia and the production of IgE (346). Eosinophils are pro-inflammatory leukocytes with diverse functions and increasing recruitment of these cells into affected tissues is a basic feature of inflammatory response and allergic reaction (347,348). Moreover, the clinical manifestations of allergies result from the effects of a complex network of cells and effector molecules that include IgE, which plays a central role in mediating allergic disease (349). Thus, the percentage of eosinophils, among the white blood cells, were estimated on peripheral blood smears. Additionally, an Ouchterlony double immunodiffusion assay was performed to detect the presence of the antibody IgE in the sera of mice, since serum IgE levels may rise in response to inhalation of an allergen (350).

The eosinophil count in the group treated with unloaded FUC microparticles was 1%, a mean value comparable with the control group (Figure 5.10). The obtained results suggest a non-pathological state as the values obtained for the treated mice fell within the haematological reference values, since the relative number of eosinophils varies between 0 – 5% in male BALB/c mice (351).

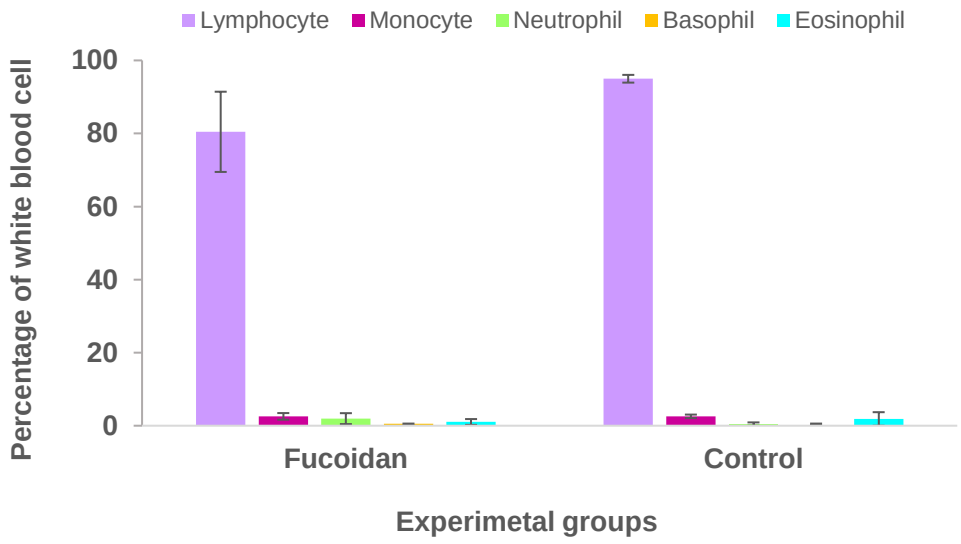

Figure 5.10. Percentage of white blood cells counted in the blood smears. Mean value ± SD.

This result demonstrates that the inhalation of the produced FUC microparticles generated no eosinophilia in the treated mice, suggesting that the biomaterial was well tolerated by the animals. It is important to highlight that blood eosinophil count is considered a biomarker of airway inflammation. Eosinophils roll onto the bronchial vascular endothelium, as the cells flow in the blood stream (348).

Thus, studies have shown that blood eosinophil measurement is associated with eosinophilic inflammation in the airway (348,352).Yet, considering all cell counts, no significant differences were perceived when comparing FUC-treated group with the control group (Figure 5.10). It is relevant to take into consideration the differential white blood cell count, since the total number of cells may increase if there is an inflammatory reaction, and more specifically, the relative numbers of the different classes of white blood cells is changed. For instance, an increase in neutrophils and lymphocytes is frequently observed along with eosinophilia (346).

Complementarily to the eosinophil count, immunodiffusion tests were conducted to evaluate the immunological response. No reaction was detected between antibody-antigen. In the Ouchterlony assay, the antigen (antiserum) and antibody solutions diffuse away from their original wells where the test solution is placed and through the agar gel, toward one another, and at the point where they meet in the agarose, if “equivalence” occurs they form a visible line of precipitation. The test samples (sera of mice before and after inhalation of microparticles) did not precipitate in contact with antiserum IgE despite using a range of concentrations in the assays. The most probable justification for this observation is that a very low level of IgE was present in the samples. In this case, it could be said that the unloaded FUC microparticles did not induce IgE production, indicating the microparticles were well tolerated by the treated mice. Nevertheless, a suitable control was needed to confirm the reaction worked properly. In this study, the sera obtained from OVA-sensitised mice, used as positive control of IgE, did not cause an immunoprecipitation when used in the Ouchterlony assay, possibly due to protein degradation. A commercial IgE sample is in this way the best control to be used in the future, in order to adequately obtain clear observations.

5.9 Conclusion

Inhalable dry powders based on FUC and loaded with first-line anti-TB drugs (INH and/or RFB) were successfully produced with high drug association efficiency (81–97%). The produced microparticles displayed MMAD between 1.9 and 3.9 µm, and FPF around 39%–55%, thus evidencing suitable aerodynamic properties for pulmonary delivery with great potential to reach the respiratory zone. Dual drug-loaded microparticles had no effect on the cell viability of alveolar epithelial cells

(A549), while a slight reduction in the viability of macrophage-differentiated THP-1 cells (65% viable cells) was observed when exposed for 24 h to concentrations as high as 1.0 mg/mL. Similarly, RFB-loaded microparticles (single drug formulation) revealed a considerable cytotoxic effect on THP-1 at the referred concentration (1.0 mg/mL), but this dose is considered overestimated comparing with the expected *in vivo* conditions. On the contrary, microparticles loaded with INH (single drug formulation) had no effect on cell viability, as indicated by metabolic assays performed on alveolar epithelial cells (A549) and macrophage-like cells (THP-1). The results of LDH assays essentially reinforced those of MTT, evidencing that RFB content was the major factor related to the observed cytotoxicity. The produced FUC microparticles were further demonstrated to be captured by macrophages and macrophage-like cells in a dose-dependent manner, reaching 87% of uptake. Moreover, they were able to induce macrophage activation by potentiating the secretion of cytokines, which is a clear indicator that the phagocytosis of drug-loaded FUC microparticles may mediate the improvement of the bactericidal effect of macrophages. Furthermore, dual drug-loaded microparticles showed potential activity against a strain of mycobacteria (95% growth inhibition) and it was demonstrated that the bactericidal activity of drugs was maintained after spray-drying. Finally, the preliminary *in vivo* study suggested that the produced microparticles were well tolerated by mice after pulmonary administration, since no blood eosinophilia was detected.

According to the obtained data, the proposed delivery carriers associating one or two anti-TB drugs, are a promising tool for the inhalable treatment of pulmonary TB. Nevertheless, unveiling the effect of a long-term administration of FUC microparticles *in vivo*, as well as the *in vivo* antibacterial efficacy, are very relevant aspects to address in the future

This page was intentionally left in blank

Chapter Six

Chitosan Microparticles: Results and Discussion

The information contained in this chapter was partially presented in the following manuscript:

Ludmylla Cunha, Susana Rodrigues, Ana M. Rosa da Costa, Leonor Faleiro, Francesca Buttini, and Ana Grenha. Inhalable chitosan microparticles for simultaneous delivery of isoniazid and rifabutin in lung tuberculosis treatment. Carbohydrate Polymers (submitted).

This page was intentionally left in blank

6. Chitosan microparticles: Results and discussion

6.1 Preparation and characterisation of chitosan microparticles

As previously mentioned, the development of inhalable microparticles for treating pulmonary tuberculosis demands the design of aerodynamically suitable systems, able to reach the alveoli, where alveolar macrophages hosting the infectious bacteria reside. Particularly, further benefit may be attained if the carriers can be recognised and phagocytosed by alveolar macrophages. This can be mediated by the chemical composition of the carriers, which may favour recognition by macrophage surface receptors. CS was selected within this context, since it is composed by *N*-acetylglucosamine and D-glucosamine residues, the former described to be recognised by macrophages (353), thus possibly potentiating phagocytosis. In addition, the polysaccharide has been widely investigated for applications in the pharmaceutical field, and therefore was used as a standard for comparisons with the other polymer selected for this work, FUC.

Spray-drying yielded 75–81% of dry powder, which is satisfactory and actually higher than other values reported for spray-dried CS microparticles (239,306). In this case, high yields could be attributed to the instrumentation design, given that the use of a high performance cyclone, instead of the manufacturer's standard separator, greatly improved the powder yield (354). INH and RFB were efficiently associated to CS microparticles either individually or together. The simultaneous incorporation of the drugs in microparticle formulations represents an important approach towards the compliance with the combined therapeutic regimen of TB that is recommended by WHO (261). Table 6.1 displays, among other properties, the mean values of drug association efficiency of the produced CS microparticles along with loading capacity and production yield. INH and RFB were associated separately with efficiencies of 90% and 97%, respectively. When associated simultaneously, 93% of INH was incorporated into the formulation, while RFB association efficiency was as high as 99%. Surprisingly, INH and RFB displayed similar association efficiencies, despite the differences in the aqueous solubility of the two drugs, which is 125 mg/mL for INH and 0.19 mg/mL for RFB, as previously stated. Moreover, the incorporation of two antibiotics in a single formulation did not interfere with the association efficiency of each drug. As a result,

loading capacities of the antibiotics were found to be around 8.1% for INH and in the range of 4.3–4.7% for RFB, values that are close to the theoretical maximum. It should be noticed that the amount of INH included in the microparticles is higher than RFB, since the latter is a more potent antibiotic (297), and also has a more toxic profile, as demonstrated in Section 6.7. In addition, CS amount was maintained purposely high in order to favour the internalisation of microparticles by macrophages (353).

These results demonstrate the efficacy of spray-drying in providing drug association, which was previously reported inclusive for CS-based microparticles associating anti-TB drugs (239,306). However, unlike the present study, the production of the referred microparticles required more than one production step and involved the use of a crosslinking agent (e.g. tripolyphosphate), which has been suggested to improve drug retention in the formulation (355). Several published articles report the production of CS microparticles loaded with one (239,306,356) or more anti-TB drugs (357), which were produced by spray-drying or other methods. However, the referred studies included dispersing agents (e.g. lactose) and other polysaccharides (e.g. alginate) in the process. Particularly, to the best of our knowledge, this is the first report that describes the preparation and evaluation of spray-dried CS microparticles with a combination of INH and RFB, which were produced in one step, with no use of other excipients, including crosslinking agents.

Table 6.1. Spray-drying production yield, drug association efficiency, loading capacity, Feret´s diameter, median volume particle size (D_v50) and density values of chitosan (CS)-based microparticles (mean ± SD, n = 3). INH: isoniazid; RFB: rifabutin.

Microparticles	Production yield (%)	Drug association efficiency (%)	Loading capacity (%)	Feret´s diameter (µm)	D_v50 (µm)	Span	Density (g/cm^3)		
							Real	Bulk	Tap
Unloaded CS	81 ± 2	–	–	1.53 ± 0.86	–		1.39 ± 0.02	0.12 ± 0.05	0.17 ± 0.01
CS/INH (10/1)	77 ± 6	90 ± 4	8.2 ± 0.3	1.54 ± 0.87	7.8 ± 0.2	2.59 ± 0.02	1.35 ± 0.02	0.10 ± 0.01	0.18 ± 0.05
CS/RFB (10/0.5)	76 ± 4	97 ± 4	4.7 ± 0.3	1.48 ± 0.80	9.3 ± 0.9	2.98 ± 0.07	1.37 ± 0.02	0.17 ± 0.02	0.26 ± 0.02
CS/INH/RFB (10/1/0.5)	75 ± 5	93 ± 4 (INH) 99 ± 5 (RFB)	8.1 ± 0.3 (INH) 4.3 ± 0.2 (RFB)	1.70 ± 0.94	5.9 ± 1.7	2.68 ± 0.03	1.37 ± 0.02	0.15 ± 0.01	0.25 ± 0.02

It is well-known that the properties of dry powders play an important role in the development of inhalable formulations, as deep lung deposition depends mainly on characteristics like particle size, shape, and density (304). Morphological analysis by SEM showed that CS microparticles are generally spherical, having a wrinkled surface that generally becomes smoother after drug incorporation (Figure 6.1). These morphologies correspond to previous descriptions on spray-dried CS microparticles (358,359).

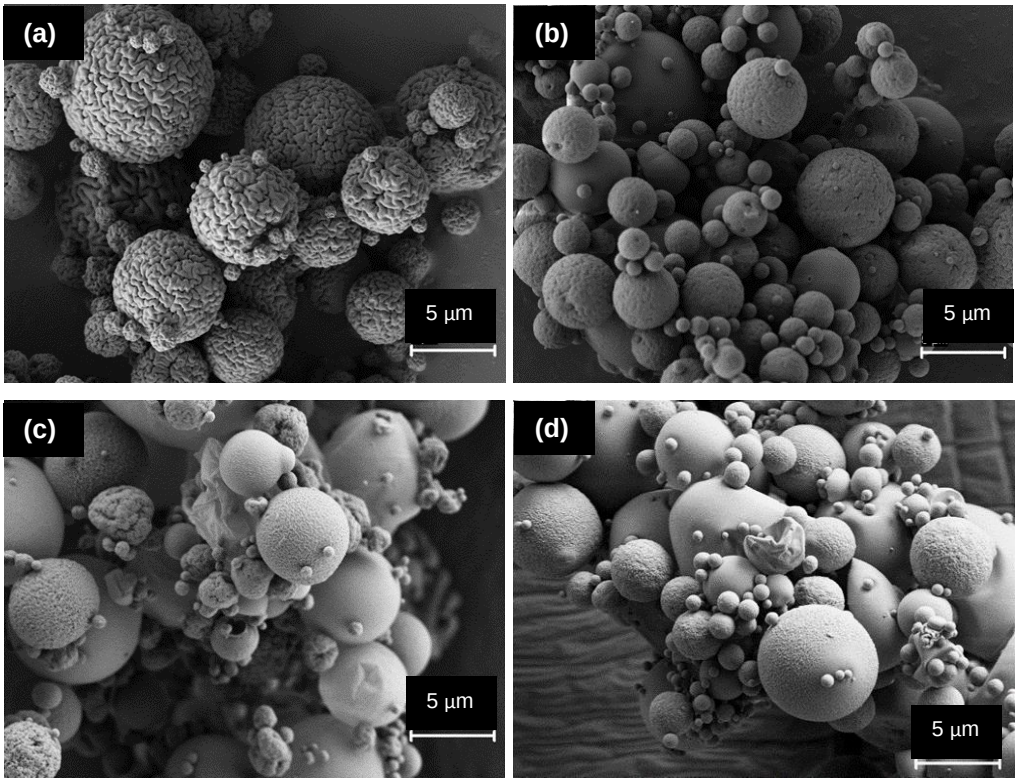

Figure 6.1. Scanning electron microphotographs of chitosan (CS)-based microparticles: (a) unloaded CS microparticles, (b) CS/INH = 10/1 (w/w) microparticles; (c) CS/RFB = 10/0.5 (w/w) microparticles; (d) CS/INH/RFB = 10/1/0.5 (w/w) microparticles. INH: isoniazid, RFB: rifabutin.

Each SEM image displays spray-dried particles with variable diameters, which is a common observation, as reported elsewhere (360,361). In fact, the volume median diameter (Dv50), estimated by laser diffraction, confirmed the production of microparticles with wide size distribution. Overall, the produced carriers presented a mean value ranging between 5.9–9.3 µm, as displayed in Table

6.1. Likewise, span values were determined to provide an indication on the width of the size distribution of drug-loaded microparticles and varied from 2.6 to 3.0 µm.

Density further influences the properties of inhalable dry powders (362). Real density was found to be approximately 1.40 g/cm^3 in all formulations (unloaded and drug-loaded microparticles), as depicted in Table 6.1. Bulk density varied between 0.10 and 0.17 g/cm^3 and tap density between 0.17 and 0.26 g/cm^3. The literature reports similar density values for spray-dried polysaccharide microparticles (303,363). Generally, Feret's diameter and density did not suffer alterations after drug association and are similar between the different drug-loaded formulations. This was expected, as the amount of drugs incorporated is not high.

6.1.1 Dry powder analysis using Powder X-Ray Diffraction (PXRD)

As performed for FUC, a study to verify any interaction between CS and the drugs was conducted using XRD and results are presented in Figure 6.2. In accordance with a published study, chitosan diffraction peaks were perceived at 10° or 20° (Figure 6.2a), correlated with hydrated and anhydrous crystals, respectively (364). Moreover, spray-dried CS (unloaded CS microparticles) showed no sharp peaks, revealing the absence of crystallinity. Crystallinity degree influences the stability of a polymer, in which the declining crystallisation could contribute to both the polymer destabilisation and, consequently, the release of drugs (365).

The analysis of free drugs was already described in Chapter 5. Briefly, it was observed that INH remains crystalline after spray-drying, although with peaks of lower intensity, while RFB assumed an amorphous form (Figure 6.2b,c). The three formulations of drug-loaded CS microparticles displayed similar X-ray patterns, despite drug compositions (Figure 6.2a). Their diffractograms evidenced broader peaks with low intensity, indicating almost amorphous state of formulations. These results are in line with other studies that demonstrated the production of amorphous microparticulate CS carriers (306,364). As stated in the previous chapter, drug amorphisation indicates its association to the CS microparticles. The amorphous state of microparticles may influence the dissolution behaviour of the carriers, leading to an enhanced bioavailability of drugs, as will be discussed later on. Moreover, the stability of an amorphous drug is influenced by environmental conditions, including humidity, temperature, and mechanical stress (366), which

may reduce the physical stability of carriers due to premature drug recrystallization from its formulation, as referred in the previous chapter.

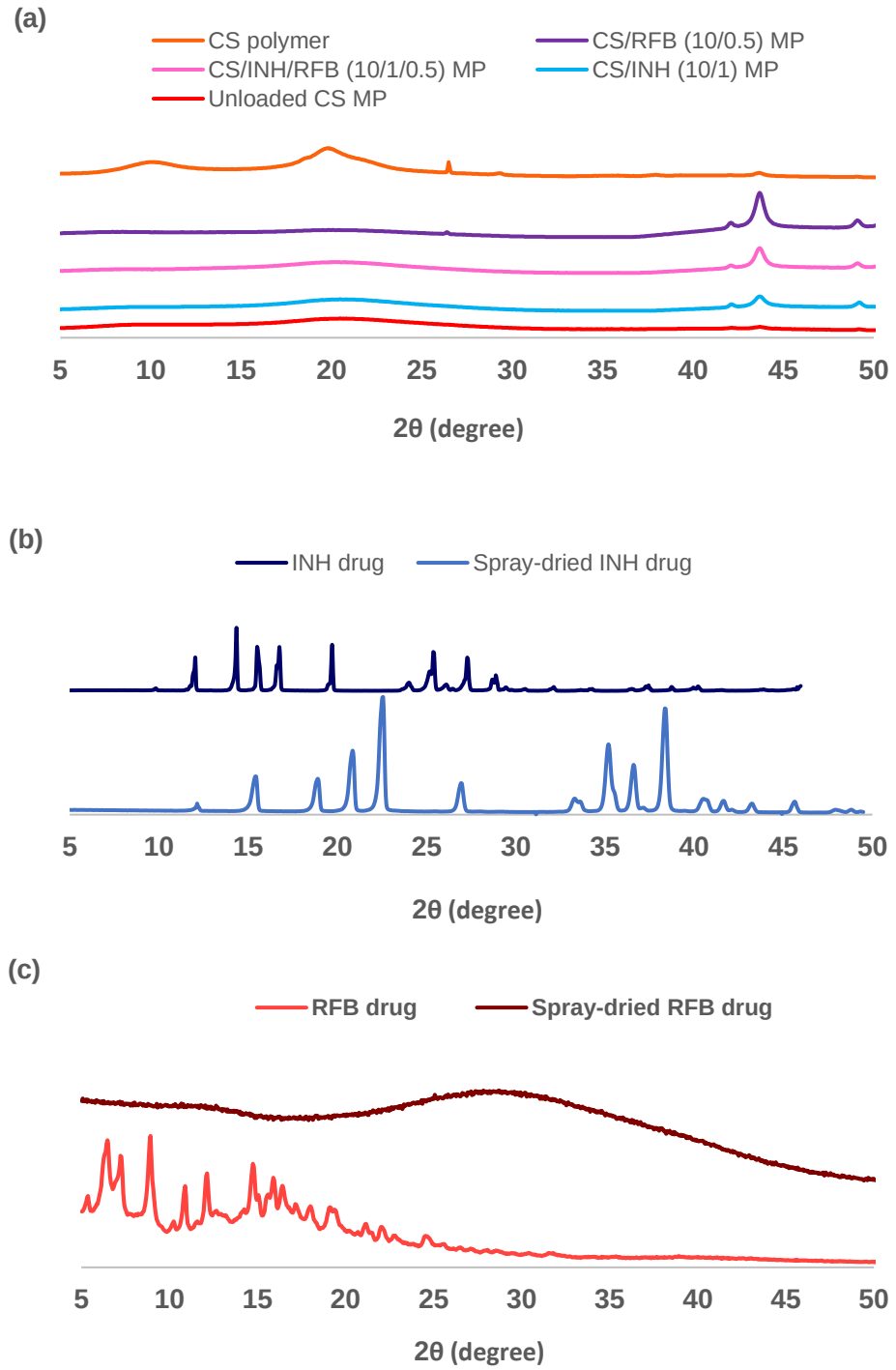

Figure 6.2. Diffractograms of (a) chitosan (CS) polymer, unloaded and drug-loaded CS microparticles; (b) free isoniazid (INH) before and after spray-drying, (c) free rifabutin (RFB), before and after spray-drying. Note to Figure 6.2: Graphics c and d represent the same set of data of Figure 5.2 and were reprinted in this chapter to facilitate reading.

6.2 Evaluation of aerodynamic properties

The aerosolisation and deposition properties of CS microparticles were investigated *in vitro* using an ACI and the obtained data are displayed in Table 6.2. The percentages of drug recovery were found to vary between 86–91 (INH) and 87–98% (RFB), complying with the recommendations of the European Pharmacopeia (75). Moreover, the assessment revealed high emitted doses (>90%) with respirable fractions (FPF ≤ 5μm) in the range of 43–63%. These results indicate adequate flowability of the produced microparticles, supporting the intended application of the systems.

It is important to highlight the use of the RS01 inhaler, a device that disperses fine particles through an effective rotating capsule movement (313), which certainly contributed to the satisfactory aerosol performance of CS microparticles.

Table 6.2. Aerodynamic properties of chitosan (CS) microparticles loaded with isoniazid (INH) and/or rifabutin (RFB). Loaded amount of powder in the capsule was 30 mg, corresponding to approximately 2.8 mg of INH and 1.5 mg of RFB, according to the drug content found in each formulation (*n* = 3, mean ± SD). FPD: fine particle dose; FPF: fine particle fraction; MMAD: mass median aerodynamic diameter.

Microparticles		Metered dose (mg)	Emitted dose (mg)	MMAD (μm)	FPD <5 μm (mg)	FPF <5μm (%)
CS/INH (10/1)		1.9 ± 0.1	1.9 ± 0.1	3.8 ± 0.1	1.2 ± 0.1	62.1 ± 0.2
CS/RFB (10/0.5)		1.0 ± 0.1	1.0 ± 0.1	2.5 ± 0.1	0.6 ± 0.1	63.4 ± 0.5
CS/INH/RFB (10/1/0.5)	**INH**	2.2 ± 0.2	2.1 ± 0.3	4.2 ± 0.1	1.1 ± 0.2	43.6 ± 4.2
	RFB	1.0 ± 0.1	1.0 ± 0.2	4.1 ± 0.2	0.5 ± 0.1	45.2 ± 3.1

The evaluation of the deposition properties of CS-based microparticles resulted in MMAD between 2.5 and 4.2 μm, indicating that the formulation generated adequate aerosol size for efficient lung penetration. Usually, particles with aerodynamic diameters around 1–5 μm can potentially reach the respiratory region, while those with less than 2 μm are prone to deposit in peripheral airways (75,315). In this sense, the produced drug-loaded CS microparticles display suitable aerodynamic diameter to reach the respiratory zone and possibly to be internalised by macrophages, the target cells, which are described to uptake particulate matters with diameter within 1–6 μm (104).

Drug deposition profiles on ACI stages are illustrated in Figure 6.3. Particularly for the formulation associating the two drugs in combination, data show great similarity between the profiles, evidencing co-deposition of both INH and RFB on the different ACI stages (Figure 6.3b). On the other hand, observing the distribution in Figure 6.3a, it is visible that CS/INH microparticles deposited more in the upper stages, in contrast with CS/RFB microparticles that accumulate on stages 3–4, which recover particles <3.2 µm, potentially capable to reach the deep zones of the lung.

These observations reinforce that spray-drying was adequate to associate anti-TB drugs to CS microparticles for an application in TB therapy, especially combining the two antibiotics in a single dry powder formulation, as the drugs are evenly distributed. Furthermore, the proposed systems exhibit suitable aerodynamic properties for deep lung delivery of anti-TB drugs.

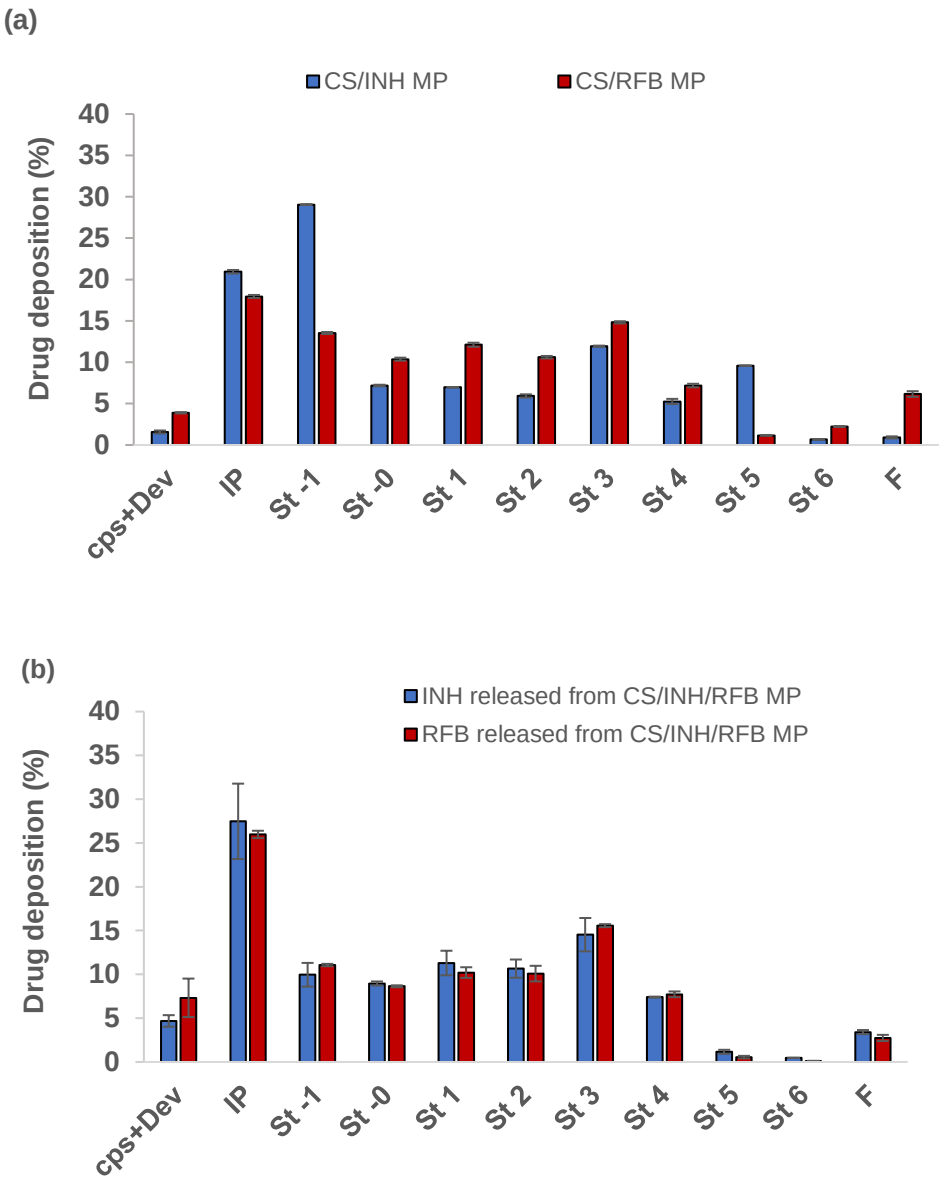

Figure 6.3. *In vitro* aerodynamic deposition of antitubercular drugs (isoniazid – INH and rifabutin – RFB) in the Andersen cascade impactor. Drugs associated with chitosan (CS) microparticles (MP) either individually (a) or together in a single formulation (b). Values are mean ± SD, *n* = 3. Cps: capsule; Dev: inhaler device; IP: induction port; F: filter, St: stage.

6.3 *In vitro* drug release profiles

The *in vitro* determination of drug release profiles was conducted in PBS pH 7.4, containing 1% (v/v) Tween® 80, mimicking the alveolar surfactant (316,317) and facilitating RFB dissolution, as referred previously. Drug release was also tested at pH 5.0, simulating the intracellular environment of alveolar macrophages (318).

As can be observed in Figure 6.4, both antibiotics are released from CS microparticles within two hours. The release of RFB from CS/RFB microparticles and the release of INH from CS/INH microparticles is very similar. At pH 7.4, there is an initial burst, resulting in 90% of released RFB at 30 min and total release of INH at the same time point (Figure 6.4a). The complete release of RFB from CS/RFB microparticles at pH 7.4 occurs after 60 min, a little faster than that observed for CS/INH/RFB formulation, from which 88% of RFB is released at the same period (Figure 6.4c). On the other hand, the release profiles of INH are very much alike regardless of the formulations.

At pH 7.4 and at initial time points, the release of RFB was slower compared to INH (Figure 6.4c, $p < 0.05$), in the dual drug-loaded formulation. In this case, about 70% of RFB is released after 30 min, whereas INH is almost completely available in the same period. However, when testing the release in acidic medium, no significant difference was perceived between INH and RFB profiles at any time point (Figure 6.4d).

Overall, drug release profiles exhibited similar pattern in both media, no significant differences being perceived, especially regarding INH. Although not statistically significant, RFB was released from both CS/RFB and CS/INH/RFB microparticles faster in pH 5.0 than at pH 7.4, certainly because of its higher solubility in acidic medium. In general, it is suggested that pH does not have significant impact on the release of the two antibiotics from CS microparticles.

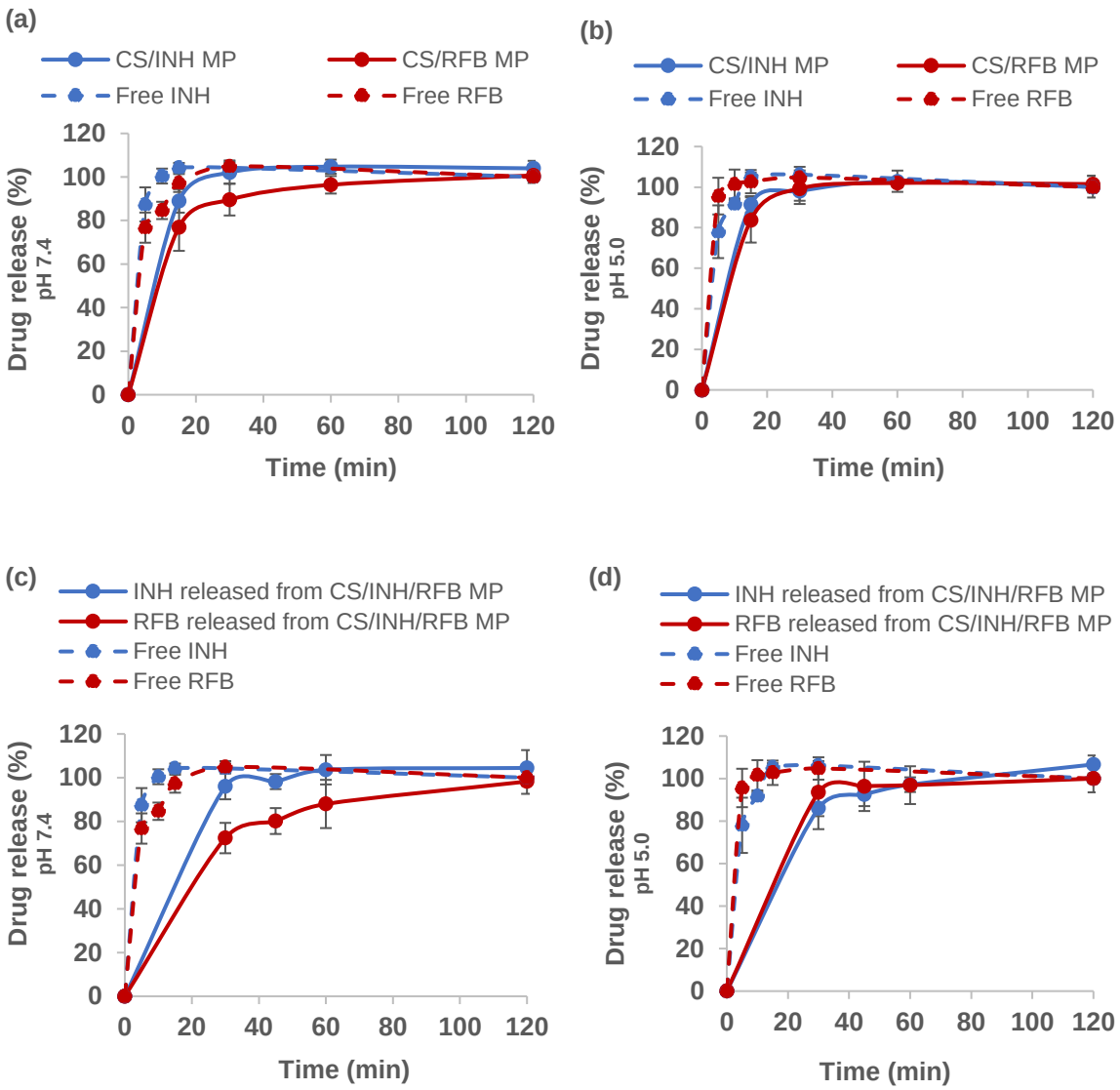

Figure 6.4. Drug dissolution and *in vitro* release profiles of isoniazid (INH) from CS/INH (10/1, w/w) microparticles and of rifabutin (RFB) from CS/RFB microparticles (10/0.5, w/w), in (a) PBS pH 7.4-Tween® 80 and (b) citrate buffer pH 5.0-Tween® 80, at 37 °C. Drug dissolution and *in vitro* release profile of INH and RFB from CS/INH/RFB (10/1/0.5, w/w) microparticles in (c) PBS pH 7.4-Tween® 80 and (d) citrate buffer pH 5.0-Tween® 80, at 37 °C. CS: chitosan; mean ± SD, *n* ≥ 3.

Importantly, the release of drugs from the produced microparticles showed different pattern compared to the respective drug dissolution profiles (Figure 6.4a-d). For instance, the release of INH from CS/INH microparticles was initially slower in comparison with free INH dissolution upon 15 min in both media (Figure 6.4a,b; $p < 0.05$). Similarly, the microencapsulation markedly delayed the RFB release from CS/RFB formulation at initial time points in neutral and acidic media (Figure 6.4a,b; $p < 0.05$). The effect of microencapsulation on the released drug was also evident

for dual drug-loaded microparticles from which drugs are completely released after 30 min (INH) and 60 min (RFB) while free drugs are completely dissolved in the media within 15 min. In general, polymers composing the carrier matrix play an important role in the modulation of drug release. Commonly, polymeric matrices that hydrate, forming gelatinous structures, which is the case of CS, can delay the diffusion of drugs through the polymeric material into the aqueous medium (367). However, in this case, although having a certain impact, CS microparticles did not extend the release of drugs for a long period.

The rapid release observed herein has also been reported for other polymeric microparticles loaded with either INH or RFB proposed for pulmonary delivery (368,369). Nevertheless, it must be considered that the used *in vitro* setting does not represent accurately the lung physiology. In fact, the volume and thickness of the alveolar lung lining fluid (around 0.01–0.1 µm) is overestimated in the assay, in which microparticles are immersed in the release media. In this way, drug release, which follows microparticle dissolution, occurs rapidly, differing from *in vivo* environment wherein microparticles would be only partially in contact with the alveolar fluid (320,321). Thus, *in vivo* profiles will probably show slower release of drugs, as has been previously published (320).

6.4 *In vitro* biocompatibility studies

6.4.1 Assessment of metabolic activity by MTT test

MTT assay was performed to evaluate the cytotoxicity of CS microparticles in cells of human alveolar epithelium (A549) and human macrophage-like cells (differentiated from THP-1 monocytes). The produced systems were tested along with free drugs, which were considered as controls. For the purpose of discussion, the occurrence of a cytotoxic effect was assumed when the material decreased cell viability below 70% (322).

The exposure of A549 cells to drug-loaded CS microparticles revealed viabilities over 70% at all tested concentrations and at both time points under evaluation (3 h and 24 h), as depicted in Figure 6.5a,b. These results indicate absence of cytotoxicity of the produced formulations. However, despite no significant differences were observed in terms of dose, viabilities of A549 cells

decreased over time upon exposure to both CS/RFB and CS/INH/RFB formulations, suggesting a time-dependent effect (Figure 6.5a,b; $p < 0.05$). In turn, macrophage-differentiated THP-1 cells were more sensitive to the contact with formulations. In fact, a dose-dependent effect was perceived on these cells, as viabilities decreased to approximately 57–59%, when cells were exposed for 24 h to CS/RFB (10/0.5) and CS/INH/RFB (10/1/0.5, w/w), at the highest tested dose (1.0 mg/mL) (Figure 6.6b). The observed toxic effect of CS microparticles on these cells is possibly an effect of RFB content, an antibiotic that has also shown to be toxic *in vivo* (327). Differently, the formulation associating only INH (CS/INH MP) revealed to be non-toxic to macrophage-differentiated THP-1 cells, since viabilities remained above 90% at all tested conditions (Figure 6.6a,b). In summary, the two formulations containing RFB had significantly more effect over cell viability, particularly on macrophage-differentiated THP-1 cells, in comparison with CS/INH formulation ($p < 0.05$).

Overall, both A549 (Figure 6.5a,b) and differentiated THP-1 cell lines (Figure 6.6a,b) tolerated well the exposure to unloaded CS microparticles, which is in agreement with other studies showing low toxicity of CS-based systems tested in the same cell lines (370,371). Moreover, upon 24 h exposure and particularly at the higher concentrations, free INH had more impact over A549 cells (Figure 6.5c) and macrophage-like THP-1 cells (Figure 6.6c) than CS/INH microparticles ($p < 0.05$), suggesting that microencapsulation may have a beneficial effect in this regard. As depicted in Figures 6.5d and 6.6d, RFB as free drug was observed to induce cytotoxicity, decreasing cell viability to around 49% in both cell lines when tested at the highest concentration (24 h). As free RFB has shown a concentration-dependent effect (Figures 6.5d and 6.6d), microparticles with lower RFB content (polymer: drug ratio = 10/0.2, w/w) were purposely produced to be tested regarding cytotoxicity. By decreasing RFB content, the viability of A549 cells remained over 90% (Figure 6.5a,b). Moreover, the decrease in RFB amount led to a viability of macrophage-like cells above 70% in all the tested conditions referred above (Figure 6.6a,b). Interestingly, free RFB was found to be toxic after 24 h incubation with macrophage-differentiated THP-1 cells at 0.025 mg/mL, but the detrimental effect was not perceived for dry powder formulations containing RFB (Figure 6.6a,b; $p < 0.05$), reinforcing the capacity of microencapsulation to improve drug toxicological profile.

It is important to mention that the highest dose tested in the present study is considered much higher than that to be observed *in vivo* upon inhalation, taking into account the large area of the alveolar zone (372). Therefore, as was also stated in Chapter 5, *in vivo* concentrations will most likely correlate those of the lower doses tested, at which no cytotoxicity were perceived. In this regard, both cell lines were considered to tolerate well the exposure to drug-loaded CS microparticles.

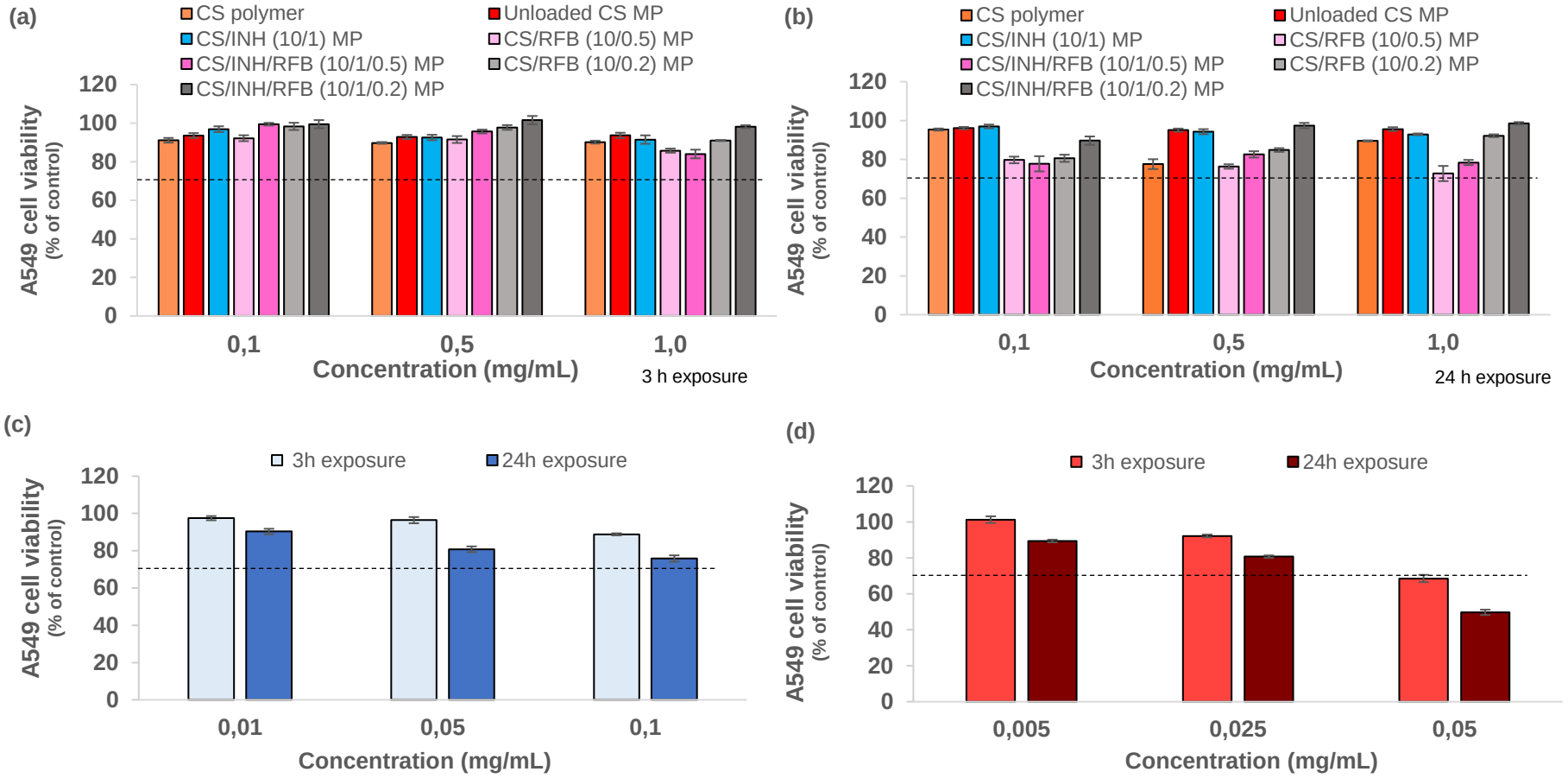

Figure 6.5. A549 cell viabilities upon (a) 3 h and (b) 24 h of exposure to chitosan (CS) polymer, unloaded and drug-loaded CS microparticles; (c) exposure to INH as a free drug; and (d) exposure to RFB as a free drug. Cell viability was calculated as a percentage of positive control (untreated cells). Data represent mean ± SEM (*n* = 3, six replicates per experiment at each concentration). Dashed line indicates 70% cell viability. INH: isoniazid; MP: microparticles; RFB: rifabutin. Note to Figure 6.5: Graphics c and d represent the same set of data of Figure 5.5 and were reprinted in this chapter to facilitate reading.

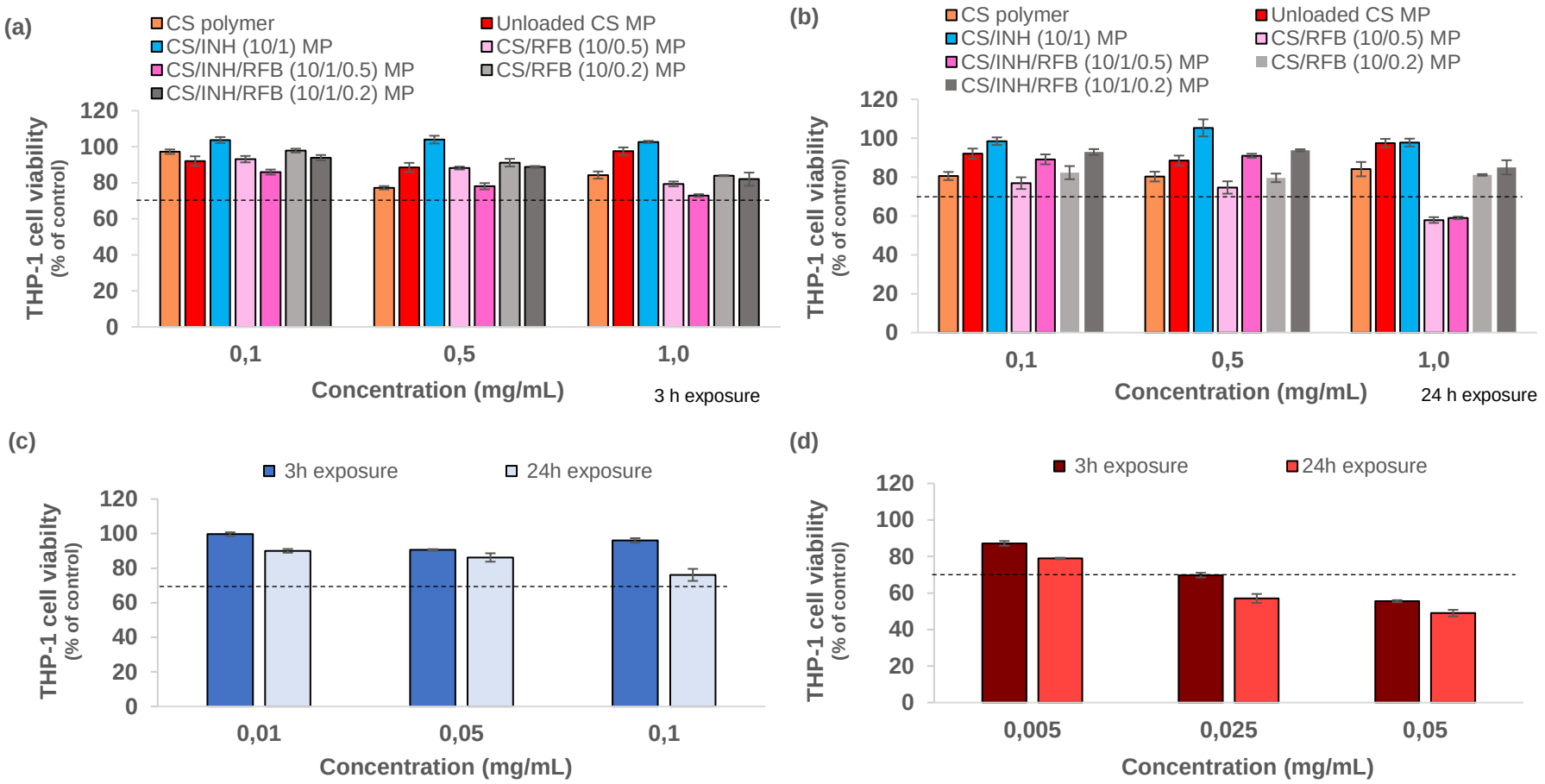

Figure 6.6. Macrophage-differentiated THP-1 cell viabilities upon (a) 3 h and (b) 24 h of exposure to chitosan (CS) polymer, unloaded and drug-loaded CS microparticles; (c) exposure to INH as a free drug and (d) exposure to RFB as a free drug. Cell viability was calculated as a percentage of positive control (untreated cells). Data represent mean ± SEM (*n* = 3, six replicates per experiment at each concentration). Dashed line indicates 70% cell viability. INH: isoniazid; MP: microparticles; RFB: rifabutin. Note to Figure 6.6: Graphics c and d represent the same set of data of Figure 5.6 and were reprinted in this chapter to facilitate reading.

6.4.2 Evaluation of cell membrane integrity

Similarly to what was performed with FUC microparticles, the integrity of cell membrane upon exposure to CS microparticles was assessed by determining the level of LDH released from alveolar epithelial (A549) and macrophage-like (THP-1) cells. Results are presented in Figure 6.7a,b. As previously reported in Chapter 5, the incubation with CCM resulted in basal release of LDH of 21% and 34%, for A549 and macrophage-differentiated THP-1 cells, respectively. Moreover, both INH and RFB as free drugs generated significantly higher release of LDH compared to control CCM ($p < 0.05$).

The results showed that unloaded CS microparticles did not raise the release of the enzyme, evidencing that CS itself does not have toxic effect on any cell line (Figure 6.7a,b), confirming what has been reported in other works (373,374). Similar to the observations of the MTT assay, microparticles loaded with RFB, either alone or in combination exhibited cytotoxic behaviour on macrophage-differentiated THP-1 cells upon 24 h exposure to 1 mg/mL. The two formulations containing RFB at the ratio polymer/RFB = 10/0.5 (w/w) released 49% (CS/INH/RFB MP) and 43% (CS/RFB MP) of LDH, amounts significantly greater than the 34% of CCM ($p < 0.05$). Such effect was not observed for microparticles associating the lower amount of RFB (polymer/RFB = 10/0.2, w/w), demonstrating that the cytotoxicity observed for the carriers is related to RFB content (Figure 6.7b).

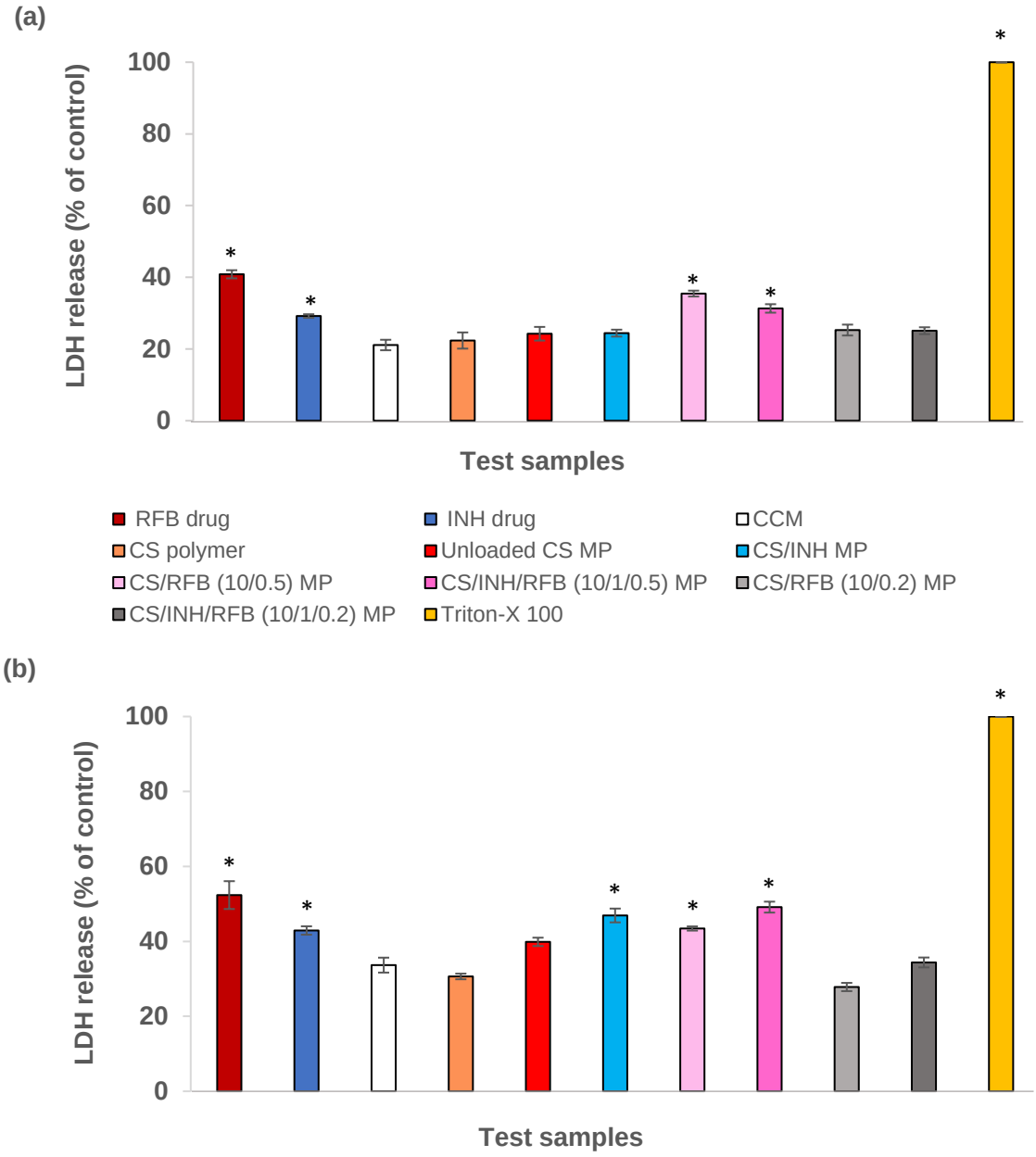

Figure 6.7. Release of lactate dehydrogenase (LDH) from (a) A549 cells and (b) macrophage-differentiated THP-1 cells exposed to chitosan (CS) polymer, CS-based microparticles (1.0 mg/mL), free rifabutin (RFB, 0.05 mg/mL), and free isoniazid (INH, 0.1 mg/mL). Cell culture medium (CCM) and Triton X-100 were used as negative and positive controls, respectively. The released LDH was calculated based on 100% assumed for positive control. Data represent mean ± SEM (*n* = 3, six replicates per experiment at each concentration). * p < 0.05 compared to CCM. Note to Figure 6.7: The set of data of free RFB, free INH, CCM and Triton is the same presented in Figure 5.7 – Chapter 5. The data were reprinted in this figure to facilitate reading

Unexpectedly, a similar observation was made in A549 cells, which also showed increased release of LDH upon exposure to CS/INH/RFB (10/1/0.5, w/w) microparticles compared with CCM (Figure 6.7a; $p < 0.05$). This slight cytotoxicity was not evidenced in the MTT assay, which showed cell viability around 80%. It should be highlighted that, despite the increased release of LDH observed in both cell lines, dual drug-loaded microparticles induced lower LDH release than free RFB ($p < 0.05$) and had an effect similar to that of free INH, thus suggesting the ability of microencapsulation to potentially reduce drug toxicological effects, as was also reported for FUC microparticles in the previous chapter.

Surprisingly, CS/INH (10/1) microparticles revealed a toxic effect on differentiated THP-1 cells, indicated by the release of approximately 46% of LDH (Figure 6.7b; $p < 0.05$). On the other hand, the single drug formulation displayed no cytotoxicity on A549 cell line, corroborating the MTT results. In addition, CS/INH (10/1) microparticles significantly promoted less LDH release than free INH ($p < 0.05$), particularly on A549 cells (Figure 6.7a).

Differently, free RFB and CS/RFB (10/0.5) microparticles induced LDH release from A549 cells at similar levels, but the former had more effect on differentated-THP-1 cells than the latter ($p < 0.05$). Additionally, the overall data demonstrated that the level of enzyme secreted after exposure to the produced microparticles is far lower than that observed for the positive control (Triton X-100).

It is worth mentioning that the different outcomes registered in both assays (MTT and LDH release) have been reported in other occasions (133,375) and was also registered in Chapter 5, referring to FUC microparticles developed in the present study. This is due the fact that the two methods assess cell-particle interactions in different ways. Microparticles possibly interact with cytoplasmic membrane, promoting cell lysis, but may not immediately interfere with intracellular organelle functions, such as mitochondrial dehydrogenase activity (376). On the other hand, particles may enhance metabolic activity, despite the small number of viable cells, leading to an overestimation of cell viability, determined by MTT assay (133). Therefore, the measurement of LDH release should be taken as a complement to the MTT assay, but there is the need to extend the range of tests to rigorously characterise the safety profile of the proposed carriers.

6.5 Macrophage activation

As described in the previous chapter for FUC microparticles, the ability of dual drug-loaded CS microparticles (CS/INH/RFB = 10/1/0.5, w/w) to activate macrophage-like cells was evaluated by determining the amount of secreted pro-inflammatory cytokines (TNF-α and lL-8) upon the exposure.

Macrophage-differentiated THP-1 cells were exposed to the microparticles for 24 h prior to cytokine quantification. As observed in Figure 6.8, dual drug-loaded CS microparticles induced the secretion of a considerable amount of cytokines, 614 pg/mL for TNF-α and 10.6 x 10^3 pg/mL for IL-8. In both cases the values were much higher than those of basal secretion, considered that produced by cells incubated with CCM, the negative control ($p < 0.05$). No significant differences were found between TNF-α secretion promoted by loaded carriers and CS polymer (Figure 6.8a), evidencing that the observed effect is induced by the polymer rather than by its particulate form. However, a significant difference was observed for IL-8, comparing the two samples (Figure 6.8b; $p < 0.05$). In that case, drug encapsulation apparently interfered with cell receptor signaling during immune activation, thus decreasing macrophage activation ability. A possible explanation for this effect is that, the length of the released polymeric chain and also the number of fractions of *N*-acetylglucosamine residues influences the level of immune activation and drug encapsulation can possibly alter this pattern (377). It is worth mentioning that *N*-acetylglucosamine moieties are reported to be recognised by macrophage receptors (353), thus, possibly, inducing cell activation.

Although the formulations induced cytokine production at lower levels compared to LPS, the overall observation is that the exposure of macrophage-like cells to CS microparticles resulted in cell activation demonstrated by the increased release of TNF-α and IL-8 in comparison with CCM. This is corroborated by other studies that described the ability of CS to promote the production of the referred cytokines by macrophage-like cells (306,378). Although the natural immunomodulatory properties of CS have been already demonstrated (379), the mechanism through which CS particles induce immune response still needs to be unveiled.

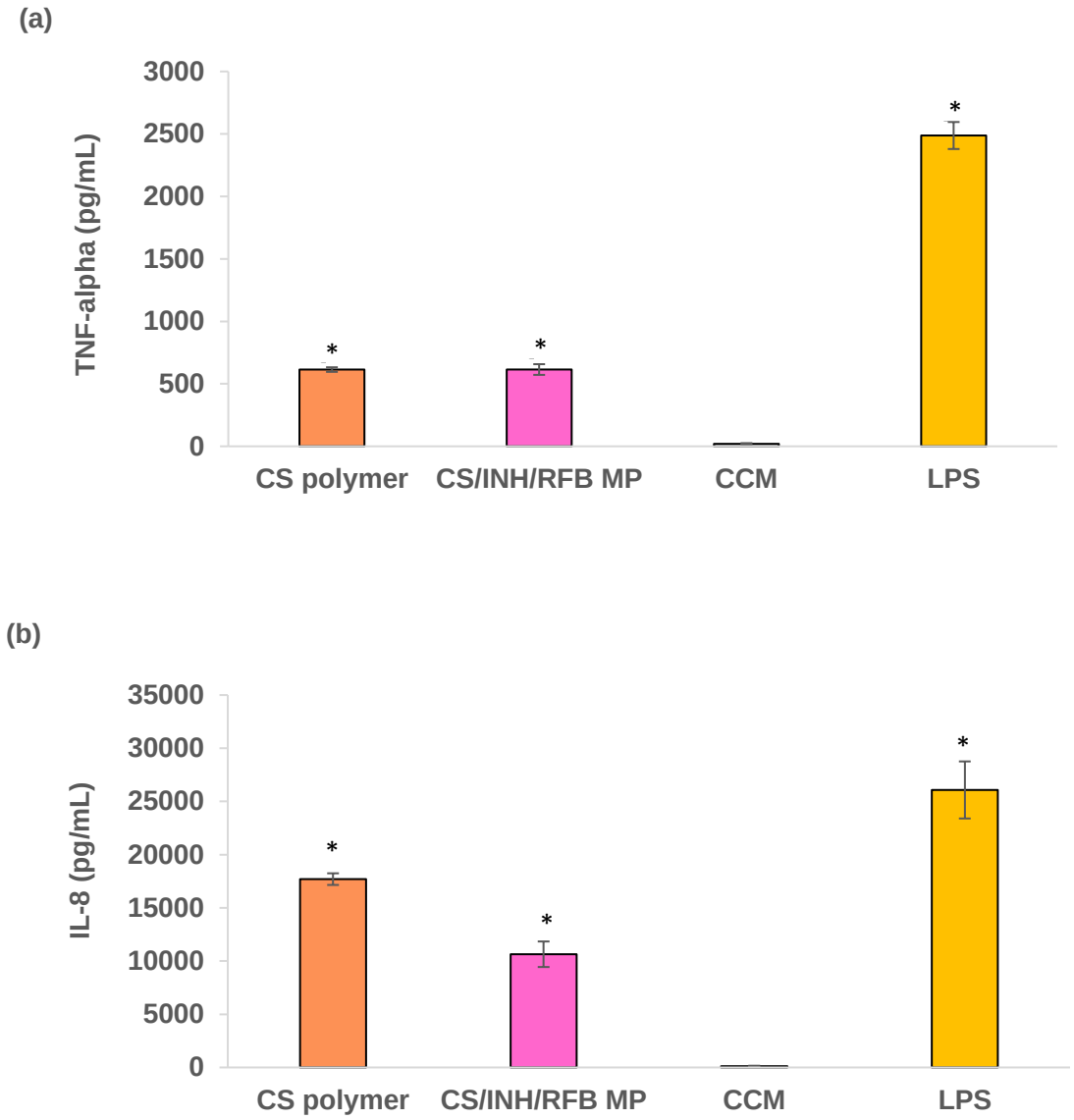

Figure 6.8. TNF-α (a) and IL-8 (b) secretion by macrophage-differentiated THP-1 cells upon 24 h exposure to CS/INH/RFB (10/1/0.5) microparticles (MP) and CS as raw material. Cell culture medium (CCM) and lipopolysaccharide (LPS) were used as negative and positive controls, respectively. CS: chitosan; INH: isoniazid; RFB: rifabutin. Data represent mean ± SEM (*n* = 3). * p < 0.05 compared to CCM. Note to Figure 6.8: The set of data of CCM and LPS is the same presented in Figure 5.8 – Chapter 5. The data were reprinted in this figure to facilitate reading.

6.6 Preliminary evaluation of microparticle uptake by macrophages

The uptake of CS microparticles was assessed in macrophage-differentiated THP-1 cells and rat alveolar macrophages NR8383. Cells were exposed to

fluorescently-labelled CS microparticles at concentrations of 50 and 200 µg/cm^2, for 2 h, and the obtained results are presented in Figure 6.9. Microparticle uptake by macrophage-differentiated THP-1 cells was demonstrated to be very high at both concentrations (94.3 ± 1.5 for 50 µg/cm^2 and 98.1 ± 1.8% for 200 µg/cm^2). Likewise, rat macrophages (NR8383 cells) internalised up to 99.9 ± 0.1, regardless of the dose. These preliminary results suggest high affinity of macrophages for CS microparticles independently of concentrations and cell type. It is well-known that macrophages are specialised cells, which recognise and engulf particulate matter, and thus the internalisation of particles was expected. Nevertheless, residues of *N*-acetylglucosamine, a structural unit of CS, have been described to be preferentially recognised by macrophages (353). The presence of such units possibly mediated the phagocytic mechanism, which could explain the high affinity of cells for the produced microparticles. However, it is deemed adequate to consider future assays providing comparison with a material devoid of units recognised by macrophages. In this way, the favourable recognition of CS-based carriers by macrophage-like cells could be unequivocally established. Furthermore, obtaining confocal microscopy images would be beneficial to corroborate cytometry data gathered so far.

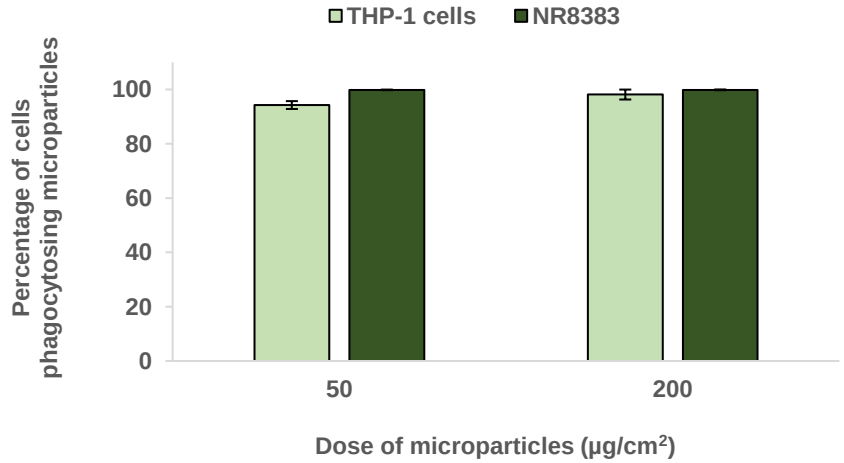

Figure 6.9. Percentage of human macrophage-differentiated THP-1 cells and rat alveolar macrophages (NR8383 cells) phagocytosing fluorescently-labelled chitosan microparticles. Cells were exposed (2 h) to 50 and 200 µg/cm^2 of microparticles. Data represent mean ± SEM (*n* ≥ 3).

6.7 Determination of minimum inhibitory concentration (MIC)

The viability of *M. bovis* cells was verified upon exposure to dual drug-loaded CS microparticles and free drugs (either alone or in combination). Due to time constraints, only the dry powder combining the two antibiotics was tested in this assay (CS/INH/RFB = 10/1/0.5, w/w), as the formulation complies with WHO recommendations for combined TB therapy, as previously mentioned.

MIC values were calculated in relation to control (culture of mycobacteria), assumed as 100% bacterial growth. As reported in Chapter 5, the MIC determined for the free drugs was 0.125 µg/mL for INH and 0.004 µg/mL for RFB, evidencing the stronger antimicrobial effect of RFB compared to INH. When in combination, free INH and RFB inhibited bacterial growth by 94 ± 1%, presenting MIC values of 0.008 µg/mL and 0.004 µg/mL, respectively. In what concerns the microcarriers, a dose of 0.08 µg/mL of drug-loaded CS microparticles was the minimum concentration needed to inhibit mycobacterial growth by 96 ± 1%. At this concentration, microparticle drug contents are approximately 0.007 µg/mL (INH) and 0.004 µg/mL (RFB), considering the association efficiencies. It is worth mentioning that these results are in line with MIC values determined for the free antibiotics in combination. In other words, no differences were perceived in terms of inhibition effects comparing drug-loaded CS microparticles (96 ± 1%) and INH/RFB solution (94 ± 1%). This indicates that the microencapsulation of the drugs in combination did not interfere with their antibacterial activity. As well, results demonstrate that the proposed formulation can potentially inhibit the growth of *M. bovis in vitro*.

6.8 Preliminary *in vivo* studies

As stated in the previous chapter, *in vivo* assays of a drug delivery system comprise a wide range of experiments. This applies not only to the developed drug-loaded carriers, but also for the biomaterial itself. Although CS has been widely proposed as biomaterial to be used in the pharmaceutical field, very few studies on *in vivo* toxicity upon pulmonary administration have been reported (380).

As performed for FUC, blood samples collected from BALB/c mice that inhaled unloaded CS microparticles were analysed in order to verify the occurrence of eosinophilia and/or the presence of IgE in the sera of treated animals.

Results from the blood smears revealed an eosinophil count of around 1% in the group of mice treated with unloaded CS microparticles, which was similar to the control mice (Figure 6.10), indicating a non-pathological state as the values obtained are within the reference range for eosinophil count in male BALB/c mice (0 – 5%), as discussed in the previous chapter. Therefore, the normal relative number of eosinophils in the sera indicates the absence of inflammatory response after inhalation of the produced CS microparticles. Furthermore, the overall count of white blood cells, which are inflammatory cells, disclosed no significant differences when comparing the two groups (Figure 6.10), reinforcing that the inhalable dry powder was well tolerated by the animals.

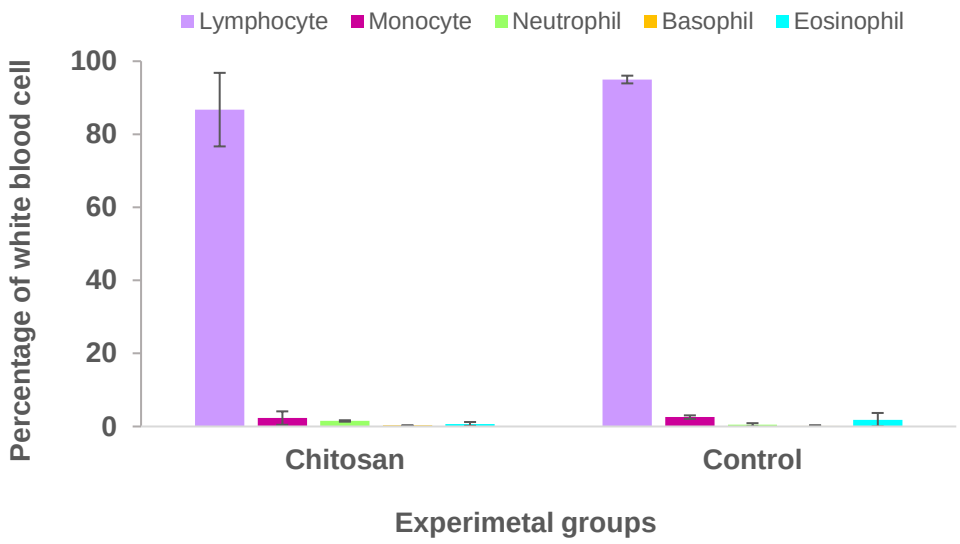

Figure 6.10. Percentage of white blood cells counted in the blood smears. Mean ± SD.

As discussed in Chapter 5, immunodiffusion tests (Ouchterlony technique) were conducted as a complementary evaluation of an allergic response, possibly induced by the carriers, and showed no visible precipitation reactions between antibody-antigen. As stated in the previous chapter, this is probably due to the fact that low levels of IgE were present in the sera of treated mice, suggesting the biomaterial did not induce allergic reaction. However, a commercial IgE sample, to be used as control, is needed to confirm that observation.

6.9 Conclusion

Inhalable CS dry powders loaded with INH and RFB, either separately or in combination, were prepared by spray-drying, with drug association efficiency varying between 90% and 99%, depending on the formulation. The developed microparticles displayed MMAD in the range of 2.5 – 4.2 µm and FPF varying from 43% to 63%, thus evidencing thus adequate aerodynamic properties for deep lung delivery. Cytotoxicity assays demonstrated good tolerability of alveolar epithelial cells to the produced formulations, while a slight decrease on cell viability of macrophage-like cells was observed at the highest tested microparticle concentration (1.0 mg/mL) after 24 h exposure to dry powders containing RFB. Nevertheless, this dose was considered as possibly overestimated comparing to real *in vivo* conditions. Furthermore, a preliminary evaluation indicated strong ability of CS microparticles for macrophage uptake *(*up to 99.9%) but complementing cytometry data with confocal microscopy would be beneficial in corroborating the data described herein. Importantly, CS-based microcarriers induced macrophage activation and demonstrated to preserve drug antibacterial activity against *M. bovis in vitro*. A preliminary *in vivo* evaluation showed no indication of allergyc reponse in mice that inhaled CS microparticles, suggesting that the biomaterial was well tolerated by the animals. In conclusion, the developed CS microparticles were considered to exhibit suitable properties to mediate inhalable therapy for pulmonary TB.

This page was intentionally left in blank

Chapter Seven

Final Considerations

This page was intentionally left in blank

7. Final considerations

7.1 General discussion

In the present study, we proposed the use of respirable carriers composed of polysaccharides, namely FUC and CS, for the treatment of pulmonary TB. Natural polymers possess several favourable characteristics in comparison with synthetic polymers used in drug delivery, including higher propensity for biocompatibility and biodegradability, and the fact that they are abundant renewable sources (132). Furthermore, FUC and CS are reported to be specifically recognised by macrophage receptors (40,245) and have been shown to potentiate macrophage activation, mediated by membrane receptors (241). The induction of macrophage activation is beneficial, in this case, as activated macrophages control more efficiently the proliferation and dissemination of pathogens, such as *M. tuberculosis* (42). Thus, the use of FUC and CS as matrix of polymeric carriers allows targeted TB therapy, particularly toward alveolar macrophages infected with mycobacteria.

We explored the potential of FUC and CS as matrixes of nano and microparticles for the pulmonary delivery of anti-TB drugs. The feasibility of the approach was demonstrated by using INH and RFB as model anti-TB drugs.

NANOPARTICLES

The production of nanoparticles initiated with a complexation between the two polymers, considering that they exhibit opposite electrical charge. As aforementioned, FUC has been used in the development of nanoparticles and polyelectrolyte complexation is the predominant technique, in most cases having CS as counterion (120,141,147,246,264,381). Nanoparticles were then produced by polyelectrolyte complexation between FUC and CS, but the technique did not allow the incorporation of drugs into the carriers. A possible explanation lies in the nature of the drugs, although drug entrapment is also influenced by the concentration of polymeric solutions, drug/polymer ratios and ionic strength among other factors (269).

In light of this, nanoprecipitation was used as an alternative production method, resulting in the formation of polymeric nanoparticles with variable size and

PdI values. Several approaches were applied aiming at obtaining particles in the submicron range with unimodal size distribution. Importantly, CS nanoparticles were not able to associate any drug during the nanoprecipitation process. Differently, the technique allowed the encapsulation of RFB in FUC nanoparticles, registering association efficiencies up to 46%, although not in a reproducible manner. Reproducibility is crucial when developing an experimental protocol. Indeed, nanoprecipitation is generally known as an easy and reproducible technique, but many operating parameters must be managed to ensure the production of nanoparticles with the adequate characteristics. These include the choice of solvent, non-solvent type and volume, stirring rate and time, polymer concentration, etc., to name a few. The referred operating conditions may have a major impact on the resulting characteristics of the carriers (274). Although nanoprecipitation has been widely applied to produce polymeric nanoparticles (271,282), the knowledge about the self-assembly of other polymers is yet needed to elucidate a generic application of such an easy method to a wide range of polymers.

In summary, two different techniques were used to produce nanoparticles based on FUC and CS. Both resulted in the formation of particles in the nanoscale, but the tested protocols did not allow drug encapsulation in a reproducible and efficacious manner. Therefore, due to time constraints, it was decided to direct the efforts to the development of microparticles.

MICROPARTICLES

Characterisation of microparticles

Respirable microparticles based on FUC and CS were successfully produced by spray-drying. This was the method of choice because it offers great control over critical parameters of the resulting microparticles, including their size, shape and density. Furthermore, it is a unique single step method for microencapsulation of drugs in polymeric carriers (95). The yields of the process varied between 74 and 85%, proving that spray-drying is a great choice for the production of FUC and CS microparticles.

In addition, the present research demonstrated the capacity of FUC and CS microparticles to associate not only one, but also two first-line anti-TB drugs

simultaneously in a single formulation. To date, this is the first study describing the use of spray-drying to produce respirable FUC-based microparticles loaded with one or two first-line anti-TB drugs. Contrarily, the production of CS microparticle loaded with one anti-TB drug has been reported in the last years (239,306). However, as far as we know, the association of two anti-TB drugs to spray-dried CS microparticles is described herein for the first time. Both polysaccharides provided microparticles with high drug association efficiencies (> 80%). However, FUC microparticles provided slightly lower and more variable association efficiency (81 – 97%) comparing with CS microparticles (90 – 99%). For each polymer, no significant differences were perceived in terms of the ability to associate the drugs, when comparing single and dual drug-loaded microparticles. In light of this, we may state that producing FUC and CS microparticles loaded with two anti-TB drugs is a better choice, since these formulations comply with the combined therapy that WHO recommends for TB (261).

Microparticles based on FUC or CS were analysed regarding size, density and morphology because these parameters strongly influences the sedimentation and dispersion properties of inhalable dry powders (66). The determined real densities were around 1.35 – 1.78 g/cm^3, suggesting that microparticles have a matrix dense core. As well, the particle shape may have a strong impact on carrier performance, and thus the developed microparticles were analysed by SEM, showing variable morphologies. FUC provided slightly convoluted microparticles with smooth surfaces that assumed a more irregular shape and acquired wrinkles, after the incorporation of RFB. The perceived changes were attributed to the drug itself, as this observation has been reported for other spray-dried microparticles loaded with RFB (239). Nevertheless, ethanol, used to dissolve RFB, was also ascribed a role in this effect. In fact, the removal of ethanol from microparticle surfaces occurs faster than water evaporation, inducing the formation of a primary shell that collapses as the water content in the core evaporates (298). In turn, the association of INH conferred to FUC microparticles a spherical shape with crystal structures, a consequence of Man deposition on particle surface. It should be noticed that the dual drug-loaded microparticles displayed a morphology comparable with those associating RFB (single drug formulation), with wrinkled irregular particles. Differently, CS rendered spherical microparticles, having irregular surface that generally becomes smoother after drug incorporation. This indicates

that drug association had less impact on the morphology of CS microparticles, comparing with FUC. As has been stated for long, the morphology of spray-dried particles depends on their composition along with the operating parameters (382).

Considering the irregular shape of FUC microparticles, one could expect enhanced dry powder aerosolisation, endowed by reduced cohesive forces between particles, thus preventing agglomeration and improving respirability (78,298). Nevertheless, both FUC and CS-based dry powders exhibited similar *in vitro* performance when evaluating aerosolisation properties using ACI. The emitted dose of drug-loaded FUC microparticles (84 – 98%) is comparable to that exhibited by CS carriers (>90%), all being in accordance with the values established by the European Pharmacopeia (75). Likewise, respirable fractions (FPF ≤ 5μm) of FUC microparticles (39 – 55%) are close to those of CS counterparts (43 – 63%). The aerodynamic diameters of FUC and CS carriers are very much alike, as dual drug-loaded microparticles and INH-loaded microparticles (single drug formulation) presented MMAD around 4 μm. Yet, dry powders containing RFB (single drug formulation) displayed MMAD of approximately 2 μm (FUC) and 2.5 μm (CS), anyway values not significantly different. These values are in the size range required for deep lung deposition of aerosols (315).

The evaluation of drug release profiles is a matter of utmost importance when designing drug delivery systems. Hence, the *in vitro* release of drugs from the developed carriers was determined in media relevant for pulmonary administration and specific of the context of this thesis: i) in PBS (pH 7.4) with the addition of 1% (v/v) Tween® 80, resembling the lung lining fluid in terms of pH and the presence of surfactant (316,317); and in more acidic medium (citrate buffer pH 5) to simulate the phagolysosomal environment, assuming macrophage uptake of microparticles (318). Overall, both INH and RFB were rapidly released from microparticles, regardless of the formulation. In general, 100% drug release was observed within 120 min. CS microparticles evidenced, however, a slightly slower profile, although not to a statistically significant level. This is easily explained with the gelling ability of CS that delays drug diffusion (367), which is not a characteristic of FUC. Moreover, the pH did not interfere with drug release profiles. As previously discussed, we expect that *in vivo* drug release will occur more slowly, considering that a lower amount of liquid is present in the alveoli compared with that involved in the assays. It is well known that the alveolar epithelium is covered by a thin layer

(0.01–0.1 µm) of lung lining fluid, and thus microparticles are expected to be only partially in contact with this fluid, and not immersed in it (320,321). This will certainly impact on drug dissolution, and thus on the release profile.

In summary, according to the observed features, it can be inferred that both FUC and CS provided spray-dried microparticles suitable for pulmonary delivery with great potential to reach the respiratory zone and capacity to release the associated drugs.

Assessment of biological behaviour

Taking into consideration that safety and biocompatibility are important parameters in the design of drug delivery systems, the cytotoxicity of the proposed polymeric carriers was assessed in human pulmonary epithelial (A549) and macrophage-differentiated THP-1 cells.

The metabolic assay MTT was performed, testing three different concentrations of microparticles (0.1, 0.5 and 1.0 mg/mL) at two time points (3 and 24 h). Cells were exposed to free drugs (INH and RFB) as well, at doses equivalent to theoretical loadings in the microparticles: 10% (w/w) for INH (0.01; 0.05 and 0.1 mg/mL) and 5% (w/w) for RFB (0.005; 0.025 and 0.05 mg/mL).

Overall, cells tolerated well the contact with both polymers and unloaded microparticles, suggesting that the selected biomaterials are non-toxic. Similarly, microparticles loaded with INH (single drug formulation) had no effect on cell viability in both cell lines. Nonetheless, macrophage-differentiated THP-1 cells were sensitive, after 24 h-exposure, to dry powders (1 mg/mL) containing RFB. The observed toxic effect was assumed to be due to RFB content, given that the free drug has been reported to be toxic *in vivo* (327,328) and the control assays with free RFB demonstrated similar effect. With this in mind, microparticles with reduced amount of RFB (2%, w/w) were produced to be purposely tested in cytotoxicity assays, revealing no toxic effect under the same conditions. The obtained results, thus, confirmed that the cytotoxicity was due to the content of RFB, although the used dose was possibly overestimated comparing to real *in vivo* conditions.

Such sensitivity was not observed in alveolar epithelial cells (A549) that showed viability over 70% in all tested conditions, considering formulations composed of either FUC or CS. To complement the observations of the MTT assay,

the release of the cytoplasmic enzyme LDH by the cells, upon exposure to microparticles, was determined. Essentially, the results obtained in the LDH release assessment were aligned with those of MTT, with only punctual differences in two of CS-based microparticle formulations. The different outcomes can be explained by the fact that the two methods assess cell-particle interactions in distinct ways. For instance, particles may enhance metabolic activity, despite the small number of viable cells, leading to an overestimation of cell viability, determined by the MTT assay (133). Therefore, the measurement of LDH release should be taken as a complement to the MTT assay, as indicated above, but there is the need to extend the range of tests to rigorously characterise the safety profile of the proposed carriers.

Furthermore, both FUC and CS microparticles, loaded with anti-TB drugs, were demonstrated to preserve *in vitro* the drug antibacterial activity against *M. bovis* (around 95% growth inhibition), the two formulations with MIC values of 0.08 µg/mL. These concentrations correspond to the MIC values determined for the two drugs when tested in combination (as free drugs). Therefore, these observations demonstrate that in both cases the process of microencapsulation preserved the bactericidal activity of drugs (evaluated *in vitro* against *M. bovis*).

Preliminary *in vivo* experiments were also conducted to evaluate a possible allergic reaction generated by the inhalation of FUC and CS microparticles (unloaded) by mice. The analysis of blood smears revealed eosinophil counts around 1% in the group of mice treated with unloaded microparticles (FUC and CS), similar to control and in agreement with the haematological reference range for eosinophil count in male BALB/c mice (351). This demonstrates that the inhalation of the produced carriers generated no sign of airway inflammation, since eosinophilia was not perceived in the peripheral blood. Thus, it was suggested that both biomaterials, FUC and CS, were well tolerated by the animals. Nevertheless, this is a very initial step in the evaluation of biocompatibility of polymers that needs to be complemented with more robust assays and dedicated studies. That will be the necessary kick-off for the solid proposal of alternative excipients that are currently one of the pin-points of lung drug delivery.

Despite presenting similar characteristics and behaviours in the more basic aspects of characterisation (drug loading, aerosolisation properties, biocompatibility), important and perhaps unexpected differences were found

between the two systems when performing specific biological assays regarding the intended application. As previously stated, the rationale of selecting FUC and CS as matrix of inhalable microparticles, aimed at the delivery of anti-TB drugs, relies on their chemical composition, including in both cases moieties that favour macrophage targeting.

This suggested that microparticle uptake by the target cells would be favoured by the matrix composition. Additionally, there was also the possibility that microparticle-cell interaction resulted in macrophage activation, enabling better control of the infection mediated by increased cytokine production (383). The literature reports that macrophages recognise preferentially fucose and mannose moieties (384). Based on this, a more favourable behaviour of FUC microparticles was expected. In fact, these had stronger impact on macrophage activation, comparing with CS carriers. However, the induced interleukin production was significantly higher than the negative control (CCM) in both cases. In parallell, the preliminary evaluation of microparticle uptake by macrophage-like cells (human differentiated macrophages and rat alveolar macrophages) revealed that FUC microparticles were internalised in a dose-dependent manner (23 – 87% uptake). In contrast and quite surprisingly, CS microparticles showed very high tendency (up to 99%) to be captured, regardless of the dose. Thus, this study has shown that alveolar macrophages can potentially uptake the proposed carriers and provided experimental evidence of the theoretical rationale of this project.

In summary, the obtained data demonstrate that the proposed respirable carriers present adequate aerodynamic properties for reaching the respiratory zone. Their biological evaluation evidenced absence of cytotoxicity, considering the doses that correspond to a more realistic *in vivo* condition. Moreover, a preliminary assessment indicated no allergic reaction in mice after pulmonary administration of the microparticles. In addition, it was revealed that the microencapsulation process had no impact on the bactericidal efficacy of the anti-TB drugs. Furthermore, a preliminary evaluation indicated strong ability of the developed carriers to undergo macrophage uptake and the ability to induce macrophage activation. Considering all above, the developed microparticles based on FUC or CS are considered to hold potential as pulmonary delivery systems for the treatment of pulmonary TB. It is worth mentioning that the developed single drug formulations are herein proposed

as add-on therapy whereas dual drug-loaded microparticles properly comply with the combined therapy for TB treatment.

7.2 Prospects for future research

Considering the entire set of data, the developed polymeric microparticles loaded with first-line anti-TB drugs, either alone or in combination, are promising tools for the implementation of an inhalable therapy of pulmonary TB. However, several aspects must be addressed in the future to permit more conclusive findings. Essentially, further investigation is required to have a more realistic view of the safety and efficacy of the proposed carriers. The relevant aspects that must be addressed in the future include:

i. To evaluate physical stability of the carriers;
ii. To complement the obtained cytometry data regarding the macrophage uptake of microparticles with confocal microscopy;
iii. To assess the capacity of the produced carriers to enhance macrophage phagocytosis mediated by the chemical groups on the polymeric structures of FUC and CS. This can be evaluated by comparison with a polysaccharide devoid of units recognised by macrophages;
iv. To further evaluate the biocompatibility of the carriers, *in vivo*, in order to determine whether or not unloaded microparticles induce an allergic response.
v. To perform *in vivo* evaluation of the capacity of drug-loaded carriers to reach alveoli by characterising the distribution of particles upon inhalation with imaging technique;
vi. To evaluate the *in vivo* antibacterial efficacy of drug-loaded microparticles;
vii. To unveil the *in vivo* effect of a long-term administration of the developed microparticles.

Reference

1. Sharma SK, Mohan A. Tuberculosis: From an incurable scourge to a curable disease - Journey over a millennium. Indian J Med Res. 2013;137(3):455–93.
2. Ducati RG, Ruffino-Netto A, Basso LA, Santos DS. The resumption of consumption - A review on tuberculosis. Mem Inst Oswaldo Cruz. 2006;101(7):697–714.
3. Dubos, René and Dubos J. The white plague: Tuberculosis, man, and society. Bulletin of the Medical Library Association.1996;42(1):142-43.
4. Saleem A, Azher M. The next pandemic - Tuberculosis: The oldest disease of mankind rising one more time. Br J Med Pract. 2013;6(1):615–23.
5. Murray JF. A century of tuberculosis. Am J Respir Crit Care Med. 2004;169:1181–6.
6. World Health Organization. Global Tuberculosis Report 2018. World Health Organization, Geneva. Geneva, Switzerland; 2018.
7. Elkington PT. Tuberculosis: Time for a new perspective? J Infect. 2013;66(4):299–302.
8. World Health Organization. Global Tuberculosis Report 2017. World Health Organization, Geneva. Geneva, Switzerland; 2017.
9. World Health Organization. Global Tuberculosis Report 2015. World Health Organization, Geneva. Geneva, Switzerland; 2015.
10. Udwadia ZF. MDR , XDR , TDR tuberculosis : ominous progression. 2012;1–2.
11. Ellis RC, Zabrowarny LA. Safer staining method for acid fast bacilli. J Clin Pathol. 1993;46(6):559–60.
12. Kaur K, Gupta A, Narang RK, Murthy RSR. Novel drug delivery systems: Desired feat for tuberculosis. J Adv Pharm Technol Res. 2010;1(2):145–63.
13. de Jong BC, Antonio M, Gagneux S. Mycobacterium africanum-Review of an important cause of human tuberculosis in West Africa. PLoS Negl Trop Dis. 2010;4(9):1–12.
14. Alexandra Aubry, Olivier Chosidow, Eric Caumes, Jérôme Robert EC. Sixty-three cases of Mycobacterium marinum infection. Arch Intern Med. 2002;162:1746–52.
15. Levine B, Chaisson RE. Mycobacterium kansasii: A cause of treatable pulmonary disease associated with advanced human immunodeficiency virus (HIV) infection. Ann Intern Med. 1991;114(10):861–8.
16. Niemann S, Richter E, Dalügge-Tamm H, Schlesinger H, Graupner D, Königstein B, et al. Two cases of Mycobacterium microti-derived tuberculosis in HIV-negative immunocompetent patients. Emerg Infect Dis. 2000;6(5):539–42.
17. Young RA, Mehra V, Sweetser D, Buchanan T, Clark-Curtiss J, Davis RW, et al.

Genes for the major protein antigens of the leprosy parasite Mycobacterium leprae. Nature. 1985;316:450–2.
18. Swenson JM, Wallace RJ, Silcox VA, Thornsberry C. Antimicrobial susceptibility of five subgroups of Mycobacterium fortuitum and Mycobacterium chelonae. Antimicrob Agents Chemother. 1985;28(6):807–11.
19. Grange JM. Mycobacterium bovis infection in human beings. Tuberculosis. 2001;81(2):71–7.
20. Wayne LG, Sramek HA. Agents of newly recognized or infrequently encountered mycobacterial diseases. Clin Microbiol Rev. 1992;5(1):1–25.
21. Field SK, Fisher D, Cowie RL. Mycobacterium avium complex pulmonary disease in patients without HIV infection. Chest J. 2004;126(2):566–81.
22. O´Reilly LM, Daborn CJ. The epidemiology of Mycobacterium bovis infections in animals and man: A review. Tuber Lung Dis. 1995;76(1):1–46.
23. Russell DG. Who puts the tubercle in tuberculosis? Nat Rev Microbiol. 2007;5(1):39–47.
24. Cole EC, Cook CE. Characterization of infectious aerosols in health care facilities: An aid to effective engineering controls and preventive strategies. Am J Infect Control. 1998;26(4):453–64.
25. Nicas M, Nazaroff WW, Hubbard A. Toward understanding the risk of secondary airborne infection: Emission of respirable pathogens. J Occup Environ Hyg. 2005;2(3):143–54.
26. Stetzenbach LD, Buttner MP, Cruz P. Detection and enumeration of airborne biocontaminants. Curr Opin Biotechnol. 2004;15(3):170–4.
27. Cheng YS. Mechanisms of pharmaceutical aerosol deposition in the respiratory tract. AAPS PharmSciTech. 2014;15(3):630–40.
28. Kleinnijenhuis J, Oosting M, Joosten LAB, Netea MG, Van Crevel R. Innate immune recognition of Mycobacterium tuberculosis. Clin Dev Immunol. 2011;2011:1–12.
29. Rohde K, Yates RM, Purdy GE, Russell DG. Mycobacterium tuberculosis and the environment within the phagosome. Immunol Rev. 2007;219(1):37–54.
30. Alonso S, Pethe K, Russell DG, Purdy GE. Lysosomal killing of Mycobacterium mediated by ubiquitin-derived peptides is enhanced by autophagy. Proc Natl Acad Sci U S A. 2007;104(14):6031–6.
31. Chan J, Xing Y, Magliozzo RS, Bloom BR. Killing of virulent Mycobacterium tuberculosis by reactive nitrogen intermediates produced by activated murine macrophages. J Exp Med. 1992 Apr;175(4):1111–22.
32. Ahmad S. New approaches in the diagnosis and treatment of latent tuberculosis

infection. Respir Res. 2010;11:1–17.
33. Kyei GB, Vergne I, Chua J, Roberts E, Harris J, Junutula JR, et al. Rab14 is critical for maintenance of Mycobacterium tuberculosis phagosome maturation arrest. EMBO J. 2006 Nov 15;25(22):5250–9.
34. Baena A, Porcelli SA. Evasion and subversion of antigen presentation by Mycobacterium tuberculosis. Tissue Antigens. 2009;74(3):189–209.
35. Clifford V. Harding; W. Henry Boom. Regulation of antigen presentation by Mycobacterium tuberculosis: a role for Toll-like receptors. Nat Rev Microbiol. 2011;8(4):296–307.
36. Rodrigues S, Grenha A. Activation of macrophages: Establishing a role for polysaccharides in drug delivery strategies envisaging antibacterial therapy. Curr Pharm Des. 2015;21(33):4869–87.
37. Geiser M. Update on macrophage clearance of inhaled micro- and nanoparticles. J Aerosol Med Pulm Drug Deliv. 2010;23(4):207–17.
38. Yamamoto K, Nishimura N, Doi T, Imanishi T, Kodama T, Suzuki K, et al. The lysine cluster in the collagen-like domain of the scavenger receptor provides for its ligand binding and ligand specificity. FEBS Lett. 1997;414:182–6.
39. Doi T, Higashino KI, Kurihara Y, Wada Y, Miyazaki T, Nakamura H, et al. Charged collagen structure mediates the recognition of negatively charged macromolecules by macrophage scavenger receptors. J Biol Chem. 1993;268(3):2126–33.
40. Aderem A, Underhill DM. Mechanisms of phagocytosis in macrophages. Annu Rev Immunol. 1999;17:593–623.
41. Fenton MJ, Vermeulen MW. Immunopathology of tuberculosis: Roles of macrophages and monocytes. Infect Immun. 1996;64(3):683–90.
42. JoAnne L. Flynn and John Chan. Immunology of tuberculosis. Annu Rev Immunol. 2001;19:93–129.
43. Getahun H, Matteelli A, Abubakar I, Abdel Aziz M, Baddeley A, Barreira D, et al. Management of latent Mycobacterium tuberculosis infection: WHO guidelines for low tuberculosis burden countries. Eur Respir J. 2015;46(6):1563–76.
44. Mack U, Migliori GB, Sester M, Rieder HL, Ehlers S, Goletti D, et al. LTBI: Latent tuberculosis infection or lasting immune responses to M. tuberculosis? A TBNET consensus statement. Eur Respir J. 2009;33(5):956–73.
45. Hossain MM, Norazmi M-N. Pattern recognition receptors and cytokines in Mycobacterium tuberculosis infection — The double-edged sword? Biomed Res Int. 2013;2013:1–18.
46. Rustad TR, Sherrid AM, Minch KJ, Sherman DR. Hypoxia: A window into Mycobacterium tuberculosis latency. Cell Microbiol. 2009;11(8):1151–9.

47. Lawn SD, Zumla AI. Tuberculosis. Lancet. 2011;378:57–72.
48. Zumla A, Raviglione M, Hafner R, Reyn CF von. Tuberculosis. N Engl J Med. 2013;368:745–55.
49. Hopewell PC, Pai M, Maher D, Uplekar M, Raviglione MC. International standards for tuberculosis care. Lancet Infect Dis. 2006;6:710–25.
50. Pai M, Minion J, Sohn H, Zwerling A, Perkins MD. Novel and improved technologies for tuberculosis diagnosis: Progress and challenges. Clin Chest Med. 2009;30(4):701–16.
51. Storla DG, Yimer S, Bjune GA. A systematic review of delay in the diagnosis and treatment of tuberculosis. BMC Public Health. 2008;8(15):1–9.
52. Mcnerney R, Maeurer M, Abubakar I, Marais B, Mchugh TD, Ford N, et al. Tuberculosis diagnostics and biomarkers: Needs, challenges, recent advances, and opportunities. J Infect Dis. 2012;205:147–58.
53. Koul A, Arnoult E, Lounis N, Guillemont J, Andries K. The challenge of new drug discovery for tuberculosis. Nature. 2011;469:483–90.
54. Floss HG, Yu T-W. Rifamycin-mode of action, resistance, and biosynthesis. Chem Rev. 2005;105:621–32.
55. Jo KW, Ji W, Hong Y, Lee S Do, Kim WS, Kim DS, et al. The efficacy of rifabutin for rifabutin-susceptible, multidrug-resistant tuberculosis. Respir Med. 2013;107(2):292–7.
56. Gülbay BE, Gürkan ÖU, Yildiz ÖA, Önen ZP, Erkekol FO, Baççioğlu A, et al. Side effects due to primary antituberculosis drugs during the initial phase of therapy in 1149 hospitalized patients for tuberculosis. Respir Med. 2006;100:1834–42.
57. Sharma SK, Sharma A, Kadhiravan T, Tharyan P. Rifamycins (rifampicin, rifabutin and rifapentine) compared to isoniazid for preventing tuberculosis in HIV-negative people at risk of active TB. Evidence-Based Child Heal. 2014;9(1):169–294.
58. Manish G, Vimukta S. Pulsatile drug delivery system: a review. Int Res J Pharm. 2011;1(2):135–8.
59. Mohanraj VJ, Chen Y. Nanoparticles – A Review. Trop J Pharm Res. 2006;5(June):561–73.
60. Nikam AP, Mukesh PR, Haudhary SP. Nanoparticles – An overview. Int J Reserach Dev Pharm Life Sci. 2014;3(5):1121–7.
61. Sharma A, Chakradhari M, Agrawal D, Khinchi MP, Sharma N, Gupta MK. Lung targeting of antitubercular drugs by microsphere: A review. Asian J Pharm Educ Res. 2013;2(1):37–59.
62. Smola M, Vandamme T, Sokolowski A. Nanocarriers as pulmonary drug delivery systems to treat and to diagnose respiratory and non respiratory diseases. Int J

Nanomedicine. 2008;3(1):1–19.
63. Kuzmov A, Minko T. Nanotechnology approaches for inhalation treatment of lung diseases. J Control Release. 2015;219:500–18.
64. Siekmeier R, Scheuch G. Treatment of systemic diseases by inhalation of biomolecules aerosols. Jounal Phisiology Pharmacol. 2009;60:15–26.
65. Darquenne C. Aerosol deposition in health and disease. J Aerosol Med Pulm Drug Deliv. 2012;25(3):140–7.
66. Kellaway GT. Pulmonary drug delivery. In: Drug delivery and targeting, editor. Anya M. Hillery, Andrew W. Lloyd JS. 1st ed. New York, USA: Taylor & Francis; 2001. p. 244–72.
67. Tsuda A, Henry FS, Butler JP. Particle transport and deposition. Compr Physiol. 2013;3(4):1437–71.
68. Dhanani J, Fraser JF, Chan H-K, Rello J, Cohen J, Roberts JA. Fundamentals of aerosol therapy in critical care. Crit Care. 2016;20(1):1–16.
69. Hassan MS, Lau RWM. Effect of particle shape on dry particle inhalation: Study of flowability, aerosolization, and deposition properties. AAPS PharmSciTech. 2009;10(4):1252–62.
70. Vehring R. Expert review pharmaceutical particle engineering via spray drying. Pharm Res. 2008;25(5):999–1022.
71. Loira-Pastoriza C, Todoroff J, Vanbever R. Delivery strategies for sustained drug release in the lungs. Adv Drug Deliv Rev. 2014;75:81–91.
72. Palazzo F, Giovagnoli S, Schoubben A, Blasi P, Rossi C, Ricci M. Development of a spray-drying method for the formulation of respirable microparticles containing ofloxacin-palladium complex. Int J Pharm. 2013;440(2):273–82.
73. European Pharmacopeia 9.0. Section 2.9.18. Preparations for inhalations: Aerodynamic assessment of fine particles. 9th ed. Strasburg, France: Council of Europe; 2016. p. 323–34.
74. Finlay WH, Stapleton KW, Zuberbuhler P. Fine particle fraction as a measure of mass depositing in the lung during inhalation of nearly isotonic nebulized aerosols. J Aerosol Sci. 1997;28(7):1301–9.
75. Buttini F, Colombo G, Kwok PCL, Wui WT. Aerodynamic assessment for inhalation products: Fundamentals and current pharmacopoeial methods. In: Inhalation drug delivery: Techniques and products, editor Colombo, P. Traini, D. and Buttini F. 1st ed. West Sussex, United Kingdom: Wiley-Blackwell; 2013. p. 91–119.
76. Patton JS, Byron PR. Inhaling medicines: Delivering drugs to the body through the lungs. Nat Rev Drug Discov. 2007;6:67–74.
77. Pilcer G, Amighi K. Formulation strategy and use of excipients in pulmonary drug

delivery. Int J Pharm. 2010;392(1–2):1–19.
78. Yang MY, Chan JGY, Chan HK. Pulmonary drug delivery by powder aerosols. J Control Release. 2014;193:228–40.
79. ISO/TS 80004-1:2015. Nanotechnology vocabulary - Part 1: Core terms. 2015. p. 1–3.
80. Huang Y, Li R, Chen J, Chen J. Biphasic release of gentamicin from chitosan fucoidan nanoparticles. Carbohydr Polym. 2016;138:114–22.
81. Wean Sin C, Tie Yi K, Hadinoto K. Amorphous nanodrugs prepared by complexation with polysaccharides: carrageenan versus dextran sulfate. Carbohydr Polym. 2015;117:549–58.
82. Srikanth K, Rama Mohan Gupta V, Manvi SR, Devanna N. Particulate carrier systems. Int Res J Pharm. 2012;3(11):22–6.
83. Fredenberg S, Wahlgren M, Reslow M, Axelsson A. The mechanisms of drug release in poly(lactic-co-glycolic acid)-based drug delivery systems—A review. Int J Pharm. 2011;415(1–2):34–52.
84. Liang Z, Ni R, Zhou J, Mao S. Recent advances in controlled pulmonary drug delivery. Drug Discov Today. 2015;20(3):380–9.
85. Gupta A, Pant G, Mitra K, Madan J, Chourasia MK, Misra A. Inhalable particles containing rapamycin for induction of autophagy in macrophages infected with Mycobacterium tuberculosis. Mol Pharm. 2014;11(4):1201–7.
86. Kadam NR, Survana V. Microsphere: A brief review. Asian J Biomed Pharm Sci. 2015;5(47):13–9.
87. Chiellini F, Piras AM, Errico C, Chiellini E. Micro/nanostructured polymeric systems for biomedical and pharmaceutical applications. Nanomedicine. 2008;3(3):367–93.
88. Chimie RR De, Cismaru L, Popa M. Polymeric nanoparticles with biomedical applications. 2010;55(8):433–42.
89. Jyothi NVN, Prasanna PM, Sakarkar SN, Prabha KS, Ramaiah PS, Srawan GY. Microencapsulation techniques, factors influencing encapsulation efficiency. J Microencapsul. 2010;27(3):187–97.
90. Siyawamwaya M, Choonara YE, Bijukumar D, Kumar P, DuToit LC, Pillaya V. A review: Overview of novel polyelectrolyte complexes as prospective drug bioavailability enhancers. Int J Polym Mater. 2015;64:955–68.
91. Lankalapalli S, Kolapalli VRM. Polyelectrolyte complexes: A review of their applicability in drug delivery technology. Indian J Pharm Sci. 2009;71(5):481–7.
92. Mohanty B, Aswal VK, Kohlbrecher J, Bohidar HB. Synthesis of gelatin nanoparticles via simple coacervation. J Surf Sci Technol. 2005;21(3–4):149–60.
93. Shimokawa KI, Saegusa K, Wada Y, Ishii F. Physicochemical properties and

controlled drug release of microcapsules prepared by simple coacervation. Colloids Surfaces B Biointerfaces. 2013;104:1–4.

94. Learoyd TP, Burrows JL, French E, Seville PC. Chitosan-based spray-dried respirable powders for sustained delivery of terbutaline sulfate. Eur J Pharm Biopharm. 2008;68(2):224–34.
95. Mishra M, Mishra B. Formulation optimization and characterization of spray-dried microparticles for inhalation delivery of doxycycline hyclate. Yakugaku Zasshi. 2011;131(12):1813–25.
96. Lee SH, Heng D, Ng WK, Chan H-K, Tan RBH. Nano spray drying: A novel method for preparing protein nanoparticles for protein therapy. Int J Pharm. 2011 Jan 17;403(1–2):192–200.
97. Manmode AS, Sakarkar DM, Mahajan NM. Nanoparticles-tremendous therapeutic potential: A review. Int J PharmTech Res. 2009;1(4):1020–7.
98. Nimitt C, Mayur P. Nanotechnology based drug delivery systems for the treatment of tuberculosis. Indian J Exp Biol. 2006;44:357–66.
99. Kohane DS. Microparticles and nanoparticles for drug delivery. Biotechnol Bioeng. 2007;96(2):203–9.
100. Zhou H, Zhang Y, Biggs DL, Manning MC, Randolph TW, Christians U, et al. Microparticle-based lung delivery of INH decreases INH metabolism and targets alveolar macrophages. J Control Release. 2005;107(2):288–99.
101. Ahmad Khanbeigi R, Kumar A, Sadouki F, Lorenz C, Forbes B, Dailey LA, et al. The delivered dose: Applying particokinetics to in vitro investigations of nanoparticle internalization by macrophages. J Control Release. 2012;162(2):259–66.
102. Gratton SEA, Ropp PA, Pohlhaus PD, Luft JC, Madden VJ, Napier ME, et al. The effect of particle design on cellular internalization pathways. Proc Natl Acad Sci U S A. 2008;105(33):11613–8.
103. Murugan K, Choonara YE, Kumar P, Bijukumar D, du Toit LC, Pillay V. Parameters and characteristics governing cellular internalization and trans-barrier trafficking of nanostructures. Int J Nanomedicine. 2015;10:2191–206.
104. Hirota K, Hasegawa T, Hinata H, Ito F, Inagawa H, Kochi C, et al. Optimum conditions for efficient phagocytosis of rifampicin-loaded PLGA microspheres by alveolar macrophages. J Control Release. 2007;119:69–76.
105. Zarogoulidis P, Chatzaki E, Porpodis K, Domvri K, Hohenforst-Schmidt W, Goldberg EP, et al. Inhaled chemotherapy in lung cancer: Future concept of nanomedicine. Int J Nanomedicine. 2012;7:1551–72.
106. Gaspar DP, Faria V, Gonçalves LMD, Taboada P, Remuñán-López C, Almeida AJ. Rifabutin-loaded solid lipid nanoparticles for inhaled antitubercular therapy:

Physicochemical and in vitro studies. Int J Pharm. 2016;497(1–2):199–209.
107. Rawal T, Parmar R, Tyagi RK, Butani S. Rifampicin loaded chitosan nanoparticle dry powder presents an improved therapeutic approach for alveolar tuberculosis. Colloids Surfaces B Biointerfaces. 2017;154:321–30.
108. Mehanna MM, Mohyeldin SM, Elgindy NA. Respirable nanocarriers as a promising strategy for antitubercular drug delivery. J Control Release. 2014;187:183–97.
109. Garcia-Contreras L, Padilla-Carlin DJ, Sung J, VerBerkmoes J, Muttil P, Elbert K, et al. Pharmacokinetics of ethionamide delivered in spray-dried microparticles to the lungs of guinea pigs. J Pharm. 2017;106(1):331–7.
110. Park JH, Jin HE, Kim DD, Chung SJ, Shim WS, Shim CK. Chitosan microspheres as an alveolar macrophage delivery system of ofloxacin via pulmonary inhalation. Int J Pharm. 2013;441(1–2):562–9.
111. Chan JGY, Duke CC, Ong HX, Chan JCY, Tyne AS, Chan H-K, et al. A novel inhalable form of rifapentine. J Pharm Sci. 2014;103(5):1411–21.
112. Geiser M, Casaulta M, Kupferschmid B, Schulz H, Semmler-Behnke M, Kreyling W. The role of macrophages in the clearance of inhaled ultrafine titanium dioxide particles. Am J Respir Cell Mol Biol. 2008;38:371–6.
113. Choi HS, Ashitate Y, Lee JH, Kim SH, Matsui A, Insin N, et al. Rapid translocation of nanoparticles from the lung airspaces to the body. Nat Biotechnol. 2010;28(12):1300–3.
114. El-Sherbiny IM, El-baz NM, Yacoub MH. Inhaled nano- and microparticles for drug delivery. Glob Cardiol Sci Pract. 2015;2:1–14.
115. Grenha A, Seijo B, Remuñán-López C. Microencapsulated chitosan nanoparticles for lung protein delivery. Eur J Pharm Sci. 2005;25(4–5):427–37.
116. Ohashi K, Kabasawa T, Ozeki T, Okada H. One-step preparation of rifampicin/poly(lactic-co-glycolic acid) nanoparticle-containing mannitol microspheres using a four-fluid nozzle spray drier for inhalation therapy of tuberculosis. J Control Release. 2009;135(1):19–24.
117. Pourshahab PS, Gilani K, Moazeni E, Eslahi H, Fazeli MR, Jamalifar H. Preparation and characterization of spray dried inhalable powders containing chitosan nanoparticles for pulmonary delivery of isoniazid. J Microencapsul. 2011;28(7):605–13.
118. Lee Y-S, Johnson PJ, Robbins PT, Bridson RH. Production of nanoparticles-in-microparticles by a double emulsion method: A comprehensive study. Eur J Pharm Biopharm. 2013;83(2):168–73.
119. Iyer R, Hsia CCW, Nguyen KT. Nano-therapeutics for the lung: state-of-the-art and future perspectives. Curr Pharm Des. 2015;21(36):5233–44.

120. Huang Y-C, Li R-Y. Preparation and characterization of antioxidant nanoparticles composed of chitosan and fucoidan for antibiotics delivery. Mar Drugs. 2014;12(8):4379–98.
121. Andrade F, Rafael D, Videira M, Ferreira D, Sosnik A, Sarmento B. Nanotechnology and pulmonary delivery to overcome resistance in infectious diseases. Adv Drug Deliv Rev. 2013;65(13–14):1816–27.
122. Campos E, Branquinho J, Carreira AS, Carvalho A, Coimbra P, Ferreira P, et al. Designing polymeric microparticles for biomedical and industrial applications. Eur Polym J. 2013;49(8):2005–21.
123. Beneke CE, Viljoen AM, Hamman JH. Polymeric plant-derived excipients in drug delivery. Molecules. 2009;14(7):2602–20.
124. Angelova N, Hunkeler D. Rationalizing the design of polymeric biomaterials. Tibtech. 1999;17:409–21.
125. Espíndola-González A, Martínez-Hernández AL, Fernández-Escobar F, Castaño VM, Brostow W, Datashvili T, et al. Natural-synthetic hybrid polymers developed via electrospinning: the effect of PET in chitosan/starch system. Int J Mol Sci. Multidisciplinary Digital Publishing Institute (MDPI); 2011;12(3):1908–20.
126. Tong R, Gabrielson NP, Fan TM, Cheng J. Polymeric nanomedicines based on poly(lactide) and poly(lactide-co-glycolide). Curr Opin Solid State Mater Sci. 2012;16(217):323–32.
127. Suarez S, O'Hara P, Kazantseva M, Newcomer CE, Hopfer R, McMurray DN, et al. Respirable PLGA microspheres containing rifampicin for the treatment of tuberculosis: screening in an infectious disease model. Pharm Res. 2001;18(9):1315–9.
128. Malathi, S. SB. PLGA nanoparticles for anti tuberculosis drug delivery. Recent Trends Adv Mater. 2012;584:465–9.
129. Hirota K, Hasegawa T, Nakajima T, Inagawa H, Kohchi C, Soma G-I, et al. Delivery of rifampicin–PLGA microspheres into alveolar macrophages is promising for treatment of tuberculosis. J Control Release. 2010 Mar;142(3):339–46.
130. Upadhyay S, Khan I, Gothwal A, Pachouri PK, Bhaskar N, Gupta UD, et al. Conjugated and entrapped HPMA-PLA nano-polymeric micelles based dual delivery of first line anti TB drugs: Improved and safe drug delivery against sensitive and resistant Mycobacterium tuberculosis. Pharm Res. 2017;34(9):1944–55.
131. Pillai O, Panchagnula R. Polymers in drug delivery. Curr Opin Chem Biol. 2001;5:447–51.
132. Nitta SK, Numata K. Biopolymer-based nanoparticles for drug/gene delivery and tissue engineering. Int J Mol Sci. 2013;14(1):1629–54.

133. Braz L, Grenha A, Ferreira D, Rosa da Costa AMAM, Gamazo C, Sarmento B. Chitosan/sulfated locust bean gum nanoparticles: In vitro and in vivo evaluation towards an application in oral immunization. Int J Biol Macromol. 2017;96:786–97.
134. Nagpal K, Singh SK, Mishra DN. Chitosan nanoparticles: a promising system in novel drug delivery. Chem Pharm Bull (Tokyo). 2010;58(11):1423–30.
135. Alves A, Cavaco J, Guerreiro F, Lourenço J, Rosa da Costa A, Grenha A. Inhalable antitubercular therapy mediated by locust bean gum microparticles. Molecules. 2016;21(702):1–22.
136. Leong KH, Chung LY, Noordin MI, Onuki Y, Morishita M, Takayama K. Lectin-functionalized carboxymethylated kappa-carrageenan microparticles for oral insulin delivery. Carbohydr Polym. 2011;86(2):555–65.
137. Gaspar R, Duncan R. Polymeric carriers: Preclinical safety and the regulatory implications for design and development of polymer therapeutics. Adv Drug Deliv Rev. 2009 Nov;61(13):1220–31.
138. Basu A, Kunduru KR, Abtew E, Domb AJ. Polysaccharide-Based Conjugates for Biomedical Applications. Bioconjug Chem. 2015 Aug 19;26(8):1396–412.
139. Laurienzo P. Marine polysaccharides in pharmaceutical applications: An overview. Mar Drugs. 2010;8(9):2435–65.
140. Manivasagan P, Oh J. Marine polysaccharide-based nanomaterials as a novel source of nanobiotechnological applications. Int J Biol Macromol. 2016;82:315–27.
141. Pinheiro AC, Bourbon AI, Cerqueira MA, Maricato É, Nunes C, Coimbra MA, et al. Chitosan/fucoidan multilayer nanocapsules as a vehicle for controlled release of bioactive compounds. Carbohydr Polym. 2015;115:1–9.
142. Kim ES, Lee JS, Lee HG. Nanoencapsulation of red ginseng extracts using chitosan with polyglutamic acid or fucoidan for improving antithrombotic activities. J Agric Food Chem. 2016;64:4765–71.
143. Yi-Cheng H, Jen-Kun C, U-Ian L, Sih-Yu C. Preparing, characterizing, and evaluating chitosan/fucoidan nanoparticles as oral delivery carriers. J Polym Res. 2014;21(5):1–9.
144. Lu KY, Li R, Hsu CH, Lin CW, Chou SC, Tsai ML, et al. Development of a new type of multifunctional fucoidan-based nanoparticles for anticancer drug delivery. Carbohydr Polym. 2017;165:410–20.
145. Lee KKW, Jeong D, Na K. Doxorubicin loading fucoidan acetate nanoparticles for immune and chemotherapy in cancer treatment. Carbohydr Polym. 2013;94(2):850–6.
146. Hwang PA, Lin XZ, Kuo KL, Hsu FY. Fabrication and cytotoxicity of fucoidan-cisplatin nanoparticles for macrophage and tumor cells. Materials (Basel).

2017;10(3).
147. Shao-Jung W, Trong-Ming D, Cheng-Wei L, Fwu-Long M. Delivery of berberine using chitosan/fucoidan-taurine conjugate nanoparticles for treatment of defective intestinal epithelial tight junction barrier. Mar Drugs. 2014;12(11):5677–97.
148. Sezer AD, Akbuğa J. Fucosphere-new microsphere carriers for peptide and protein delivery: Preparation and in vitro characterization. J Microencapsul. 2006;23(5):513–22.
149. Sezer AD, Akbuğa J. Comparison on in vitro characterization of fucospheres and chitosan microspheres encapsulated plasmid DNA (pGM-CSF): Formulation design and release characteristics. AAPS PharmSciTech. 2009;10(4):1193–9.
150. Sezer AD, Akbuğa J. The design of biodegradable ofloxacin-based core-shell microspheres: influence of the formulation parameters on in vitro characterization. Pharm Dev Technol. 2012;17(1):118–24.
151. Situ W, Xiang T, Liang Y. Chitosan-based particles for protection of proteins during storage and oral administration. Int J Biol Macromol. 2018;117:308–14.
152. Abnoos M, Mohseni M, Mousavi SAJ, Ashtari K, Ilka R, Mehravi B. Chitosan-alginate nano-carrier for transdermal delivery of pirfenidone in idiopathic pulmonary fibrosis. Int J Biol Macromol. 2018;118:1319–25.
153. Tang P, Sun Q, Zhao L, Pu H, Yang H, Zhang S, et al. Mesalazine/hydroxypropyl-β-cyclodextrin/chitosan nanoparticles with sustained release and enhanced anti-inflammation activity. Carbohydr Polym. 2018;198:418–25.
154. Garrido-Maestu A, Ma Z, Paik S-Y-R, Chen N, Ko S, Tong Z, et al. Engineering of chitosan-derived nanoparticles to enhance antimicrobial activity against foodborne pathogen Escherichia coli O157:H7. Carbohydr Polym. 2018;197:623–30.
155. Tan C, Xie J, Zhang X, Cai J, Xia S. Polysaccharide-based nanoparticles by chitosan and gum arabic polyelectrolyte complexation as carriers for curcumin. Food Hydrocoll. 2016;57:236–45.
156. Luque-Alcaraz AG, Lizardi-Mendoza J, Goycoolea FM, Higuera-Ciapara I, Argüelles-Monal W. Preparation of chitosan nanoparticles by nanoprecipitation and their ability as a drug nanocarrier. RSC Adv. 2016;6(64):59250–6.
157. Katsarov P, Pilicheva B, Uzunova Y, Gergov G, Kassarova M. Chemical cross-linking: A feasible approach to prolong doxylamine/pyridoxine release from spray-dried chitosan microspheres. Eur J Pharm Sci. 2018;123:387–94.
158. Yildiz-Peköz A, Akbal O, Tekarslan SH, Sagirli AO, Mulazimoglu L, Morina D, et al. Preparation and characterization of doripenem-loaded microparticles for pulmonary delivery. J Aerosol Med Pulm Drug Deliv. 2018;31:1–11.
159. Zhang L, Yang L, Zhang X, Jiaqi L, Fan L, Beck-Broichsitter M, et al. Sustained

therapeutic efficacy of budesonide-loaded chitosan swellable microparticles after lung delivery: Influence of in vitro release, treatment interval and dose. J Control Release. 2018;283:163–74.

160. Moreno JAS, Mendes AC, Stephansen K, Engwer C, Goycoolea FM, Boisen A, et al. Development of electrosprayed mucoadhesive chitosan microparticles. Carbohydr Polym. 2018;190:240–7.
161. Cunha L, Grenha A. Sulfated seaweed polysaccharides as multifunctional materials in drug delivery applications. Mar Drugs. 2016;14(42):1–41.
162. Li B, Lu F, Wei X, Zhao R, Bo L, Fei L, et al. Fucoidan: structure and bioactivity. Molecules. 2008;13(8):1671–95.
163. Holtkamp AD, Kelly S, Ulber R, Lang S. Fucoidans and fucoidanases-focus on techniques for molecular structure elucidation and modification of marine polysaccharides. Appl Microbiol Biotechnol. 2009;82(1):1–11.
164. Wijesinghe WAJP, Jeon Y. Biological activities and potential industrial applications of fucose rich sulfated polysaccharides and fucoidans isolated from brown seaweeds: A review. Carbohydr Polym. 2012;88(1):13–20.
165. Tsutomu F, Yusuke S, Shigeru M, Kazue T, Takashi K, Tomohiko S, et al. Fucoidan is the active component of Fucus vesiculosus that promotes contraction of fibroblast-populated collagen gels. Biol Pharm Bull. 2000;23(10):1180–4.
166. Xing R, Liu S, Yu H, Chen X, Qin Y, Li K, et al. Extraction and separation of fucoidan from Laminaria japonica with chitosan as extractant. Biomed Res Int. 2013;1:1–4.
167. Duarte MER, Cardoso MA, Noseda MD, Cerezo AS. Structural studies on fucoidans from the brown seaweed Sargassum stenophyllum. Carbohydr Res. 2001;333:281–93.
168. Marais MF, Joseleau JP. A fucoidan fraction from Ascophyllum nodosum. Carbohydr Res. 2001;336:155–9.
169. Woo-jung K, Sung-min K, Hyun Guell K, Hye-rim O, Kyung-bok L, Yoo-kyung L, et al. Purification and anticoagulant activity of a fucoidan from Korean Undaria pinnatifida sporophyll. Algae. 2007;22(3):247–52.
170. Guangling J, Guangli Y, Junzeng Z, Ewart HS. Chemical structures and bioactivities of sulfated polysaccharides from marine algae. Mar Drugs. 2011;9(2):196–233.
171. Xiangdong Q, Amarasekara A, Doctor V. Effect of oversulfation on the chemical and biological properties of fucoidan. Carbohydr Polym. 2006;63:224–8.
172. Chizhov AO, Dell A, Morris HR, Haslam SM, McDowell RA, Shashkov AS, et al. A study of fucoidan from the brown seaweed Chorda filum. Carbohydr Res.

1999;320(1–2):108–19.

173. Kusaykin MI, Chizhov AO, Grachev AA, Alekseeva SA, Bakunina IY, Nedashkovskaya OI, et al. A comparative study of specificity of fucoidanases from marine microorganisms and invertebrates. J Appl Phycol. 2006;18:369–73.
174. Hahn T, Lang S, Ulber R, Muffler K. Novel procedures for the extraction of fucoidan from brown algae. Process Biochem. 2012;47(12):1691–8.
175. Ale MT, Mikkelsen JD, Meyer AS. Important determinants for fucoidan bioactivity: A critical review of structure-function relations and extraction methods for fucose-containing sulfated polysaccharides from brown seaweeds. Mar Drugs. 2011;9(10):2106–30.
176. Ponce NMA, Pujol CA, Damonte EB. Fucoidans from the brown seaweed Adenocystis utricularis : extraction methods , antiviral activity and structural studies. Carbohydr Res. 2003;338:153–65.
177. Bo L, Xin-Jun W, Jun-Liang S, Shi-Ying X. Structural investigation of a fucoidan containing a fucose-free core from the brown seaweed, Hizikia fusiforme. Carbohydr Res. 2006;341(9):1135–46.
178. Bilan MI, Bilan MI, Grachev A a, Grachev A a, Ustuzhanina NE, Ustuzhanina NE, et al. Structure of a fucoidan from the brown seaweed Fucus evanescens. Carbohydr Res. 2002;337:719–30.
179. Bilan MI, Grachev AA, Ustuzhanina NE, Shashkov AS, Nifantiev NE, Usov AI. A highly regular fraction of a fucoidan from the brown seaweed Fucus distichus L. Carbohydr Res. 2004;339(3):511–7.
180. Chevolot L, Mulloy B, Ratiskol J, Foucault A, Colliec-Jouault S. A disaccharide repeat unit is the major structure in fucoidans from two species of brown algae. Carbohydr Res. 2001;330(4):529–35.
181. Usui T, Asari K, Takashi M. Isolation of highly purified “fucoidan” from Eisenia bicyclis and its anticoagulant and antitumor activities. Agric Biol Chem. 1980;44(8):1965–6.
182. Colliec S, Boisson-Vidal C, Jozefonvicz J. A low molecular weight fucoidan fraction from the brown seaweed Pelvetia canaliculata. Phytochemistry. 1994;35(3):697–700.
183. Pomin VH. Fucanomics and galactanomics: Marine distribution, medicinal impact, conceptions, and challenges. Mar Drugs. 2012;10(4):793–811.
184. Zvyagintseva TN, Shevchenko NM, Chizhov AO, Krupnova TN, Sundukova EV, Isakov VV. Water-soluble polysaccharides of some far-eastern brown seaweeds. Distribution, structure, and their dependence on the developmental conditions. J Exp Mar Bio Ecol. 2003;294(1):1–13.

185. Black WAP. The seasonal variation in the combined L-fucose content of the common British Laminariaceae and fucaceae. J Sci Food Agric. 1954;5(9):445–8.
186. Taylor P, Nishino T, Aizu Y, Nagumo T. The relationship between the molecular weight and the anticoagulant activity of two types of fucan sulfates from the brown seaweed Ecklonia kurome. Agric Biol Chem. 1991;55(3):791–6.
187. Fitton JH, Stringer DN, Karpiniec SS. Therapies from fucoidan: An update. Mar Drugs. 2015;13:5920–46.
188. Rupérez P, Ahrazem O, Leal JA. Potential antioxidant capacity of sulfated polysaccharides from the edible marine brown seaweed Fucus vesiculosus. J Agric Food Chem. 2002;50:840–5.
189. Synytsya A, Copicová J, Woo JK, Yong II P. Marine algal biotechnology. In: Springer Handbook of Marine Biotechnology, editor. Se-kwon K. 1st ed. London, New York: Springer; 2015. p. 1–8.
190. Venugopal V. Polysaccharide from seaweed and microalgae. In: Marine polysaccharides: Food applications, editor Zollo S. 1st ed. Boca Raton, FL, USA: Taylor and Francis Group; 2011. p. 111–22.
191. Silva TH, Alves A, Popa EG, Reys LL, Gomes ME, Sousa RA, et al. Marine algae sulfated polysaccharides for tissue engineering and drug delivery approaches. Biomatter. 2012;2:278–89.
192. Kwak J. Fucoidan as a marine anticancer agent in preclinical development. Mar Drugs. 2014;12:851–70.
193. Young H, Ho M, Park C, Jin C, Gi-Young K, Il-Whan C, et al. Anti-inflammatory effects of fucoidan through inhibition of NF-κB , MAPK and Akt activation in lipopolysaccharide-induced BV2 microglia cells. Food Chem Toxicol. 2011;49(8):1745–52.
194. Jung-Bum L, Hayashi K, Hashimoto M, Nakano T, Hayashi T. Novel antiviral fucoidan from Sporophyll of Undaria pinnatifida (Mekabu). Chem Pharm Bull. 2004;52(9):1091–4.
195. Raghavendran HRB, Srinivasan P, Rekha S. Immunomodulatory activity of fucoidan against aspirin-induced gastric mucosal damage in rats. Int Immunopharmacol. 2011;11(2):157–63.
196. Teng H, Yang Y, Wei H, Liu ZZ, Liu ZZ, Ma Y, et al. Fucoidan suppresses hypoxia-induced lymphangiogenesis and lymphatic metastasis in mouse hepatocarcinoma. Mar Drugs. 2015;13(6):3514–30.
197. Cumashi A, Ushakova NA, Preobrazhenskaya ME, D'Incecco A, Piccoli A, Totani L, et al. A comparative study of the anti-inflammatory, anticoagulant, antiangiogenic, and antiadhesive activities of nine different fucoidans from brown seaweeds.

Glycobiology. 2007;17(5):541–52.
198. Croci DO, Cumashi A, Ushakova NA, Preobrazhenskaya ME, Piccoli A, Totani L, et al. Fucans, but not fucomannoglucuronans, determine the biological activities of sulfated polysaccharides from Laminaria saccharina brown seaweed. PLoS One. 2011;6(2):1–10.
199. Kuznetsova TA, Besednova NN, Mamaev AN, Momot AP, Shevchenko NM, Zvyagintseva TN. Anticoagulant activity of fucoidan from brown algae Fucus evanescens of the Okhotsk Sea. Bull Exp Biol Med. 2003;136(11):471–3.
200. Burtseva YV, Kusaikin MI, Sova VV, Shevchenko NM, Skobun AS, Zvyagintseva TN. Distribution of fucoidan hydrolases and some glycosidases among marine invertebrates. Russ J Mar Biol. 2000;26(6):453–6.
201. Silchenko ASAS, Kusaykin MIMI, Kurilenko VVV, Zakharenko AMAM, Isakov VVV, Zaporozhets TSTS, et al. Hydrolysis of fucoidan by fucoidanase isolated from the marine bacterium, formosa algae. Mar Drugs. 2013;11:2413–30.
202. Weiss DJ, Liggitt D, Clark JG. In situ histochemical detection o beta-galactosidase activity in lung: Assessment of X-Gal reagent in distinguishing lacZ gene expression and endogenous beta-galactosidase activity. Hum Gene Ther. 1997;8:1545–54.
203. Zhao Y-J, Ju Q, Li G-C. Tumor markers for hepatocellular carcinoma (Review). Mol Clin Oncol. 2013;1:593–8.
204. Chan JY, Nwokoro NA, Schachter H. L-fucose metabolism in mammals. J Biol Chem. 1979;254(15):7060–8.
205. Sinha VR, Singla AK, Wadhawan S, Kaushik R, Kumria R, Bansal K, et al. Chitosan microspheres as a potential carrier for drugs. Int J Pharm. 2004;274(1–2):1–33.
206. Rinaudo M. Chitin and chitosan: Properties and applications. Prog Polym Sci. 2006;31(7):603–32.
207. Younes I, Rinaudo M. Chitin and chitosan preparation from marine sources. Structure, properties and applications. Mar Drugs. 2015;13(3):1133–74.
208. Aiba S. Preparation of N-acetylchitooligosaccharides by hydrolysis of chitosan with chitinase followed by N-acetylation. Carbohydr Res. 1994 Dec;265(2):323–8.
209. Ilyina A V, Yu Tatarinova N, Varlamov VP. The preparation of low-molecular-weight chitosan using chitinolytic complex from Streptomyces kurssano6ii. Process Biochem. 1999;34:875–8.
210. No HK, Meyers SP. Preparation and Characterization of Chitin and Chitosan—A review. J Aquat Food Prod Technol. 1995;4(2):27–52.
211. Kumari S, Rath PK. Extraction and Characterization of Chitin and Chitosan from (Labeo rohit) Fish Scales. Procedia Mater Sci. 2014;6:482–9.

212. Rodrigues S, Dionísio M, López CR, Grenha A. Biocompatibility of chitosan carriers with application in drug delivery. J Funct Biomater. 2012;3(4):615–41.
213. Luangtana-anan M, Opanasopit P, Ngawhirunpat T, Nunthanid J, Sriamornsak P, Limmatvapirat S, et al. Effect of Chitosan Salts and Molecular Weight on a Nanoparticulate Carrier for Therapeutic Protein. Pharm Dev Technol. 2005;10(2):189–96.
214. Orienti I, Cerchiara T, Luppi B, Bigucci F, Zuccari G, Zecchi V. Influence of different chitosan salts on the release of sodium diclofenac in colon-specific delivery. Int J Pharm. 2002;238(1–2):51–9.
215. Zargar V, Asghari M, Dashti A. A review on chitin and chitosan polymers: Structure, chemistry, solubility, derivatives, and applications. ChemBioEng Rev. 2015;2(3):204–26.
216. Aranaz I, Mengíbar M, Harris R, Paños I, Miralles B, Acosta N, et al. Functional characterization of chitin and chitosan. Curr Chem Biol. 2009;3:203–30.
217. Paul W, Sharma CP. Chitosan, a drug carrier for the 21st century: A review. STP Pharma Sci. 2000;10(1):5–22.
218. Aiba S. Evidence for the presence of random and block copolymer structures in partially N-acetylated chitosans. Int J Biol Macromol. 1991;13(1):40–4.
219. Kasaai M, Arul J, Charlet G. Intrinsic viscosity — Molecular weight relationship for chitosan. J Polym Sci Part B Polym Phys. 2000;38:2591–2598.
220. Costa CN, Teixeira VG, Delpech MC, Virginia J, Souza S, Costa MAS. Viscometric study of chitosan solutions in acetic acid / sodium acetate and acetic acid / sodium chloride. Carbohydr Polym. 2015;133:245–50.
221. Sarbon NM, Sandanamsamy S, Kamaruzaman SFS, Ahmad F. Chitosan extracted from mud crab (Scylla olivicea) shells: Physicochemical and antioxidant properties. J Food Sci Technol. 2014;52(7):4266–75.
222. Mourya VKK, Inamdar NN. Chitosan-modifications and applications: Opportunities galore. React Funct Polym. 2008 Jun;68(6):1013–51.
223. Pillai CKS, Paul W, Sharma CP. Chitin and chitosan polymers: Chemistry, solubility and fiber formation. Prog Polym Sci. 2009;34:641–78.
224. Lee D, Lockey R, Mohapatra S. Folate receptor-mediated cancer cell specific gene delivery using folic acid-conjugated oligochitosans. J Nanosci Nanotechnol. 2006;6(9–10):2860–6.
225. Thanou M, Henderson S, Kydonieus A, Elson C. N-sulfonato-N,O-carboxymethylchitosan: A novel polymeric absorption enhancer for the oral delivery of macromolecules. J Control Release. 2007;117(2):171–8.
226. Aruna U, Rajalakshmi R, Y IM, Vinesha V, Sushma M, Kr V, et al. Role of chitosan

nanoparticles in cancer therapy. Int J Innov Pharm Res. 2013;4(3):318–24.
227. Bernkop-Schnürch A, Dünnhaupt S. Chitosan-based drug delivery systems. Eur J Pharm Biopharm. 2012;81(3):463–9.
228. Azuma K, Osaki T, Minami S, Okamoto Y. Anticancer and anti-inflammatory properties of chitin and chitosan oligosaccharides. J Funct Biomater. 2015;6(1):33–49.
229. Younes I, Hajji S, Frachet V, Rinaudo M, Jellouli K, Nasri M. Chitin extraction from shrimp shell using enzymatic treatment. Antitumor, antioxidant and antimicrobial activities of chitosan. Int J Biol Macromol. 2014;69:489–98.
230. Barakat AA. Hypolipidemic and antiatherogenic effects of dietary chitosan and wheatbran in high fat- high cholesterol fed rats. 2011;5(10):30–7.
231. Harisa GI, Attia SM, Zoheir KMA, Alanazi FK. Chitosan treatment abrogates hypercholesterolemia-induced erythrocyte's arginase activation. Saudi Pharm J. 2017;25(1):120–7.
232. Harish Prashanth K V., Tharanathan RN. Chitin/chitosan: Modifications and their unlimited application potential-an overview. Trends Food Sci Technol. 2007;18(3):117–31.
233. Kerch G. The potential of chitosan and its derivatives in prevention and treatment of Age-related diseases. Mar Drugs. 2015;13(4):2158–82.
234. Croisier F, Jérôme C. Chitosan-based biomaterials for tissue engineering. Eur Polym J. 2013;49:780–92.
235. Dash M, Chiellini F, Ottenbrite RMM, Chiellini E. Chitosan - A versatile semi-synthetic polymer in biomedical applications. Prog Polym Sci. 2011 Aug;36(8):981–1014.
236. Zeng L, Qin C, Wang W, Chi W, Li W. Absorption and distribution of chitosan in mice after oral administration. Carbohydr Polym. 2008;71:435–40.
237. Rodriguez-Vazquez M, Vega-Ruiz B, Ramos-Zuniga R, Saldana-Koppel DA, Quinones-Olvera LF. Chitosan and its potential use as a scaffold for tissue engineering in regenerative medicine. BioMed Res Int Int. 2015;2015:1–15.
238. Dajani R, Zhang Y, Taft PJ, Travis SM, Starner TD, Olsen A, et al. Lysozyme secretion by submucosal glands protects the airway from bacterial infection. Am J Respir Cell Mol Biol. 2005;32:548–52.
239. Pai R V., Jain RR, Bannalikar AS, Menon MD. Development and evaluation of chitosan microparticles based dry powder inhalation formulations of rifampicin and rifabutin. J Aerosol Med Pulm Drug Deliv. 2015;28:1–17.
240. António J. Almeida, Grenha A. Technosphere®: An inhalation system for pulmonary delivery of biopharmaceutical. In: Mucosal Delivery of

Biopharmaceuticals, editor: Neves, J. and Sarmento, B. 1st ed. Springer: New York, USA; 2014. p. 483–98.

241. Teruya T, Tatemoto H, Konishi T, Tako M. Structural characteristics and in vitro macrophage activation of acetyl fucoidan from Cladosiphon okamuranus. Glycoconj J. 2009;26(8):1019–28.
242. Jiang Z, Ueno M, Nishiguchi T, Abu R, Isaka S, Okimura T, et al. Importance of sulfate groups for the macrophage-stimulating activities of ascophyllan isolated from the brown alga Ascophyllum nodosum. Carbohydr Res. 2013;380:124–9.
243. Lira MCB, Santos-Magalhães NS, Nicolas V, Marsaud V, Silva MPC, Ponchel G, et al. Cytotoxicity and cellular uptake of newly synthesized fucoidan-coated nanoparticles. Eur J Pharm Biopharm. 2011;79(1):162–70.
244. Kunjachan S, Gupta S, Dwivedi AK, Dube A, Chourasia MK. Chitosan-based macrophage-mediated drug targeting for the treatment of experimental visceral leishmaniasis. J Microencapsul. 2011 Jun 17;28(4):301–10.
245. Chong AS, Parish CR. Cell surface receptors for sulphated polysaccharides: A potential marker for macrophage subsets. Immunology. 1986;58(2):277–84.
246. Lee EJ, Lim KH. Polyelectrolyte complexes of chitosan self-assembled with fucoidan: An optimum condition to prepare their nanoparticles and their characteristics. Korean J Chem Eng. 2014;31(4):664–75.
247. Saikia C, Gogoi P. Chitosan: A promising biopolymer in drug delivery applications. J Mol Genet Med. 2015;S4:006:1–10.
248. Onishi H, Machida Y. Improvement of oral drug absorption by chitosan and its derivatives. In: Enhancement in Drug Delivery, editors Touitou E and Barry B. New York, USA: Taylor & Francis Group; 2007. p. 57–66.
249. Hwang SM, Kim DD, Chung SJ, Shim CK. Delivery of ofloxacin to the lung and alveolar macrophages via hyaluronan microspheres for the treatment of tuberculosis. J Control Release. 2008;129(2):100–6.
250. Kamaly N, Yameen B, Wu J, Farokhzad OC. Degradable controlled-release polymers and polymeric nanoparticles: Mechanisms of controlling drug release. Chem Rev. 2016;116(4):2602–63.
251. Chin SF, Pang SC, Tay SH. Size controlled synthesis of starch nanoparticles by a simple nanoprecipitation method. Carbohydr Polym. 2011;86(4):1817–9.
252. Kimura R, Rokkaku T, Takeda S, Senba M, Mori N. Cytotoxic effects of fucoidan nanoparticles against osteosarcoma. Mar Drugs. 2013;11(11):4267–78.
253. Garg T, Rath G, Goyal AK. Inhalable chitosan nanoparticles as antitubercular drug carriers for an effective treatment of tuberculosis. Artif Cells, Nanomedicine, Biotechnol. 2015;1–5.

254. Zahoor A, Sharma S, Khuller GK. Inhalable alginate nanoparticles as antitubercular drug carriers against experimental tuberculosis. Int J Antimicrob Agents. 2005;26:298–303.
255. Hamman JH. Chitosan based polyelectrolyte complexes as potential carrier materials in drug delivery systems. Mar Drugs. 2010;8(4):1305–22.
256. Lee EJ, Lim K-H. Relative charge density model on chitosan-fucoidan electrostatic interaction: Qualitative approach with element analysis. J Biosci Bioeng. 2015;119(2):237–46.
257. Yu SH, Tang DW, Hsieh HY, Wu WS, Lin BX, Chuang EY, et al. Nanoparticle-induced tight-junction opening for the transport of an anti-angiogenic sulfated polysaccharide across Caco-2 cell monolayers. Acta Biomater. 2013;9(7):7449–59.
258. Sonam S, Chaudhary H, Arora V, Kholi K, Kumar V. Effect of physicochemical properties of biodegradable polymers on nano drug delivery. Polym Rev. 2013;53(4):546–67.
259. Huang Y-C, Yang Y-T. Effect of basic fibroblast growth factor released from chitosan–fucoidan nanoparticles on neurite extension. J Tissue Eng Regen Med. 2013;10(5):418–27.
260. Yang H-C, Hon M-H. The effect of the molecular weight of chitosan nanoparticles and its application on drug delivery. Microchem J. 2009;92(1):87–91.
261. World Health Organization. WHO treatment guidelines for drug-resistant tuberculosis 2016. Geneva, Switzerland; 2016.
262. Di Martino A, Pavelkova A, Maciulyte S, Budriene S, Sedlarik V. Polysaccharide-based nanocomplexes for co-encapsulation and controlled release of 5-fluorouracil and temozolomide. Eur J Pharm Sci. 2016;92:276–86.
263. Briones AV, Sato T. Encapsulation of glucose oxidase (GOD) in polyelectrolyte complexes of chitosan-carrageenan. React Funct Polym. 2010;70(1):19–27.
264. Huang Y-C, Lam U-I, Yi-Cheng H, U-Ian L. Chitosan/fucoidan pH sensitive nanoparticles for oral delivery system. J Chinese Chem Soc. 2011;58(6):779–85.
265. Carvalho ELS, Grenha A, Remuñán-López C, Alonso M, Seijo B. Mucosal delivery of liposome–chitosan nanoparticle complexes. In: Methods in Enzymology: Liposomes, Part G, Vol 465, editor Nejat Duzgunes. Burlington: Academic Press; 2009. p. 289–312.
266. Ho TTM, Bremmell KE, Krasowska M, Stringer DN, Thierry B, Beattie DA. Tuning polyelectrolyte multilayer structure by exploiting natural variation in fucoidan chemistry. Soft Matter. 2015;11:2110–24.
267. Skaugrud Ø, Hagen A, Borgersen B, Dornish M. Biomedical and pharmaceutical applications of alginate and chitosan. Biotechnol Genet Eng Rev. 1999;16(1):23–

40.
268. Vostrikov V V., Selishcheva AA, Sorokoumova GM, Shakina YN, Shvets VI, Savel'ev OY, et al. Distribution coefficient of rifabutin in liposome/water system as measured by different methods. Eur J Pharm Biopharm. 2008;68(2):400–5.
269. Magalhães Jr. GA, Moura Neto E, Sombra VG, Richter AR, Abreu CMWS, Feitosa JPA, et al. Chitosan/Sterculia striata polysaccharides nanocomplex as a potential chloroquine drug release device. Int J Biol Macromol. 2016;88:244–53.
270. Bilati U, Allémann E, Doelker E. Development of a nanoprecipitation method intended for the entrapment of hydrophilic drugs into nanoparticles. Eur J Pharm Sci. 2005;24(1):67–75.
271. Saari H, Fuentes C, Sjöö M, Rayner M, Wahlgren M. Production of starch nanoparticles by dissolution and non-solvent precipitation for use in food-grade Pickering emulsions. Carbohydr Polym. 2017;157:558–66.
272. Khan SA, Schneider M. Improvement of nanoprecipitation technique for preparation of gelatin nanoparticles and potential macromolecular drug loading. Macromol Biosci. 2013;13(4):455–63.
273. Salatin S, Barar J, Barzegar-Jalali M, Adibkia K, Kiafar F, Jelvehgari M. Development of a nanoprecipitation method for the entrapment of a very water soluble drug into Eudragit RL nanoparticles. Res Pharm Sci. 2017;12(1):1–14.
274. Schubert S, Delaney JT, Schubert US. Nanoprecipitation and nanoformulation of polymers: From history to powerful possibilities beyond poly (lactic acid). Soft Matter. 2011;7:1581–8.
275. Rauf A, Bhatnagar A, Sisodia SS, Khar RK, Ahmad FJ. Lungs deposition and pharmacokinetic study of submicron budesonide particles in Wistar rats intended for immediate effect in asthma. EXCLI J. 2017;16:236–44.
276. Monjezi M, Saidi MS, Ahmadi G. Submicron particle deposition in pulmonary alveoli during cyclic breathing. Sci Iran. 2017;24(4):1975–84.
277. Mora-Huertas CE, Fessi H, Elaissari A. Polymer-based nanocapsules for drug delivery. Int J Pharm. 2010;385(1–2):113–42.
278. Tay SH, Pang SC, Chin SF. A facile approach for controlled synthesis of hydrophilic starch-based nanoparticles from native sago starch. Starch/Staerke. 2012;64(12):984–90.
279. Kaur M, Malik B, Garg T, Rath G, Goyal AK. Development and characterization of guar gum nanoparticles for oral immunization against tuberculosis. Drug Deliv. 2015;22(3):328–34.
280. Limayem Blouza I, Charcosset C, Sfar S, Fessi H. Preparation and characterization of spironolactone-loaded nanocapsules for paediatric use. Int J Pharm.

2006;325:124–31.
281. Budhian A, Siegel SJ, Winey KI. Haloperidol-loaded PLGA nanoparticles: Systematic study of particle size and drug content. Int J Pharm. 2007;336(2):367–75.
282. Guhagarkar SA, Malshe VC, Devarajan P V. Nanoparticles of polyethylene sebacate: A new biodegradable polymer. AAPS PharmSciTech. 2009;10(3):935–42.
283. Vandervoort J, Ludwig A. Preparation and evaluation of drug-loaded gelatin nanoparticles for topical ophthalmic use. Eur J Pharm Biopharm. 2004;57(2):251–61.
284. Martínez Rivas CJ, Tarhini M, Badri W, Miladi K, Greige-Gerges H, Nazari QA, et al. Nanoprecipitation process: From encapsulation to drug delivery. Int J Pharm. 2017;532(1):66–81.
285. Martinelli F, Balducci AG, Kumar A, Sonvico F, Forbes B, Bettini R, et al. Engineered sodium hyaluronate respirable dry powders for pulmonary drug delivery. Int J Pharm. 2017;517(1–2):286–95.
286. Ota A, Istenič K, Skrt M, Šegatin N, Žnidaršič N, Kogej K, et al. Encapsulation of pantothenic acid into liposomes and into alginate or alginate–pectin microparticles loaded with liposomes. J Food Eng. 2018;229:21–31.
287. Prabu C, Latha S, Selvamani P, Ahrentorp F, Johansson C, Takeda R, et al. Layer-by-layer assembled magnetic prednisolone microcapsules (MPC) for controlled and targeted drug release at rheumatoid arthritic joints. J Magn Magn Mater. 2017;427:258–67.
288. Carmichael J, Degraff WG, Gazdar AF, Minna JD, Mitchell JB. Evaluation of a tetrazolium-based semiautomated colorimetric assay: Assessment of chemosensitivity testing. Am Assoc Cancer Res. 1987;47:936–42.
289. Ahmadi Z, Verma G, Jha D. Evaluation of antimicrobial activity and cytotoxicity of pegylated aminoglycosides. J Bioact Compat Polym. 2018;333(3):295–309.
290. Gaspar DP, Gaspar MM, Eleutério C V., Grenha A, Blanco M, Gonçalves LMD, et al. Microencapsulated solid lipid nanoparticles as a hybrid platform for pulmonary antibiotic delivery. Mol Pharm. 2017;14(9):2977–90.
291. O'Connell KE, Mikkola AM, Stepanek AM, Vernet A, Hall CD, Sun CC, et al. Practical murine hematopathology: A comparative review and implications for research. Comp Med. 2015;65(2):96–113.
292. Waggett BE, Gannon S, McGorum BC. Use of the Ouchterlony double immunodiffusion method to observe antigen/antibody interactions in serum taken from Equine Grass Sickness cases and Co-grazers of Equine Grass Sickness.

2010. p. 1–7.
293. Rodrigues S, Alves AD, Cavaco JS, Pontes JF, Guerreiro F, Rosa da Costa AM, et al. Dual antibiotherapy of tuberculosis mediated by inhalable locust bean gum microparticles. Int J Pharm. 2017;529(1–2):433–41.
294. Zhang L, Li Y, Zhang Y, Zhu C. Sustained release of isoniazid from polylactide microspheres prepared using solid/oil drug loading method for tuberculosis treatment. Sci China Life Sci. 2016;59(7):724–31.
295. Anshakova A V, Yu Konyukhov V. Study by inverse gas chromatography of the solubility of rifabutin in water in the presence of cyclodextrin. Russ J Appl Chem. 2017;90(2):209–13.
296. O'Toole MG, Henderson RM, Soucy PA, Fasciotto BH, Hoblitzell PJ, Keynton RS, et al. Curcumin encapsulation in submicrometer spray-dried chitosan/tween 20 particles. Biomacromolecules. 2012;13(8):2309–14.
297. Jabes D, Della Bruna C, Rossi R, Olliaro P. Effectiveness of rifabutin alone or in combination with isoniazid in preventive therapy of mouse tuberculosis. Antimicrob Agents Chemother. 1994;38(10):2346–50.
298. Daman Z, Gilani K, Rouholamini Najafabadi A, Eftekhari H, Barghi M. Formulation of inhalable lipid-based salbutamol sulfate microparticles by spray drying technique. DARU J Pharm Sci. 2014;22(1):1–9.
299. Maas SG, Schaldach G, Littringer EM, Mescher A, Griesser UJ, Braun DE, et al. The impact of spray drying outlet temperature on the particle morphology of mannitol. Powder Technol. 2011;213(1–3):27–35.
300. Belotti S, Rossi A, Colombo P, Bettini R, Rekkas D, Politis S, et al. Spray dried amikacin powder for inhalation in cystic fibrosis patients: A quality by design approach for product construction. Int J Pharm. 2014;471(1–2):507–15.
301. Ni R, Zhao J, Liu Q, Liang Z, Muenster U, Mao S. Nanocrystals embedded in chitosan-based respirable swellable microparticles as dry powder for sustained pulmonary drug delivery. Eur J Pharm Sci. 2017;99:137–46.
302. Dalpiaz A, Fogagnolo M, Ferraro L, Capuzzo A, Pavan B, Rassu G, et al. Nasal chitosan microparticles target a zidovudine prodrug to brain HIV sanctuaries. Antiviral Res. 2015;123:146–57.
303. Sinsuebpol C, Chatchawalsaisin J, Kulvanich P. Preparation and in vivo absorption evaluation of spray dried powders containing salmon calcitonin loaded chitosan nanoparticles for pulmonary delivery. Drug Des Devel Ther. 2013;7:861–73.
304. Kundawala A, Patel V, Patel H, Choudhary D. Preparation, in vitro characterization, and in vivo pharmacokinetic evaluation of respirable porous microparticles containing rifampicin. Sci Pharm. 2014;82(3):665–81.

305. Chauhan A, Chauhan P. Powder XRD technique and its applications in science and technology. J Anal Bioanal Tech. 2014;5(5):1–5.
306. Oliveira PM, Matos BN, Pereira PAT, Gratieri T, Faccioli LH, Cunha-Filho MSS, et al. Microparticles prepared with 50–190 kDa chitosan as promising non-toxic carriers for pulmonary delivery of isoniazid. Carbohydr Polym. 2017;174:421–31.
307. Mahajan HS, Dusunge SB, Gundare SA. Xyloglucan based microspheres for pulmonary delivery of rifabutin dry powder inhaler. Int J Pharm Sci Nanotechnol. 2017;10(3):3709–14.
308. Yousef Javadzadeh SH and SA. Recrystallization of drugs: Significance on Parmaceutical Processing. In: Recrystallization, editor. K Sztwiertnia. 1st ed. London. U.K: INTECH Open; 2012. p. 425–47.
309. Alhalaweh A, Alzghoul A, Mahlin D, Bergström CAS. Physical stability of drugs after storage above and below the glass transition temperature: Relationship to glass-forming ability. Int J Pharm. 2015;495(1):312–7.
310. Mishra B, Mishra M, Yadav SK. Antibacterial loaded spray dried chitosan polyelectrolyte complexes as dry powder aerosol for the treatment of lung infections. Iran J Pharm Res. 2017;16(1):74–92.
311. Saffari M, Ebrahimi A, Langrish T. Highly-porous mannitol particle production using a new templating approach. Food Res Int. 2015;67:44–51.
312. European Medicines Agency. Guideline on Quality of Oral Modified Release Products; EMA: Volume EMA/CHMP/QWP/428693/2013. London. U.K; 2014.
313. Martinelli F, Balducci AG, Rossi A, Sonvico F, Colombo P, Buttini F. “Pierce and inhale” design in capsule based dry powder inhalers: Effect of capsule piercing and motion on aerodynamic performance of drugs. Int J Pharm. 2015;487(1–2):197–204.
314. Buttini F, Hannon J, Saavedra K, Rossi I, Balducci AG, Smyth H, et al. Accessorized DPI: A shortcut towards flexibility and patient adaptability in dry powder inhalation. Pharm Res. 2016;3012–20.
315. Buttini F, Brambilla G, Copelli D, Sisti V, Balducci AG, Bettini R, et al. Effect of flow rate on in vitro aerodynamic performance of NEXThaler ® in comparison with Diskus ® and Turbohaler ® Dry Powder Inhalers. J Aerosol Med Pulm Drug Deliv. 2016;29(2):167–78.
316. Eleftheriadis GK, Akrivou M, Bouropoulos N, Tsibouklis J, Vizirianakis IS, Fatouros DG. Polymer−lipid microparticles for pulmonary delivery. Langmuir. 2018;34:3438–48.
317. Mulla JAS, Mabrouk M, Choonara YE, Kumar P, Chejara DR, du Toit LC, et al. Development of respirable rifampicin-loaded nano-lipomer composites by

microemulsion-spray drying for pulmonary delivery. J Drug Deliv Sci Technol. 2017;41:13–9.

318. Vieira AC, Magalhães J, Rocha S, Cardoso MS, Santos SG, Borges M, et al. Targeted macrophages delivery of rifampicin-loaded lipid nanoparticles to improve tuberculosis treatment. Nanomedicine. 2017;12(24):2721–36.
319. Azad M, Moreno J, Davé R. Stable and fast-dissolving amorphous drug composites preparation via impregnation of Neusilin®UFL2. J Pharm Sci. 2018;107(1):170–82.
320. Haghi M, Ong HX, Traini D, Young P. Across the pulmonary epithelial barrier: Integration of physicochemical properties and human cell models to study pulmonary drug formulations. Pharmacol Ther. 2014;144(3):235–52.
321. Bur M, Huwer H, Muys L, Lehr C-M. Drug transport across pulmonary epithelial cell monolayers: Effects of particle size, apical liquid volume, and deposition technique. J Aerosol Med Pulm Drug Deliv. 2010;23(3):119–27.
322. ISO 10993-5. Biological Evaluation of Medical Devices Part 5: Tests for In Vitro Cytotoxicity. International Organization for Standardization. Geneva, Switzerland; 2009.
323. Alwarsamy M, Gooneratne R, Ravichandran R. Effect of fucoidan from Turbinaria conoides on human lung adenocarcinoma epithelial (A549) cells. Carbohydr Polym. 2016;152:207–13.
324. Lee H, Kim JS, Kim E. Fucoidan from Seaweed Fucus vesiculosus Inhibits Migration and Invasion of Human Lung Cancer Cell via PI3K-Akt-mTOR Pathways. PLoS One. 2012;7(11).
325. Senthilkumar K, Manivasagan P, Venkatesan J, Kim S-K. Brown seaweed fucoidan: Biological activity and apoptosis, growth signaling mechanism in cancer. Int J Biol Macromol. 2013;60:366–74.
326. Lanone S, Rogerieux F, Geys J, Dupont A, Maillot-Marechal E, Boczkowski J, et al. Comparative toxicity of 24 manufactured nanoparticles in human alveolar epithelial and macrophage cell lines. Part Fibre Toxicol. 2009;6(14):1–12.
327. Barluenga J, Aznar F, García AB, Cabal MP, Palacios JJ, Menéndez MA. New rifabutin analogs: Synthesis and biological activity against Mycobacterium tuberculosis. Bioorganic Med Chem Lett. 2006;16(22):5717–22.
328. Chien J-Y, Chien S-T, Huang S-Y, Yu C-J. Safety of rifabutin replacing rifampicin in the treatment of tuberculosis: A single-centre retrospective cohort study. J Antimicrob Chemother. 2013;69(3):790–6.
329. Chakraborty P, Kulkarni S, Rajan R, Sainis K. Mycobacterium tuberculosis strains from ancient and modern lineages induce distinct patterns of immune responses. J Infect Dev Ctries. 2017;11(12):904–11.

330. Mwandumba HC, Squire SB, White SA, Nyirenda MH, Zijlstra EE, Molyneux ME, et al. Alveolar macrophages from HIV-infected patients with pulmonary tuberculosis retain the capacity to respond to stimulation by lipopolysaccharide. Microbes Infect. 2007;9:1053–60.
331. Duque GA, Descoteaux A. Macrophage cytokines: involvement in immunity and infectious diseases. Front Immunol. 2014;5:1–12.
332. Vidarsson MMS, Gudjónsdóttir M, Marteinsdottir G, Stefaniak-Vidarsson MM, Gudjónsdóttir M, Marteinsdottir G, et al. Evaluation of bioactivity of fucoidan from laminaria with in vitro human cell culture (THP-1). Funct Foods Heal Dis. 2017;7(9):688–701.
333. Zhang W, Oda T, Yu Q, Jin J-O, Jun-O J. Fucoidan from macrocystis pyrifera has powerful immune-modulatory effects compared to three other fucoidans. Mar Drugs. 2015;13(3):1084–104.
334. Beatrice C, Telles S, Mendes-Aguiar C, Pereira Fidelis G, Frasson AP, Wogelsanger &, et al. Immunomodulatory effects and antimicrobial activity of heterofucans from Sargassum filipendula. J Appl Phycol. 2017;30:569–78.
335. Borazjani NJ, Tabarsa M, You S, Rezaei M. Purification, molecular properties, structural characterization, and immunomodulatory activities of water soluble polysaccharides from Sargassum angustifolium. Int J Biol Macromol. 2018;109:793–802.
336. Jin, J, Park H-Y, Xu, Q, Park, J-I, Zvyagintseva T, Stonik VA, et al. Ligand of scavenger receptor class A indirectly induces maturation of human blood dendritic cells via production of tumor necrosis factor-α. Blood. 2009;113(23):5839–48.
337. Jin, J, Yu Q. Fucoidan delays apoptosis and induces pro-inflammatory cytokine production in human neutrophils. Int J Biol Macromol. 2015;73(1):65–71.
338. Li J, Chen K, Li S, Liu T, Wang F, Xia Y, et al. Pretreatment with fucoidan from fucus vesiculosus protected against conA-induced acute liver injury by inhibiting both intrinsic and extrinsic apoptosis. PLoS One. 2016;11(4):1–16.
339. Park J, Cha JD, Choi KM, Lee KY, Han KM, Jang YS. Fucoidan inhibits LPS-induced inflammation in vitro and during the acute response in vivo. Int Immunopharmacol. 2017;43:91–8.
340. Marianelli C, Armas F, Boniotti MB, Mazzone P, Pacciarini ML, Di Marco Lo Presti V. Multiple drug-susceptibility screening in Mycobacterium bovis: New nucleotide polymorphisms in the embB gene among ethambutol susceptible strains. Int J Infect Dis. 2015;33:39–44.
341. Sturegård E, Ängeby KA, Werngren J, Juréen P, Kronvall G, Giske CG, et al. Little difference between minimum inhibitory concentrations of Mycobacterium

tuberculosis wild-type organisms determined with BACTEC MGIT 960 and Middlebrook 7H10. Clin Microbiol Infect. 2015;21:148.e5–148.e7.

342. Pinheiro M, Silva AS, Reis S. Molecular interactions of rifabutin with membrane under acidic conditions. Int J Pharm. 2015;479:63–9.
343. Pinheiro M, Nunes C, Caio JM, Moiteiro C, Lúcio M, Brezesinski G, et al. The influence of Rifabutin on human and bacterial membrane models: Implications for its mechanism of action. J Phys Chem B. 2013;117:6187–93.
344. Ritz N, Tebruegge M, Connell TG, Sievers A, Robins-Browne R, Curtis N. Susceptibility of Mycobacterium bovis BCG vaccine strains to antituberculous antibiotics. Antimicrob Agents Chemother. 2009;53(1):316–8.
345. Sirgel FA, Warren RM, Böttger EC, Klopper M, Victor TC, van Helden PD. The rationale for using rifabutin in the treatment of MDR and XDR tuberculosis outbreaks. PLoS One. 2013;8(3):1–5.
346. Oberholzer HM, Vieira WA, Pretorius E. Investigating the effect of the homeopathic immunomodulator, MODUL8® on blood count, bronchial lavage and fibrin ultrastructure on experimental asthmatic BALB/c Mice. Int J Morphol. 2009;27(3):955–63.
347. Ghosh S, Hoselton SA, Dorsam GP, Schuh JM. Eosinophils in fungus-associated allergic pulmonary disease. Front Pharmacol. 2013;1–18.
348. George L, Brightling CE. Eosinophilic airway inflammation: Role in asthma and chronic obstructive pulmonary disease. Ther Adv Chronic Dis. 2016;7(1):34–51.
349. Wu LC, Scheerens H. Targeting IgE production in mice and humans. Curr Opin Immunol. 2014;31:8–15.
350. Zosky GR, Larcombe AN, White OJ, Burchell JT, Janosi TZ, Hantos Z, et al. Ovalbumin-sensitized mice are good models for airway hyperresponsiveness but not acute physiological responses to allergen inhalation. Clin Exp Allergy. 2008;38(5):829–38.
351. Santos EW, Oliveira DC de, Hastreiter A, Silva GB da, Beltran JS de O, Tsujita M, et al. Hematological and biochemical reference values for C57BL/6, Swiss Webster and BALB/c mice. Brazilian J Vet Res Anim Sci. 2016;53(2):138–45.
352. Shin SH, Park HY, Kang D, Cho J, Kwon SO, Park JH, et al. Serial blood eosinophils and clinical outcome in patients with chronic obstructive pulmonary disease. Respir Res. 2018;19:1–9.
353. East L, Isacke CM. The mannose receptor family. Biochim Biophys Acta - Gen Subj. 2002;1572(2–3):364–86.
354. Maury M, Murphy K, Kumar S, Shi L, Lee G. Effects of process variables on the powder yield of spray-dried trehalose on a laboratory spray-dryer. Eur J Pharm

Biopharm. 2005;59(3):565–73.
355. Ko J., Park H., Hwang S., Park J., Lee J. Preparation and characterization of chitosan microparticles intended for controlled drug delivery. Int J Pharm. 2002;249(1–2):165–74.
356. Lacerda L, Parize AL, Fávere V, Laranjeira MCM, Stulzer HK. Development and evaluation of pH-sensitive sodium alginate/chitosan microparticles containing the antituberculosis drug rifampicin. Mater Sci Eng C. 2014;39:161–7.
357. Pandey R, Khuller GK. Chemotherapeutic potential of alginate-chitosan microspheres as anti-tubercular drug carriers. J Antimicrob Chemother. 2004;53(4):635–40.
358. Desai KGH, Park HJ. Encapsulation of vitamin C in tripolyphosphate cross-linked chitosan microspheres by spray drying. J Microencapsul. 2005;22(2):179–92.
359. Corrigan DO, Healy AM, Corrigan OI. Preparation and release of salbutamol from chitosan and chitosan co-spray dried compacts and multiparticulates. Eur J Pharm Biopharm. 2006;62(3):295–305.
360. da Silva Carvalho AG, da Costa Machado MT, da Silva VM, Sartoratto A, Rodrigues RAF, Hubinger MD. Physical properties and morphology of spray dried microparticles containing anthocyanins of jussara (Euterpe edulis Martius) extract. Powder Technol. 2016;294:421–8.
361. Anton N, Jakhmola A, Vandamme TF. Trojan microparticles for drug delivery. Pharmaceutics. 2012;4(1):1–25.
362. Takeuchi I, Taniguchi Y, Tamura Y, Ochiai K, Makino K. Effects of l-leucine on PLGA microparticles for pulmonary administration prepared using spray drying: Fine particle fraction and phagocytotic ratio of alveolar macrophages. Colloids Surfaces A Physicochem Eng Asp. 2018;537:411–7.
363. Cabral RP, Sousa AML, Silva AS, Paninho AI, Temtem M, Costa E, et al. Design of experiments approach on the preparation of dry inhaler chitosan composite formulations by supercritical CO2-assisted spray-drying. J Supercrit Fluids. 2016;116:26–35.
364. Mesquita PC, Oliveira AR, Pedrosa MFF, De Oliveira AG, Da Silva-Júnior AA. Physicochemical aspects involved in methotrexate release kinetics from biodegradable spray-dried chitosan microparticles. J Phys Chem Solids. 2015;81:27–33.
365. Uthaman N, Majeed A, Pandurangan. Impact modification of polyoxymethylene (POM). Polym Eng Sci. 2016;56(12):1432–6.
366. Nurzyńska K, Booth J, Roberts CJ, McCabe J, Dryden I, Fischer PM. Long-Term Amorphous Drug Stability Predictions Using Easily Calculated, Predicted, and

Measured Parameters. Mol Pharm. 2015;12(9):3389–98.
367. Chauhan D, Patel A, Shah S. Influence of selected natural polymers on in-vitro release of colon targeted Mebeverine HCl matrix tablet. Int J Drug Dev Res. 2012;4(2):247–55.
368. Upadhyay TK, Fatima N, Sharma D, Saravanakumar V, Sharma R. Preparation and characterization of beta-glucan particles containing a payload of nanoembedded rifabutin for enhanced targeted delivery to macrophages. EXCLI J. 2017;16:210–28.
369. Kundawala AJ, Patel V a, Patel H V, Choudhary D. Influence of formulation components on aerosolization properties of isoniazid loaded chitosan microspheres. Intenational J Pharm Sci Drug Res. 2011;3(4):297–302.
370. Abbas Y, Azzazy HME, Tammam S, Lamprecht A, Ali ME, Schmidt A, et al. Development of an inhalable, stimuli-responsive particulate system for delivery to deep lung tissue. Colloids Surfaces B Biointerfaces. 2016;146:19–30.
371. Boyles MSP, Kristl T, Andosch A, Zimmermann M, Tran N, Casals E, et al. Chitosan functionalisation of gold nanoparticles encourages particle uptake and induces cytotoxicity and pro-inflammatory conditions in phagocytic cells, as well as enhancing particle interactions with serum components. J Nanobiotechnology. 2015;13:1–20.
372. Fröhlich E, Mercuri A, Wu S, Salar-Behzadi S. Measurements of deposition, lung surface area and lung fluid for simulation of inhaled compounds. Front Pharmacol. 2016;7:1–10.
373. Caetano LA, Almeida AJ, Gonçalves LMD. Effect of experimental parameters on alginate / chitosan microparticles for BCG encapsulation. Mar Drugs. 2016;14:1–30.
374. Fu YN, Li Y, Li G, Yang L, Yuan Q, Tao L, et al. Adaptive chitosan hollow microspheres as efficient drug carrier. Biomacromolecules. 2017;18(7):2195–204.
375. Fotakis G, Timbrell JA. In vitro cytotoxicity assays: Comparison of LDH, neutral red, MTT and protein assay in hepatoma cell lines following exposure to cadmium chloride. Toxicol Lett. 2006;160(2):171–7.
376. Wang C, Muttil P, Lu D, Beltran-Torres AA, Garcia-Contreras L, Hickey AJ. Screening for potential adjuvants administered by the pulmonary route for tuberculosis vaccines. AAPS J. 2009;11(1):139–47.
377. Brodaczewska K, Wolaniuk N, Lewandowska K, Donskow-Łysoniewska K, Doligalska M. Biodegradable chitosan decreases the immune response to Trichinella spiralis in mice. Molecules. 2017;22(11):1–16.
378. Caires HR, Esteves T, Quelhas P, Barbosa MA, Navarro M, Almeida CR. Macrophage interactions with polylactic acid and chitosan scaffolds lead to

improved recruitment of human mesenchymal stem/stromal cells: A comprehensive study with different immune cells. J R Soc Interface. 2016;13:1–12.

379. Singh B, Maharjan S, Cho K-H, Cui L, Park I-K, Choi Y-J, et al. Chitosan-based particulate systems for the delivery of mucosal vaccines against infectious diseases. Int J Biol Macromol. 2018;110:54–64.
380. Wu T, Liao W, Wang W, Zhou J, Tan W, Xiang W, et al. Genipin-crosslinked carboxymethyl chitosan nanogel for lung-targeted delivery of isoniazid and rifampin. Carbohydr Polym. 2018;197:403–13.
381. Liu Y, Yao W, Wang S, Di G, Zheng Q, Chen A. Preparation and characterization of fucoidan-chitosan nanospheres by the sonification method. J Nanosci Nanotechnol. 2014;14(5):3844–9.
382. Nuzzo M, Millqvist-Fureby A, Sloth J, Bergenstahl B. Surface composition and morphology of particles dried individually and by spray drying. Dry Technol. 2015;33(6):757–67.
383. Fujihara M, Muroi M, Tanamoto K, Suzuki T. Molecular mechanisms of macrophage activation and deactivation by lipopolysaccharide: Roles of the receptor complex. Pharmacol Ther. 2003;100:171–94.
384. Allavena P, Chieppa M, Monti P, Piemonti L. From pattern recognition receptor to regulator of homeostasis: The double-faced macrophage mannose receptor. Crit Rev Immunol. 2004;24(3):179–92.